TAMPEREEN TEKNILLINEN YLIOPISTO
TAMPERE UNIVERSITY OF TECHNOLOGY

LINDA URBAŃSKI

FABRICATION AND CHARACTERIZATION OF COLLAGEN, HYALURONIC ACID AND CHONDROITIN SULFATE SCAFFOLDS FOR CARTILAGE TISSUE ENGINEERING APPLICATIONS

Master of Science Thesis

Examiners: Professor Dr. Tech. Minna Kellomäki
M.Sc. Eng. Anne-Marie Haaparanta

Examiners and topic accepted in the faculty meeting on 8th of October 2014.

TIIVISTELMÄ

TAMPEREEN TEKNILLINEN YLIOPISTO
Biotekniikan koulutusohjelma
URBAŃSKI, LINDA: Fabrication and characterization of collagen, hyaluronic acid and chondroitin sulphate scaffolds for cartilage tissue engineering applications
Diplomityö, 92 sivua, 48 liitesivua
Kesäkuu 2015
Pääaine: Kudosteknologia
Tarkastajat: Professori Minna Kellomäki
DI Anne-Marie Haaparanta
Avainsanat: Kudosteknologia, rusto, skaffoldi, kollageeni, hyaluronihappo, kondroitiinisulfaatti, kylmäkuivaus, 1-etyyli-3-(3-dimetyyliaminopropyyli)-karbodi-imidi hydrokloridi, N-hydroksisukkiini-imidi, genipin

Rustokudoksen paranemiskyky on hyvin rajoittunutta eivätkä nykyiset kliiniset metodit tarjoa varmaa tapaa uuden toiminnallisen rustokudoksen aikaansaamiseksi. Viime vuosikymmeninä ruston korjaukseen liittyvä tutkimus on keskittynyt yhä enemmän kudosteknologisiin ratkaisuihin, jotka tarjoavat skaffoldi-pohjaisia strategioita uuden ruston muodostamiseksi. Kollageenin (COL) ja kahden glykosaminoglykaanin, kondroitiinisulfaatin (CS) ja hyaluronihapon (HA) yhdistäminen on saanut osakseen laajaa mielenkiintoa, sillä kaikki kolme ovat natiivin rustokudoksen peruskomponentteja.

Tämän diplomityön tavoitteena oli valmistaa ruston kudosteknologiaan soveltuvia COL, HA ja/tai CS skaffoldeja ja tutkia niiden ominaisuuksia. Huokoiset kolmiulotteiset skaffoldit valmistettiin kylmäkuivaamalla ja ristisilloitettiin käyttäen joko 1-etyyli-3-(3-dimetyyliaminopropyyli)-karbodi-imidi hydrokloridi / N-hydroksisukkiini-imidia (EDC/NHS) tai genipiniä (GP). Valmistettujen COL+CS/HA/CS+HA skaffoldien ominaisuuksia tutkittiin puristus- ja nesteenimeytymistestein, mikrotietokonetomografialla sekä Fourier-muunnos infrapunaspektroskopialla (FTIR).

Yleisesti ottaen, 80 wt.% COL komposiittiskaffoldit kestivät valmistuksen ja ristisilloituksen 60 wt.% COL komposiittiskaffoldeja paremmin. Lisäksi ne imivät 60 wt.% skaffoldeja enemmän vettä. Myös GP-ristisilloitettujen ja COL+HA skaffoldien vedenottokyvyn havaittiin olevan EDC/NHS-ristisilloitettuja ja COL+CS skaffoldeja suurempi. Veden imeytymistesteissä kaikkien skaffoldien turpoaminen/kutistuminen huomattiin pysyvän alle 20%:ssa; suurimmaksi osaksi muutokset olivat noin 10%:n luokkaa. FTIR-tulokset varmistivat ristisilloituksen tapahtuneen kaikissa GP ja EDC/NHS käsitellyissä skaffoldeissa. Mikrotietokonetomografia mittaukset paljastivat kaikkien skaffoldien olevan erittäin huokoisia (88-94%) ja huokoset toisiinsa liittyneitä (mitatut huokoskoot 26-57 µm).

Kuivien skaffoldien puristuslujuus oli huomattavasti suurempi kuin vastaavien märkien skaffoldien; suurin ero havaittiin GP-ristisilloitettujen skaffoldien välillä. Korkeimmat puristusmodulit, niin kuivilla kuin märillä skaffoldeilla, mitattiin CS:ää sisältävistä komposiiteista. Kahdesta COL:ia ja HA:a sisältävästä skaffoldiryhmästä taas mitattiin pienimmät puristusmodulit. Kaikki skaffoldit (märkinä että kuivina) palautuivat hyvin puristuksesta.

Tässä diplomityössä onnistuttiin valmistamaan kylmäkuivaamalla erittäin huokoisia, kolmiulotteisia ja ruston kudosteknologiaan soveltuvia COL+CS/HA/CS+HA skaffoldeja. Lisäksi, GP osoittautui ristisilloittajana lupaavaksi vaihtoehdoksi perinteiselle EDC/NHS:lle.

ABSTRACT

TAMPERE UNIVERSITY OF TECHNOLOGY
Master's Degree Programme in Biotechnology
URBAŃSKI, LINDA: Fabrication and characterization of collagen, hyaluronic acid and chondroitin sulphate scaffolds for cartilage tissue engineering applications
Master of Science Thesis, 92 pages, 48 Appendix pages
June 2015
Major: Tissue Engineering
Examiners: Professor Dr. Tech. Minna Kellomäki
M.Sc. Eng. Anne-Marie Haaparanta
Keywords: Tissue engineering, cartilage, scaffold, collagen, hyaluronic acid, chondroitin sulfate, freeze-drying, 1-ethyl-3-(3-dimethylaminopropyl)-carbodiimide hydrochloride, N-hydroxysuccinimide, genipin

Native cartilage has very little capacity for self-healing and even the current clinical methods have limited ability to regenerate functional cartilage. In the recent decade research related to cartilage repair has been increasingly focused on tissue engineering solutions that offer scaffold-based strategies for new cartilage formation. The combination of collagen (COL) with two glycosaminoglycans, chondroitin sulfate (CS) and hyaluronic acid (HA) has received widespread interest because all three are naturally abundant in the native cartilage tissue.

The objective of this thesis was to fabricate and characterize COL, HA and/or CS containing scaffolds applicable for cartilage tissue engineering. Porous 3D scaffolds were fabricated by freeze-drying and cross-linked with either 1-ethyl-3-(3-dimethylaminopropyl)-carbodiimide hydrochloride / N-hydroxysuccinimide (EDC/NHS) or genipin (GP). Fabricated COL+CS/HA and COL+CS+HA scaffolds were characterized by compression and water uptake testing, Fourier transform infrared (FTIR) spectroscopy and micro-computed tomography (micro-CT) imaging.

In general, the 80 wt.% COL containing composite scaffolds endured fabrication and both cross-linking procedures better than the 60 wt.% COL containing composite scaffolds. Water uptake ability was higher in GP cross-linked versus EDC/NHS cross-linked scaffolds, in the 80 wt.% COL containing versus 60 wt.% COL containing scaffolds and in COL+HA versus COL+CS composite scaffolds. The swelling/shrinkage upon water uptake of all of the scaffolds was below 20%; in most cases around 10%. FTIR spectra confirmed successful cross-linking with both GP and EDC/NHS and micro-CT images revealed highly porous microstructure (88-94%) with interconnected pores (pore sizes 26-57 µm) in all the scaffolds.

The dry scaffolds had significantly higher compressive modulus than the corresponding wet scaffolds; the difference being bigger with GP cross-linked scaffolds. In case of both dry and wet scaffolds the three highest compressive modulus values were measured from CS containing scaffolds. Two scaffold groups with the lowest compressive modulus contained COL and HA. Both wet and dry scaffolds recovered well from compression.

This thesis demonstrated successful incorporation of CS and/or HA to COL in order to fabricate a highly porous freeze-dried 3D scaffold applicable for cartilage TE. In addition, the novel crosslinker GP proved to be a promising alternative to the conventional EDC/NHS crosslinker.

PREFACE

This Master of Science thesis was conducted at the Tampere University of Technology, Department of Biomedical Engineering (Department of Electronics and Communications Engineering from January 1st, 2013).

I want to express my sincere gratitude to Professor Minna Kellomäki and M.Sc. Eng. Anne-Marie Haaparanta for making my graduation possible in such supportive and interesting way. Thank you for giving me the chance to work in a professional environment, trusting me and supporting me all the way from start to finish.

I also want to thank my fellow Master's Thesis workers for sharing their personal experiences with their work. Thanks are also in order for the staff and co-worker of the Department of Biomedical Engineering for making room for me and providing me such pleasant working environment. Last but not least, I want to thank my family and friends for reminding me to dance in the rain. Without your constant love and support this journey could not have been possible.

I want to dedicate my Master's Thesis to my loved ones but especially to my "camel boots" mother. Thank you for making me strong by always believing in me!

June 2015, Tampere

_____

Linda Urbański

TABLE OF CONTENT

ABBREVIATIONS

2D	Two-dimensional
3D	Three-dimensional
dH_2O	Distilled water
D2O	Heavy water
ADH	Adipic dihydrazide
AFM	Atomic force microscopy
BP	Benzophenone
BSA	Bovine serum albumin
CAD	Computer aided design
CDI	1,1-carbonyldiimidazole
Chi	Chitosan
CL	Cross-linking
CLer	Crosslinker
COL1 or COL2	Collagen type I or II
CS	Chondroitin sulfate
CS-A or C4S	Chondroitin sulfate type A or chondroitin-4-sulfate
CS-C or C6S	Chondroitin sulfate type C or chondroitin-6-sulfate
CS-E or C4,6S	Chondroitin sulfate type E or chondroitin-4,6-sulfate
CSMA	Chondroitin sulfate methacrylic anhydride
DCS	Differential scanning calorimetry
DHT	Dehydrothermal
DIW	Deionized water
DMEM	Dulbecco's modified Eagle's medium
DPBS	Dulbecco's PBS (see PBS)
ECM	Extracellular matrix
EDC	1-ethyl-3-(3-dimethylaminopropyl)-carbodiimide hydrochloride
EDGE	Ethylene glycol diglycidyl ether
ELN	Elastin
FD	Filter dried
GA	Glutaraldehyde
GAG	Glycosaminoglycan
Gel	Gelatin
GlcNAc	N-acetylglucosamine
GMHA	Glycidyl methacrylate-modifed hyaluronic acid
GP	Genipin
GTA	Glutaraldehyde
HA	Hyaluronic acid
HAMA	Hyaluronic acid methacrylic anhydride
HCl	Hydrocloric acid

HCPDE	Hollow-centered parallel disc electrode
IPN	Interpenetrating polymeric network
(h)MSC	(human) Mesenchymal stem cell
M_W	Molecular weight
NSC	Neural stem cell
NHS	N-hydroxysuccinimide
OA	Osteoarthritis
PBS	Phosphate buffered saline solution
PEM	Polyelectrolyte multilayer
PIC	Polyion complex
PU	Polyurethane
RT	Room temperature
T_d	Denaturation temperature
TE	Tissue engineering or tissue engineered
TEM	Transmission electron microscopy
TG	Thermogravimetric analysis
TIPS	Thermally induced phase separation
TPP	Two photon polymerization
SD	Standard deviation
(E)SEM	(Environmental) Scanning electron microscopy
SW	Soaking wet
WST	Water soluble tetrazolium
XPS	X-ray photoelectron spectroscopy
XRD	X-ray diffraction
UNS	Unspecified

DEFINITIONS

Bioabsorbable	Capable of being degraded or dissolved and subsequently metabolized within an organism.
Biocompatibility	The ability of a material to perform with an appropriate host response in a specific application, and the quality of not having toxic or injurious effects on biological systems.
Biodegradation	Gradual breakdown of a material mediated by specific biological activity or a biological system. Series of processes by which living systems render chemicals less noxious to the environment.
Biomaterial	Synthetic, natural or modified natural material intended to be in contact and interact with the biological system in order to evaluate, treat, augment or replace any tissue, organ or function of the body.
Biopolymer	Any polymer that is used as a biomaterial. (see polymer)
Biostability	The ability of a material to maintain its physical and chemical integrity after implantation in living tissue.
Blend	A uniform combination of two or more materials.
Buffer solution	Solution whose pH value is not appreciably changed by additions of acid or alkali.
Chondrocyte	Mature cartilage cell.
Chondrogenesis	A process by which cartilage tissue is formed.
Chondrogenic	Cartilage forming.
Composite material	Structural material made of two or more distinctly different materials, where each component contributes positively to the final properties.
Cross-linking	Formation of covalent side bonds between different chains in a polymer.
Cross-linking agent	Substance that is used as an initiator of the reaction that establishes cross-links between reactive sites in polymer chains.
Cytotoxic	Able to kill or damage cells.
Degradation	Deleterious change in the chemical structure, physical properties, or appearance of a material.
Denaturation	Destruction of the native conformation or state of a biological molecule by heat, extremes of pH, heavy metal ions, chaotropic agents etc., resulting in loss of biological activity.
Extracellular matrix	Matrix of proteins and glycoproteins surrounding cells in some tissues; located or occurring outside the cell.
Fibrous tissue	Form of connective-tissue consisting mainly of bundles of white fibres.

Hydrolysis	Chemical reaction of a compound with water.
Hydrophopic	Having an affinity for water.
Hydrophilic	Not readily absorbing or interacting with water.
in vitro	Literally, “in glass” or “test tube”, used to refer to processes that are carried outside the living body, usually in the laboratory.
in vivo	Within the living body.
Osteogenic	Bone forming.
Porogen	Any of a mass of particles (of a specified shape and size) used to make pores in molded structures used for tissue engineering (dissolved away after the structure has set).
Scaffold	A temporary supporting structure for growing cells and tissues; also called synthetic extracellular matrix.
Tissue engineering	Application of principles and methods of engineering and life sciences to the design, construction, modification, growth and maintenance of living tissues. Creation of devices for the study, restoration, modification and assembly of functional tissues from native or synthetic sources.

NOTATIONS

Table 1. Scaffold groups and their composition.

Notations of the test scaffold groups	Interpretation of the abbreviations
C100E	1.0 wt.% (v/v) COL; plain collagen scaffold, EDC/NHS cross-linked
C100G	1.0 wt.% (v/v) COL; plain collagen scaffold, genipin cross-linked
C80HE	1.0 wt.% (v/v) COL + 1.0 wt.% (m/v) HA | 80:20 wt.% (v/v); collagen-hyaluronic acid composite scaffold, EDC/NHS cross-linked
C80HG	1.0 wt.% (v/v) COL + 1.0 wt.% (m/v) HA | 80:20 wt.% (v/v); collagen-hyaluronic acid composite scaffold, genipin cross-linked
C60HE	1.0 wt.% (v/v) COL + 1.0 wt.% (m/v) HA | 60:40 wt.% (v/v); collagen-hyaluronic acid composite scaffold, EDC/NHS cross-linked
C80CSE	1.0 wt.% (v/v) COL + 1.0 wt.% (m/v) CS | 80:20 wt.% (v/v); collagen chondroitin sulfate composite scaffold, EDC/NHS cross-linked
C80CSG	1.0 wt.% (v/v) COL + 1.0 wt.% (m/v) CS | 80:20 wt.% (v/v); collagen-chondroitin sulfate composite scaffold, genipin cross-linked
C60CSE	1.0 wt.% (v/v) COL + 1.0 wt.% (m/v) CS | 60:40 wt.% (v/v); collagen-chondroitin sulfate composite scaffold, EDC/NHS cross-linked
C80CS15HE	1.0 wt.% (v/v) COL + 1.0 wt.% (m/v) CS + 1.0 wt.% (m/v) HA | 80:15:5 wt.% (v/v); collagen-chondroitin sulfate-hyaluronic acid composite scaffold, EDC/NHS cross-linked
C80CS15HG	1.0 wt.% (v/v) COL + 1.0 wt.% (m/v) CS + 1.0 wt.% (m/v) HA | 80:15:5 wt.% (v/v); collagen-chondroitin sulfate-hyaluronic acid composite scaffold, genipin cross-linked
C60CS30HE	1.0 wt.% (v/v) COL + 1.0 wt.% (m/v) CS + 1.0 wt.% (m/v) HA | 60:30:10 wt.% (v/v); collagen-chondroitin sulfate-hyaluronic acid composite scaffold, EDC/NHS cross-linked

1 INTRODUCTION

Cartilage reconstruction has become an important topic in modern medicine for both functional and esthetic surgery [104]. The need for treatments options is strongly associated with the fact that native cartilage is a hypocellular, avascular and not innervated tissue and thus heals poorly [133]. Osteoarthritis (OA) is a common joint disorder that progressively leads to the loss of cartilage. In addition, injuries to the articular cartilage tissue can occur through various mechanisms. Most common injury is a blunt trauma (caused by e.g. a car accident or a fall from a height) that breaks piece of cartilage from the end of the bone. [28] After such traumas, articular cartilage often remains unhealed due to incomplete bonding of the fractured surfaces [27]. Since current clinical methods have limited ability to regenerate functional cartilage [111], especially OA has become a major socio-economic burden [66]. In recent years, the cartilage repair-related research has focused on tissue engineering solutions that provide templates (scaffolds) to fill the tissue lesion, and ultimately form new cartilage [130].

Scaffolds intended for cartilage regeneration have many requirements, including adequate nutrient and waste transport, adhesion to the defect site, minimally invasive implantation or injection, biocompatibility and biodegradability [60]. A temporary three-dimensional (3D) scaffold mimics the physiological properties and functions of the cartilage extracellular matrix (ECM) [111] enabling a microenvironment that can induce chondrocytes into appropriate differentiation and functional state under *in vitro* conditions [64]. Furthermore, one of the most important criteria that ultimately leads to the success or failure of the scaffold is its ability to provide structural support during new tissue formation [111].

In terms of choosing a suitable material for a cartilage scaffold, it is favorable to design a scaffold based on the natural cartilage composition. Cartilage matrix is a gel-like substance composed of water and the macromolecular polyanionic substances (proteoglycans and collagen). Proteoglycans are elastic molecules that expand in solution and strongly resist compression into a smaller volume. In the cartilage matrix, proteoglycans are arranged in high-molecular-weight aggregates formed by noncovalent association between proteoglycan subunits (hyaluronic acid and a linkage protein, collagen). Glycosaminoglycans, from which chondroitin sulfate is the prominent one, are attached to the collagen core or backbone. [84] Given the nature and composition of native cartilage, combination of collagen with chondroitin sulfate and/or hyaluronic acid have received a deserved and widespread interest in the field of cartilage tissue engineering [6]. In fact, modification of collagen scaffolds by chondroitin sulfate and hyaluronic acid has been

proposed to enhance chondrocyte differentiation into better cartilage and to provide the necessary molecules for cell attachment [64].

The aim of this thesis was to fabricate and characterize porous freeze-dried 3D composite scaffolds with different amounts (wt.%) of collagen I, chondroitin sulfate and hyaluronic acid that mimic the native cartilage composition. The scaffolds were evaluated in terms of applicability for cartilage reconstruction as well as keeping in mind the basic requirements of a porous 3D tissue engineering scaffold. The theoretical background gives an overview of the basic material properties of collagen, hyaluronic acid and chondroitin sulfate as well as their use in tissue engineering. It also provides basic information concerning the two cross-linking agents used in the present study; 1-ethyl-3-(3-dimethylaminopropyl)-carbodiimide hydrochloride / N-hydroxysuccinimide (EDC/NHS) and genipin. Different processing methods for porous scaffold fabrication are also presented; focus being on freeze-drying, the method used for manufacturing the scaffolds in this work.

The scaffolds were fabricated by freeze-drying and cross-linked with EDC/NHS or genipin. To study the effects between EDC/NHS and genipin cross-linking as well as the different collagen, hyaluronic acid and/or chondroitin sulfate compositions, the compression properties, recovery from compression, water uptake and swelling of the scaffolds were investigated. The compressive modulus and compressive stiffness values were determined separately for dry and wet scaffolds. The water uptake and swelling abilities of the scaffolds were evaluated after immersion in PBS (37ºC) for 24 hours. The dimensional changes of the scaffolds were investigated in connection with water uptake and compression (i.e. recovery after the compression) tests. Fourier transform infrared (FTIR) spectroscopy was used to analyze the cross-linking treatments and micro-computer tomography (micro-CT) imaging to study the microstructure of the scaffolds.

2 BIOABSORBABLE NATURAL POLYMERS

2.1 Collagen

Collagen is a ubiquitous protein in mammalian tissues, accounting around 20-30% of total body proteins [72]. For most soft and hard connective tissues, collagen fibrils and their networks function as the ECM (i.e. highly organized, 3D architecture surrounding various cells) [12]. It prevails in the ECM of skin, cartilage, bone, tendon and ligaments and forms the structural framework of tissues like cornea and blood vessels [68]. Fibroblasts are responsible for the production of most collagens in connective tissue [104].

The basic unit of collagen is a polypeptide composed of repeating sequence of three amino acids: glycine, proline and hydroxyproline [68]. There exists over 20 genetically different collagen molecules with varying abundance, functionality and distributions in tissues [141]. The most abundant and widespread group of collagens are the fibril-forming collagens (types I, II, III, V, XI), which comprise about 90% of the total collagen content in tissues [32]. Their distinctive feature is high tensile strength [33]. Different collagen types are listed in Table 2.1 according to their family and tissue distribution. For instance, bone tissues are mainly constructed from type I and V collagens that form a framework anchoring nano-sized hydroxyapatite crystals. In cartilage type II collagen is the main component, accounting approximately 60% of the dry weight of the tissue. Other collagen types found in cartilage are VI, IX and XI collagens and even trace amounts of type I collagen can be detected in it. Type II, IX, and XI collagens form a fibrillar network that gives the cartilage tissue tensile stiffness and strength. Type VI collagen forms part of the cartilage matrix that immediately surrounds the chondrocytes and may help the chondrocytes to attach to the macromolecular framework of the matrix. [8]

Table 2.1. *Various collagen types divided into individual families according to their distinctive features and tissue distribution. Modified from [32].*

Family and type	Tissue distribution
Fibril-forming collagens	
I	bone, dermis, tendon, ligaments, cornea
II	cartilage, vitreous body, nucleus pulposus
III	skin, vessel wall, reticular fibers in most tissues (lungs, liver, spleen etc.)
V	lung, cornea, bone, fetal membranes; together with type I collagen
XI	cartilage, vitreous body
Basement membrane collagens	
IV	basement membranes
Microfibrillar collagens	
VI	widespread: dermis, cartilage, placenta, lungs, vessel wall, intervertebral disc
Anchoring fibrils	
VII	skin, dermal– epidermal junctions; oral mucosa, cervix
Hexagonal network-forming collagens	
VIII	endothelial cells, Descemet's membrane
X	hypertrophic cartilage
FACIT collagens	
IX	cartilage, vitreous humor, cornea
XII	perichondrium, ligaments, tendon
XIV	dermis, tendon, vessel wall, placenta, lungs, liver
XIX	human rhabdomyosarcoma
XX	corneal epithelium, embryonic skin, sternal cartilage, tendon
XXI	blood vessel wall
Transmembrane collagens	
XIII	epidermis, hair follicle, endomysium, intestine, chondrocytes, lungs, liver
XVII	dermal-epidermal junctions
Multiplexins	
XV	fibroblasts, smooth muscle cells, kidney, pancreas
XVI	fibroblasts, amnion, keratinocytes
XVIII	lungs, liver

Despite the vast diversity of structurally different collagen molecules, all members have one common characteristic feature: three left-handed polypeptide α-chains wrapped around each other forming a right-handed triple helix (procollagen) [32, 72]. A procollagen peptidase removes loose termini to create a tropocollagen molecule. Tropocollagen molecules then self-assemble to microfibrils that further bundle up as collagen fibrils. These growing fibrils finally self-assemble to form a collagen fiber. [38] Each collagen molecules has a molecular weight of approximately 300 kiloDaltons [72] and each individual polypeptide chain of collagen contains approximately 1000 amino acid residues [92]. The pre-described process of the collagen assembly is shown in Figure 2.1 (a). Figure 2.1 (b) illustrates the collagen structure from a tropocollagen helix to the form of a collagen fiber.

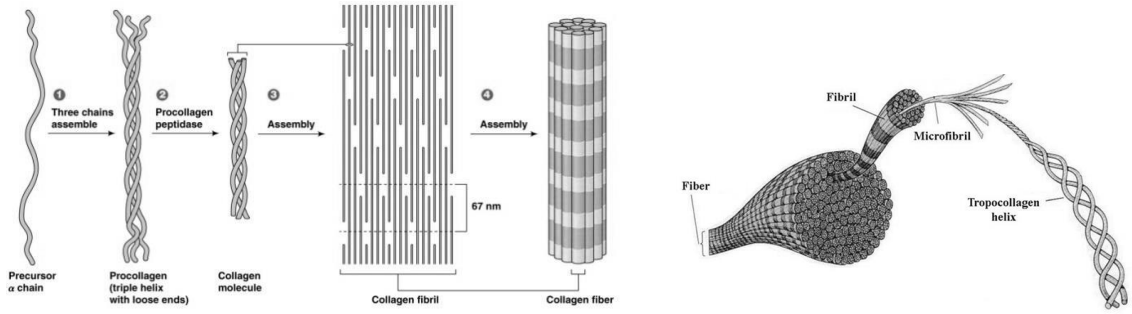

(a) (b)

Figure 2.1. *The collagen self-assembly (a) and the structure of collagen from tropocollagen to a collagen fiber (b). Modified from [121, 38].*

There are approximately 25 different α-chain conformations, each of which is produced by their unique gene [104]. The triple helix structure is important to the nature of collagen, since it protects its integrity against proteases and plays an important role in cell adhesion and the assembly of the ECM [20]. Additionally, the ability of the polypeptide strands to self-aggregate enables stable fibers formation in the physiological condition and thus provides mechanical support [147].

Collagen has numerous structural and functional roles depending on the tissue where it is located in. It induces important events in the cell microenvironment and is involved in the storage and release of cell mediators, such as growth factors. [33] Cell-matrix interactions are induced mostly by the interaction of cells with collagen, either directly or indirectly. Direct cell-collagen interactions imply cell receptors that recognize specific peptide sequence located within the collagen molecule. The indirect interactions between cells and collagen are normally the ones that achieve stable adhesion of cell to the ECM. [104] The ability to withstand tensile loads is directly related to the fibrous nature [68] and the intramolecular crosslinks of collagen [46]. Collagen plays a dominant role in maintaining the biologic and structural integrity of vertebrates and other organisms [33, 12]. It is highly dynamic molecule that undergoes constant remodeling for proper physiologic functions [12].

2.2 Hyaluronic acid

Hyaluronic acid (also known as hyaluronan or hyaluronate [120]) is a highly hydrophilic polysaccharide [30] and a major intracellular component of connective tissues [19]. It was first discovered and isolated in 1934 from the vitreous body of the eye. However, it was not until 20 years later that its structure was completely determined. [39] Hyaluronic acid is a non-sulfated linear polymer that is homogenous in its primary structure [29]. It is composed of repeating disaccharide units, ß-1,4-D-glucuronic acid and ß-1,3-N-acetyl-D-glucosamine (Figure 2.2). Hyaluronic acid is chemically classified to the family of glycosaminoglycans (GAGs). [39] It is considerably larger compared to the other GAGs [29] with a molecular weight of 1000-10^4 kiloDaltons [30]. Hyaluronic acid is widely distributed component in the ECM of vertebrate's tissues. Its pronounced viscoelastic properties and the biophysical basis (related to its 'non-ideal' behavior) have made hyaluronic acid a source of great interest and speculation. [39]

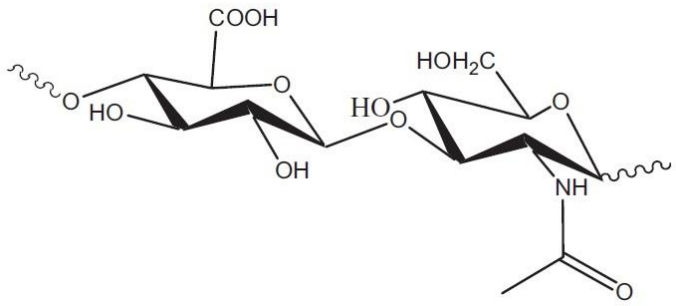

Figure 2.2. *Chemical structure of hyaluronic acid. [97]*

After the early work of researchers Laurent (1955) and Balazs (1970), it was concluded that hyaluronic acid chains behave as a stiffened random coil in solution. In recent years this relative simple model has been challenged by proposing that hyaluronic acid chains self-associate, and thereby dominate the solution properties. The abundant data found in the current literature suggests that hyaluronic acid chains do not strongly self-associate in aqueous solution, but their self-association might be very weak and transient and contribute to the so-called 'non-ideal' behavior. Today, based on the bulk solution properties hyaluronic acid is in fact best described as a random coil with considerable internal stiffness; attributed to direct or water-mediated intramolecular hydrogen-bonding pattern across the glycosidic linkages. The conformation of the individual saccharide units in hyaluronic acid is an important factor that contributes to the overall shape of the molecule. Both glucuronic acid and the N-acetylglucosamine moieties appear to exits mainly in chair forms, which limits the flexibility of the molecule. However, the conformation of hyaluronic acid has been shown to vary due to the binding of proteins. [39]

Since its initial isolation, the physical properties of hyaluronic acid have been the dominant feature that distinguish it from other ECM components. In addition to not being covalently bound to proteins of any tissue, hyaluronic acid is the only non-sulfated GAG. However, specific hyaluronic acid-protein interactions have been shown; foremost the

association with CD44 antigen (a cell-surface glycoprotein). [39] Hyaluronic acid is an important component of native ECM and most tissues including synovial fluids of joints, skin and articular cartilage [6, 98]. This ubiquitous polyanion is also responsible for several structural and biological properties that mediate cellular signaling, cell growth and differentiation, morphogenesis and matrix organization [109]. In addition, hyaluronic acid has an essential role in wound repair [109], in controlling tissue permeation and hydration, in macromolecular transport between cells and in bacterial invasiveness [39]. While numerous investigations have focused on the extracellular roles of hyaluronic acid, there is a growing interest towards its putative intracellular roles. Hyaluronic acid has been suggested to contribute in cell cycle. It may also modulate the trafficking of specific kinases in the cell and thereby regulate cell behavior. [39]

Hyaluronic acid plays an important role in regulating the water and electrolyte balance of tissues [113]. Compared to other ECM molecules, hyaluronic acid has unique hygroscopic, rheological and viscoelastic properties. When not bound to other molecules, it has the ability to self-associate into 3D structures in solutions and bind up to 1000 times its weight in water, which gives it a stiff viscous quality similar to gel-like gelatin [49, 97, 30]. The hydrophilic nature of hyaluronic acid creates an environment permissive for migration of cells to new tissue sites, while its free-radical scavenging and protein exclusion properties offer protection to cells and ECM molecules against free-radical and proteolytic damage [6]. Other unique properties of hyaluronic acid are its ability to promote angiogenesis and modulate wound site inflammation. It is recognized by receptors on a number of different cells associated with tissue repair. It promotes mesenchymal and epithelial cell migration and differentiation, and thereby enhances collagen deposition alongside with angiogenesis. [97]

2.3 Chondroitin sulfate

Chondroitin sulfate (also known as chondroitin, chonsurid or chondroitin sulfuric acid [15]) is another representative of the GAG family. The natural abundance and wide distribution of chondroitin sulfate in all living creatures apart from plants reflect its central role in biological processes. [70] Chondroitin sulfate is the prevalent GAG in the articular cartilage [97], varying from 20 to 80% of its total GAG content [147]. Structurally this linear polymer comprises of repeating disaccharide units of D-glucuronic acid and N-acetyl-D-galactosamine (GalNac) with a molecular weight of 50-100 kiloDaltons [9, 54]. Other than containing 25-30 such units in the average chain, chondroitin sulfate does not have a uniform structure. Naturally occurring modifications of chondroitin are a result of varying sulfate residue distribution along the chains. The classification and type of chondroitin sulfate is determined by the sulfate group placing: most commonly located in carbon 4 (CS-A or C4S), carbon 6 (CS-C or C6S) or in both 4 and 6 carbons (CS-E or C4, 6S). [139] CS-B is no longer classified as a form of chondroitin sulfate, since it later turned out to be a fellow GAG called dermatan sulfate [91]. The changes in terminology with time are due to the fact that chondroitin sulfate was originally isolated well before

its structure was characterized. Early scientists used letters as nomenclature. [76] Later also numbers have been used to indicate the sulfate group including carbon unit [91]. The different types of chondroitin sulfate are presented in Table 2.2.

Table 2.2. *Different types of chondroitin sulfate and their nomenclature. Modified from [91].*

Letter identification	Site of sulfation	Systematic name	Number identification
CS-A	carbon 4 of the GalNAc sugar	chondroitin-4-sulfate	C4S
CS-C	carbon 6 of the GalNAc sugar	chondroitin-6-sulfate	C6S
CS-D	carbon 2 of the glucuronic acid and 6 of the GalNAc sugar	chondroitin-2,6-sulfate	C2,6S
CS-E	carbons 4 and 6 of the GalNAc sugar	chondroitin-4,6-sulfate	C4,6S

Most abundant variations of chondroitin sulfate found in the joint tissue are C4S and C6S [66]. Their chemical structures are shown in Figure 2.3.

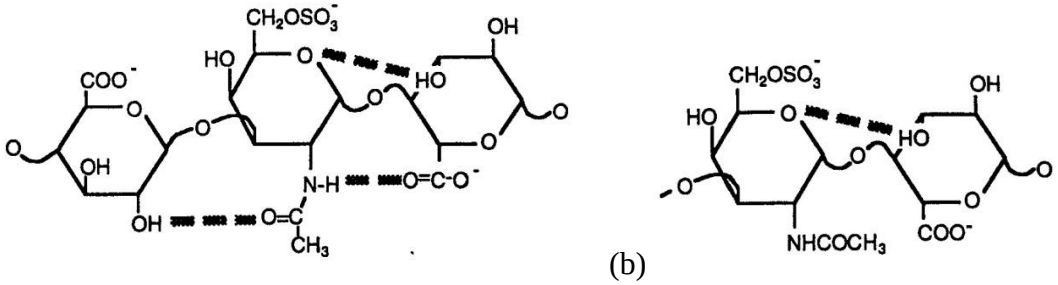

(a) (b)

Figure 2.3. *Chemical structure of (a) chondroitin 4-sulphate and (b) chondroitin 6-sulphate [23].*

The composition and concentration of chondroitin sulfate depends on the function of the relevant organism and tissue [93]. It is found mostly in large aggregating proteoglycans (PGs) with 20-100 GAG chains of 15-70 kiloDaltons [29]. Chondroitin sulfate is a major component in the ECM of connective tissue [62]. It is present both in cancellous and compact bones [115], tendon and ligaments [79]. But more importantly, chondroitin sulfate is the key constituent of aggrecan (cartilage-specific proteoglycan protein) [62], shown in Figure 2.4. Chondroitin sulfate plays an important role in cartilage by regulating the expression of the chondrocyte phenotype and stimulating the metabolic response of cartilage tissue. Most importantly, chondroitin sulfate plays a major role in creating osmotic pressure that expands the matrix and places the collagen network under tension. This creates water-trapping system of PGs that absorbs compression while moving. [62]

This is explained more specifically in the next paragraph alongside with the structure of native cartilage (Figure 2.4).

Cartilage matrix is a gel-like substance. Its abundant ECM surrounds chondrocytes and is composed of water and the macromolecular polyanionic substances, i.e. PGs and collagen. [79] Collagen fibrils form the framework of articular cartilage and help it to resist tensile stress [93]. PGs consist of a protein core or backbone that has side chains of chondroitin and keratin sulfate attached to it. Because of their repelling negative charges, chondroitin sulfate side chains are attached to a protein core at nearly right angles [79]. In the cartilage matrix PGs are arranged in high-molecular-weight aggrecans formed by noncovalent association between PG subunits, hyaluronic acid and linkage protein. PGs are elastic molecules that expand in solution exerting a swelling pressure to the tissue. [79] They strongly resist compression into a smaller volume by being constantly restrained by the collagen network in which they are entrapped [93, 79]. Small PGs, such as decorin, biglycan and fibromodulin, bind to other matrix macromolecules and thereby help to stabilize the matrix. They may also bind growth factors and influence the function of the chondrocytes. [8] Together the collagen framework and the PGs give the cartilage matrix its unique load-bearing properties [70]. Figure 2.4 shows an illustrative presentation of the cartilage matrix.

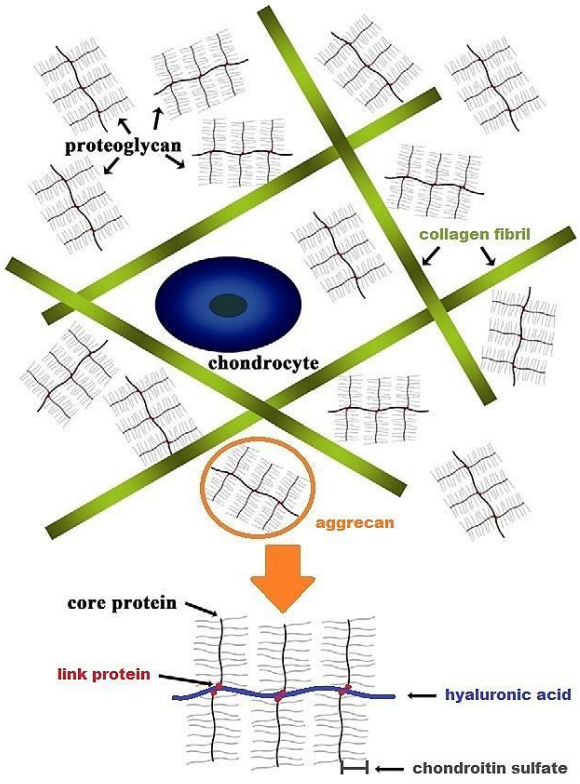

Figure 2.4. *Schematic presentation of cartilage structure. Modified from [66].*

Chondroitin sulfate was first identified as a component of cartilage in 1940, and since the 1980s its effectiveness has been continuously investigated. [133] The best described function is its structural role within cartilage [70]. In cartilage, multiple chondroitin sulfate

including aggrecan molecules bind to hyaluronic acid via a protein link and form large aggregated proteoglycans (PGs) that carry a negative charge and therefore attract cations. This phenomenon increases the osmolality, which in turn draws water into the ECM resulting in resistance towards compression stress. [133] Chondroitin sulfate helps to maintain healthy cartilage by absorbing fluid (particularly water) into the connective tissue. Supposedly it also blocks enzymes that break down cartilage and provides the building blocks for the body to produce new cartilage. [15]

Other than its roles within cartilage, chondroitin sulfate has important biological functions in the development of brain [145]. It possess anti-inflammatory activity [54] and is known to involve in intracellular signaling, cell recognition and connecting ECM components to cell-surface glycoproteins. Furthermore, chondroitin sulfate has been reported to involve in a process of long bone growth (endochondral ossification). [62]

3 THE USE OF NATURAL POLYMERS IN TISSUE ENGINEERING

After a century of developing synthetic polymers, scientists are turning back towards the usage of natural polymers [60]. In general, the use of natural polymers for tissue engineering applications is a beneficial choice due to their excellent biocompatibility and because their structures mimic closely native cellular environments. Moreover, natural polymers have unique mechanical properties, and are biodegraded by an enzymatic or hydrolytic mechanism. [98] For cartilage tissue engineering natural biomaterials are commonly used due to their abundant availability because they possess many intrinsic prochondrogenic properties and are commonly involved in native cellular processes [60]. Hyaluronic acid and chondroitin sulfate are the most valued GAGs in the market because of their prevalence in mammalian tissues, beneficial biological and physiological functions such as high bioactivity [139].

The wide distribution in nature, natural biocompatibility and biodegradation make their use as biomaterials beneficial as well as practical. However, while some of the characteristics of natural polymers are considered as remarkable advantages, some of them may also restrict their use. In most cases, poor mechanical strength and relatively fast degradation constrain natural biomaterial design. Usually these problems are overcome by different cross-linking treatments, combining mechanically stronger materials with weaker ones, adding fibers to the structure etc. [33] The following chapters give insight into the applications of collagen, hyaluronic acid and chondroitin sulfate in tissue engineering, as individual biomaterials as well as composite scaffolds. Given the nature and composition of the ECM architecture of native cartilage, together collagen, hyaluronic acid and chondroitin sulfate could well be a promising composite material designed especially for cartilage tissue engineering purposes.

3.1 Collagen in tissue engineering

Collagens, the oldest and most well understood class of biomaterials [141] have shown superior advantages not only as a scaffold material in tissue engineering, but also as a coating material for implants [23]. Its well-understood structure, low antigenicity and remarkable biochemical and physical properties have made it widely used biomaterial in a variety of applications [141, 72] from injectable collagen matrices to bone regeneration scaffolds [104]. Scientific investigations involving collagen have inspired tissue engineering, since collagen fibrils and their networks primarily regulate and define most tissues. The collagen networks form a highly organized 3D architecture that entraps other ingredients. [12]

The tissue engineering applications exploiting collagen as a biomaterial have been intensively growing in the past decades. The fact that it is easily available and highly

versatile makes it an attractive choice. Major advantages of collagen as a biomaterial include its synergy with bioactive components, easy modifiability and abilities to promote blood coagulation. Collagen can be processed into numerous different structures and shapes such as sponges, fibers, films, 3D gels, fleeces and beads without harming the basic molecule structure. In tissue engineering it has been used for skin replacement, bone substitutes and artificial blood vessels and valves. [72] Collagen is a naturally occurring abundant protein within native cartilage, where it induces intrinsic cell-binding motifs and enzyme-specific degradation [60]. Fibril-forming collagens are the most commonly used in the production of collagen-based biomaterials, from which type I collagen is currently the gold standard in the field of tissue engineering [104].

Collagen possesses also some major disadvantages that limit or complicate more or less its clinical use. Collagen has relatively weak mechanical endurance and thermal stability, due to its protein nature [46, 33]. In addition, all collagens are very soft and can contract during culture [60], which makes it difficult to sterilize them without altering their structure [104]. Isolated collagens have various cross-link densities, fiber sizes, trace impurities etc. and in addition they bear the risk of viral infection such as bovine spongiform encephalopathy (BSE) [33, 72]. The hydrophilicity of collagen does not only lead to e.g. swelling and rapid release of incorporated drugs but results also in its fast degradation [72]. In some cases the use of biological materials for medical applications can trigger an immune response in patients. Type I collagen has, nonetheless been regarded as a suitable material for implantation, since only a small amount of people possess humoral immunity against it and a simple allergic test can verify patient's response to the biomaterials based on this type of collagen. [104]

Collagen, being the most abundant proteins on earth can be extracted from almost every living animal [104]. Desired collagens can be isolated from tissues that are rich in the relevant collagen type. An extraction of isolated collagen triple helices has been referred to as ''monomeric'', whereas extracted collagen with a retained fibrillar structure have been referred to as ''polymeric''. [128] Currently the majority of industrial collagens are extracted from animal derivatives such as porcine, calf and bovine skin, bovine tendon and rat tail [72].

Collagen constitutes over 30% of total body proteins of mammalian tissues, which makes it abundant and easily purified from living organisms [72]. However, animal-derived collagen raises concerns over the possible transmission of infectious agents. Therefore complementary alternatives, such as recombinant collagens are also used and studied. Compared to animal-derived collagens, the recombinant sources of human collagen (rhC) provide more reliable, predictable and chemically defined source of collagens. [33] Today, in addition to animal-derived collagens, the recombinant collagens are acknowledged as one of the most useful biomaterials available and currently widely used in the field of tissue engineering, cosmetic surgery and drug delivery systems [12]. For example, a company called Fibrogen® have been distributing recombinant human collagen since 2004. Their product is marketed potentially less immunogenic than animal sources and

their different production lots identical in composition. Products like this may well be paving the way for the future of collagen scaffolds. [104]

Another area of research is the development of artificial collagen-like materials. As an example, Paramonov et al. [103] have prepared collagenous peptide polymers using native chemical ligation techniques; more precisely by a solid phase peptide synthesis, polymerization and self-assembly. Their product is presented as a mesh of nanofibers that resembles natural collagen fibrils by maintaining the characteristic circular dichroism signal for collagen triple helices. [103]

3.2 Hyaluronic acid in tissue engineering

Hyaluronic acid and its derivatives (both in solution and hydrogel form have) shown a great promise as a biomaterial in many medical products for over three decades [9]. Its ability to maintain hydrated environment is ideal for cell infiltration [19]. Applications range from various areas of tissue culture scaffolds to cosmetic surgery [109]. Soluble hyaluronic acid has been used in ocular surgery, viscosupplementation for arthritis and wound repair. However, its poor mechanical properties and rapid degradation *in vivo* hinder its direct clinical use. [26]

For the past decade hyaluronic acid has been used as an important building block for the creation of new biomaterials for the use in cell therapy and 3D tissue culture scaffolds [109]. Its abilities to act as a space filler and a lubricant for movable parts of the body, makes hyaluronic acid one of the most beneficial research subjects particularly in the fields of orthopedics [49]. Furthermore, hyaluronic acid is known to bind to specific proteins called hyaladherins, found in the ECM and on the cell surface, which stabilize especially the cartilage matrix and mediate cell adhesion and motility, cellular proliferation, cancer metastasis and inflammation [110, 118].

The fact that hyaluronic acid enhances collagen deposition and angiogenesis by promoting mesenchymal epithelial cell migration and differentiation, in addition to its immunoneutrality, makes it an ideal biomaterial for tissue engineering and drug delivery applications. Also, its water solubility allows hyaluronic acid to be fabricated into various types of porous and 3D structures. [97] However, its water solubility and fast resorption also preclude its use in many medical applications [33]. For particular tissue engineering purposes, hyaluronic acid is too weak and fluid as a homopolymer to create a supportive scaffold [134]. It needs to be hydrophobically modified or chemically cross-linked to gain better chemical and mechanical stability [118]. Due to the high functionality and charge density of hyaluronic acid, it can be cross-linked with a variety of chemical and physical methods [97]. Chemical modifications of hyaluronic acid target three functional groups: the glucuronic acid carboxylic acid, the primary and secondary hydroxyl groups and the N-acetyl group [6]. Chemically modified HA can be transformed into numerous physical forms without loss of biocompatibility [6] and has been proven to reduce significantly the degradation rate of the polymer [97]. These forms include viscoelastic solutions, soft or

stiff hydrogels, nanoparticulate fluids, electrospun fibers, non-woven meshes, powder, macroporous and fibrillar sponges, flexible sheets and films [9].

Hyaluronic acid has been studied and used extensively as a hydrogel in numerous biomedical applications. In many occasions hyaluronic acid hydrogel is designed for encapsulation and delivery of cells, drugs or molecules like growth factors and DNA. Similar designs have also been exploited to produce tumor models, where cancer cells are encapsulated and injected *in vivo*; introducing a "tumor engineering" strategy for creation of orthopedic xenografts. Various modifications of hyaluronic acid enable the fabrication of stable and enzymatically degradable hydrogels, including aldehyde-modified hyaluronic acid, tyramine-modified hyaluronic acid, dihydrazide-modified hyaluronic acid etc. [9] In one study the researchers fabricated collagen-hyaluronic acid composite hydrogels for DNA delivery by cross-linking hyaluronic acid with poly(ethylene glycol) diglycidyl ether [116]. Moreover, hyaluronic acid-based materials have replaced collagen-based materials as the standard soft tissue filler [28].

Hyaluronic acid can be extracted from natural mammalian sources of vitreous body, synovial fluid, umbilical cord and rooster comb [111]. Marine wastes have also been explored in search of new sources of hyaluronic acid. So far it has been found in the vitreous humor of various fish species and in cartilage of chondrichthyes. [139] Other sources for extraction have been certain strains of *streptococci* [71]. Since 2007 the usage of bioprocess methods for hyaluronic acid synthesis has gained interest and in 2011 the first animal-free (recombinant) hyaluronate was synthesized with *Bacillius subtilis* by a company called Novozymes [97, 134]. Since 2012 hyaluronic acid has been extracted from *Streptococci bacteria* through fermentation to eliminate the possibility of transferring interspecies diseases. The production of hyaluronic acid through fermentation has gradually been replacing the hyaluronic acid obtained from animal origin. [19] In terms of microbial production of hyaluronic acid, several culture variables have been studied and optimized. These include e.g. lysozyme or hyaluronidase addition, agitation and aeration conditions, the type of bioreactor, effect of pH-gradient stress, continuous culture, medium optimization and fed-batch operation. [139]

3.3 Chondroitin sulfate in tissue engineering

Chondroitin sulfate is another human carbohydrate that has shown promise as a nontoxic and biocompatible biomaterial [134, 56]. Scientists have been particularly interested in its anti-inflammatory properties, ability to reduce pain and improve articular functions [54]. Chondroitin sulfate has also been widely used to treat OA by oral dosing [62]. In some studies, chondroitin supplements have shown to decrease the pain associated with OA. However, not all studies are positive. In fact, several of them have not shown any beneficial effect from taking chondroitin. It is not clear, why the studies have different results, and therefore experts disagree on whether chondroitin is indeed helpful in treating OA or not. [135] Other applications include its use against psoriasis and atherosclerosis [54], bladder conditions [135] and high cholesterol [62]. It has also been suggested to

affect positively on Alzheimer's disease, heart disease and weak bones (osteoporosis). However, so far there have not been any studies to evaluate these claims. [135]

Chondroitin sulfate can also be found in cosmetics, eye drops and creams [70] and it can be used as dietary supplements; most of them made from cow cartilage. As an example of a commercialized dietary supplement is BioCell Collagen®, where chondroitin sulfate is mixed together with collagen and hyaluronic acid. It provides nutrients essential for maintaining cartilage, tendon and ligament connective tissue health, and has clinically shown to improve joint comfort and mobility. [6] The central role of chondroitin sulfate in natural wound healing and chondrogenesis has made it also a subject of extensive research as a hydrogel for wound dressings and cartilage tissue engineering scaffolds [134].

The number of commercial applications of chondroitin sulfate has continuously been increased due to its high biocompatibility [139] and its central role in natural wound healing and chondrogenesis [134]. Similar to hyaluronic acid, several chemical and physical cross-linking techniques have been developed for chondroitin sulfate to form hydrogels for biomedical applications [97]. When included in hydrogels, chondroitin sulfate participates in re-epithelialization, stimulation of neovascularization and supply of growth factors and cytokines. Its combination with other biopolymers, such as collagen, PGs and hyaluronic acid in order to formulate scaffolds with slow and controlled biodegradability that promote and accelerate the regeneration of damaged structures has been studied mainly in the engineering of biological tissues associated with the processes of bone repair, cartilage and cutaneous wound. [139]

Many studies have reported chondroitin sulfate having the ability to stimulate and promote significantly the bioactivity of seeded chondrocytes [97]. *In vitro* studies suggest that chondroitin sulfate can impact processes associated with cartilage degeneration by promoting synthesis of proteoglycans, which are lost during cartilage degeneration, reducing gene expression for a range of proteolytic enzymes and reducing subchondral bone resorption in combination with glucosamine [70]. Recent studies have demonstrated that CS-E is a potent antiviral, whereas chondroitin sulfate-PG is a potential target for the development of vaccines against malaria. In addition, there have been reports of new findings concerning the sulfation pattern of chondroitin sulfate and its relation to cancer cell mechanisms. [139]

Currently the route of chondroitin sulfate administration is oral and the most successful commercial products of chondroitin sulfate by market volume still remain associated with OA. The effectiveness of chondroitin sulfate for the treatment of OA has been evident through three main mechanisms: 1) stimulation of ECM production by chondrocytes; 2) suppression of inflammatory mediators; and 3) inhibition of cartilage degeneration. [66] In the field of cartilage tissue engineering many researches aim to discover, whether tissue engineering scaffolds can provide similar advantages. An example of exploiting the bioactive abilities of chondroitin sulfate for a tissue engineering application is a study by Kangjian et al. [56], in which they created a collagen-chitosan-chondroitin sulfate scaffold. Chondroitin sulfate was added to the composite construct in order to provide the

biological activity of polysaccharides and to further improve scaffold's stability and biocompatibility [56].

Chondroitin sulfate has also shown promise in bone tissue engineering. Schneiders et al. [114] demonstrated in their study that the addition of chondroitin sulfate to hyaluronic acid/collagen composites enhances bone remodeling and new bone formation. Chondroitin has shown to influence directly on the osteogenetic differentiation of human mesenchymal stem cells (MSC) and osteogenesis *in vivo* through functional groups (sulphate, carboxyl) that interact with mineral components of bone such as hydroxyapatite. This makes the addition of chondroitin sulfate to bone substitutes an attractive choice in order to increase their osteoconductive properties. [115]

There are several reported sources for the isolation of chondroitin sulfate. Commercial chondroitin sulfate can be extracted from mammalian derivatives such as nasal and trachea from bovine and swine. [139] Other natural sources from chondroitin are marine substrates from shark cartilage [70], ray [139] and sea cucumber [62]. Chondroitin sulfate derived from fish is as a better source than mammalian because of its sulfation pattern and safety [139]. The source organism and tissue, location within a tissue as well as age affect chondroitin sulfate structure, which in turn affects its function *in vivo*. The different molecular functions of chondroitin sulfate offer potential for different therapeutic impacts. Clinical studies of commercial chondroitin have all confirmed the safety of chondroitin sulfate as a nontoxic and biocompatible biomaterial, regardless of its origin. [70, 66] Nevertheless, due to concerns over the BSE disease and other food chain crisis, search for other alternative sources for the isolation of chondroitin sulfate continues. The exploration of micro-organisms and marine organisms as a source material has received increasing attention. [139]

The types of applications for the formulations of chondroitin sulfate or its derivatives, and thus their market price are dependent on the concentration and purity of this GAG in the commercial products. Different compounds, including chemical solvents and detergents from the isolation step as well as peptides, proteins, nucleic acids or organic compounds from tissues commonly contaminate the scaffolds and therefore reduce its commercial value and limit its usage areas. Clinical applications demand highly concentrated and pure chondroitin sulfate compared to cosmetic, dietary supplements or other food ingredients. In general, the methods for the isolation of chondroitin sulfate from cartilage include following steps (defined during several years): (1) chemical hydrolysis of cartilage; (2) breakdown of proteoglycan core; (3) elimination of proteins and chondroitin sulfate recovery; and (4) purification of chondroitin. [139]

In order to avoid the health and ecological problems caused by the use of mammalian and fishery wastes as a substrate, different approximations to microbial production of chondroitin sulfate-like polymers have been reported in recent years. Initially, *Pasteurella multocida* was one of the bacteria selected as a chondroitin sulfate producer, but its well-known cholera pathogenicity has hindered and reduced its interest. Excellent results have been obtained in the production of capsular polysaccharide chondroitin sulfate precursor (CS-C) by *Escherichia coli*. However, *E. coli* is a low virulent pathogen, which limits its

large scale production. Moreover, CS-C is a non-sulfated structure of chondroitin (CS-O) with a furanose residue of fructose, which needs a subsequent step of chemical sulfation and hydrolysis of the fructose monomer. Nevertheless, chondroitin sulfate production by combined fermentation and chemical developments is a reckoned complementary alternative. [139]

3.4 Natural polymer based composite scaffolds

The composition and properties of biomaterials used to produce a tissue engineering scaffold significantly affect the regeneration of neo-tissues and influence the conditions of collagen engineering [12]. From a biological point of view the natural polymers are more desirable option to prepare a tissue engineering scaffolds than synthetic material because their properties are more similar to native ECM [70]. Furthermore, possible cytotoxic effects of the degradation products released from synthetic polymers are not an issue, when using naturally derived molecules [20]. Natural polymers are derived from renewable resources, namely from plants, animals and micro-organisms, which gives them the beneficial ability to be degraded by naturally occurring enzymes. In addition, they possess many functional groups (i.e. amino, carboxylic and hydroxyl groups) available for chemical and enzymatic modification such as hydrolysis, oxidation, conjugation with other molecules, and cross-linking reactions. This makes an overwhelming variety of products with tailor-made chemistries and properties possible. Addition of protein materials may offer an additional advantage, since they are able to interact favorably with cells through specific recognition domains present in their structure. [33]

Cartilage tissue has many unique characteristics that demand specialized features from a chondrogenic tissue engineering scaffold [133]. In terms of material design a degradable bioactive polymer with proper mechanic properties can be regarded as a promising choice for cartilage regeneration [44]. Other facts that need to be taken into account, when designing a cartilage-regenerative scaffold are that the cartilage lacks of vascular supply and that the cartilage tissue has no innervation. [133] Somehow the scaffolds should be fabricated as such, which restrain angio- and neurogenesis after being cultured with cells *in vitro* and finally implanted *in vivo*. This is major challenge that has not yet been overcome. All in all, studies have shown that successful cartilage regeneration can be achieved through the use of a tissue engineered implant only if the seeded cells undergo normal proliferation and differentiation within the biodegradable scaffold alongside with the production of a new cartilage-specific ECM [97].

Tissue engineered scaffolds that combine collagen (COL) with GAGs were initially developed for the use in skin grafting, but after their composition was adapted for orthopedic applications, results have demonstrated their strong ability to support both chondrogenesis and osteogenesis [20]. Currently chondroitin sulfate (CS) and hyaluronic acid (HA) are the most valued GAGs in market because of their abundance in mammalian tissues, their physiological functions and high activity [139]. During the past decade, combining HA and/or CS to COL has been the subject of several investigations. Many of

those studies show a strong correlation between the use of either two (COL+HA/CS) or all three (COL+HA+CS) polymers and their usefulness for cartilage tissue engineering [94, 147, 147 etc.; found in the Appendices 11-12]. Researchers have been experimenting on numerous different composite structures such as membranes, microspheres, gels, fibers and porous 3D scaffolds.

Tables presented in the Appendices 9-12 show some of the studies concerning the manufacture and characterization of COL+CS/HA/CS+HA scaffolds. The studies are listed from top to bottom according to their resemblance to the present study; i.e. freeze-dried cylindrical scaffolds composed of COL, CS and/or HA, cross-linked with either EDC/NHS or genipin. If some other material component than the three is added to the scaffold matrix, such composites are presented at the bottom of each table. Some of the essential results of the studies are further presented and discussed in the following three chapters.

3.4.1 Collagen and hyaluronic acid composite scaffolds

A vast number of studies have demonstrated that COL+HA scaffolds have a positive impact on cellular response [140, 22, 142, 107, 61, 83, 31, 18]. HA is known to accelerate tissue repair by promoting mesenchymal and epithelial cell migration and differentiation, thereby enhancing COL deposition and production in tissues [97]. These observations support the idea of combining COL and HA as a functional tissue engineering scaffold. In porous COL+HA scaffolds HA is known to play a part in the survival and proliferation of cells as well as the maintenance and regeneration of tissue by cell receptor (CD44), whereas COL is known to constitute the ECM in most tissues of the human body and to be advantageous for cell adhesion [59]. Moreover, Park et al. [26] have stated that the biological benefits of HA become present without mechanical limitations with the addition of HA in COL-based scaffolds, making the two even more beneficial as a pair.

A study by Matsiko et al. [89] has revealed the ability of COL+HA scaffolds to facilitate MSC differentiation down to a chondrogenic lineage and to promote cartilage-specific matrix production *in vitro*. Furthermore, a study by Kim et al. [59] support the benefits of HA and COL in cartilage regeneration. Fabricated COL+HA scaffolds underwent *in vitro* and *in vivo* tests, both showing positive results towards cartilage formation. *In vitro* cell culture test with human chondrocytes demonstrated increase in cell proliferation with greater COL concentration, even cell distribution and good adhesion. Following *in vivo* cell culture test with rabbits showed increased GAG concentration in COL+HA scaffolds compared to plain HA scaffold, indicating cartilage formation. [59]

While HA and COL serve for cell adhesion and growth within the native cartilage ECM, they also provide the tissue with necessary tensile strength [96]. This statement is supported by a study conducted by Kim et al. [61]. Their results in tensile characterization of COL+HA scaffolds reported an increase in tensile strength with greater COL content, while simultaneously the nanofibrous structure of HA was thought to contribute to the enhanced mechanical strength. [61] Another study by Kim et al. [59] also confirmed that adding more COL in COL+HA scaffolds result in increased tensile strength. Furthermore,

another research group had evidence that with a higher HA content, the tensile strength of COL-based scaffolds could be increased [83].

However, without any further processing of the mechanical properties of *in vitro* fabricated scaffolds, they still quite often remain too weak to support heavy loads associated with cartilage tissue. Therefore it is often required to enhance the mechanical properties of fabricated scaffolds e.g. by cross-linking. [19] Two examples of such successful enhancement on mechanical properties are studies by Boss et al. [7] and Wang et al. [142], where they fabricated HA+COL-based scaffolds by freeze-drying and cross-linked them using EDC for better mechanical stability. In a study by Davidenko et al. [22] HA has even reportedly enhanced the EDC/NHS cross-linking efficiency.

3.4.2 Collagen and chondroitin sulfate composite scaffolds

For the past decade researchers have investigated the efficacy of using composite scaffolds composed of CS and other biopolymers such as COL or synthetic biodegradable polymers for cartilage tissue engineering [97]. Many studies have been reported on type I and II COL+CS scaffolds, in which they are produced either by co-precipitation of COL and CS, or by a covalent attachment of CS to collagenous matrix (ratios of COL:CS usually being 1.5-44:1) [128].

Several investigations have revealed a strong correlation between the use of CS and the bioactivity of the seeded chondrocytes [97]. For example, *in vitro* cell culture test with bovine chondrocytes demonstrated a positive influence of CS on bioactivity of chondrocytes [138]. Chondrocytes are crucial for the adequate cartilage matrix balance and function because they are the only cells in articular cartilage [66]. van Susante et al. [138] demonstrated, how the proliferation of chondrocytes and the total amount of PGs and cells was significantly higher in COL matrix with CS present compared to plain COL scaffolds.

In a number of other studies (in the Appendix 10) concerning the combination of COL and CS, CS has been shown to stimulate chondrogenesis *in vitro* [89, 147] and to maintain chondrocytic phenotype [36, 61]. Moreover CS has been shown to promote cellular ingrowth as well as cartilaginous tissue formation *in vivo* [89, 59], while COL have reportedly increased tensile strength of the composite construct [21, 61]. In a study by Kim et al. [61] the seeded chondrocytes maintained round morphology throughout the experiment (2 weeks) and only sparse elongated cells with fibroblastic appearance were detected. In addition to promoting cartilage-specific cell viability and attachment, COL+CS scaffolds have been reported to support the viability, metabolic activity and proliferation of tendon cells [11].

Adding CS to a COL-based composite has been reported to bring many beneficial properties to freeze-dried composite scaffolds; including increased mechanical strength and water uptake abilities. Kangjian et al. [56] fabricated membrane shape, freeze-dried COL+Chi+CS scaffolds for skin tissue engineering purposes. From their tensile test results became clear that the addition of CS to COL+Chi-based scaffolds increased the mechanical durability of the matrix when compared to COL+Chi scaffolds without CS. [56]

Daamen et al. [21], in turn, fabricated freeze-dried COL+CS+ELN scaffolds, whose water binding abilities were shown to increase up to 65% with the attachment of CS.

Douglas et al. [23] conducted an interesting interaction study between types I and II COL and different types of CS (CS-A, CS-B, CS-C). These composite scaffolds were composed of COL I/II+CS as a surface coating on titanium disks. COL was prepared as fibrils and cross-linked with EDC/NHS. The scaffold fabrication method of Douglas et al. [23] differed from the present study by not being freeze-drying but being fibrillogenesis instead. Nevertheless their findings are worth of mentioning in the present context. Their study demonstrated that COL II bound more CS (more precisely CS-C) than COL I. However, all CS types caused COL I/II fibrils to become thinner, and the fibrils of both COL types bound a higher mass of CS-C than CS-B and a greater mass of CS-B than CS-A. [23] Evidently CS binding favors COL II, which is the dominant COL type in native cartilage [8]. These results could be important, when choosing COL or CS type for the construction of scaffolds for cartilage tissue engineering purposes.

3.4.3 Collagen, hyaluronic acid and/or chondroitin sulfate composite scaffolds

Matsiko et al. [89] expected a significant enhancement of the biofunctionality of COL-based scaffolds for chondrogenesis with the addition of either HA or CS. Both variations (i.e. COL+HA and COL+CS) actually demonstrated ability to facilitate MSC differentiation down to a chondrogenic lineage and to promote cartilage-specific matrix production *in vitro*. The results indicated also that the quality of the cartilage matrix, produced within COL+HA scaffolds was superior compared to COL+CS or GAG-free COL scaffolds (as early as 14 days). The COL+HA scaffolds showed greater levels of MSC infiltration as well as significant acceleration of early stage gene expression of type II COL and cartilage production compared to the COL+CS scaffolds. In the case of HA, the researchers speculated that HA might stimulate migration of MSCs into scaffolds conceivably through chemotaxis or through the high anionic charge of HA that may have altered the interaction of cells and matrices. [89]

The results reported by Matsiko et al. [89] suggest that COL+HA scaffolds may have superior biochemical properties in terms of cartilage regeneration as opposed to COL+CS scaffolds. On the other hand the inclusion of both HA and CS to COL have also shown promising results. An interesting remark related to freeze-dried COL+CS+HA composite scaffolds is that so far there are only few studies in the literature associated with the composition of all three components [147, 63, 64, 36], indicating that the idea is relatively new. Since all the above mentioned investigations resulted in positive impacts on mechanical properties, swelling abilities, degradation, pore architecture and *in vitro* cell cultures (see the Appendix 12 for details), it is evident that the combination of COL, HA and CS has been successful. Furthermore, the biochemical fact that speaks on behalf of combining HA and CS to COL-based scaffolds is that CS and HA together with N-acetylglucosamine (GlcNAc; found naturally in the body) are known to repair cartilage after surgery. CS increases the synthesis of HA, glucosamine and COL type II in cartilage, while

it inhibits cartilage ECM degrading enzymes and therefore promotes cartilage repair *in situ*. [96] Moreover, HA have been reported to induce a variety of stimulatory signals to regulate chondrocyte proliferation as well as matrix synthesis in cartilage microenvironment [51], thus facilitating the integration of engineered scaffold [147]. Consequently, the combination of COL+CS+HA may partly mimic the cartilage ECM and yield out biomimetic environment for chondrocytes when the cells are incorporated into the construct [147]. Composite scaffolds with the composition of these three polymers have all been fabricated by freeze-drying (at some point of processing) and cross-linked with either GP (mostly) [147, 63, 64], EDC/NHS [147], ADH [147] or by polymerization [36].

Biological criterion is not the only important aspect to be considered when designing a suitable scaffold for the cartilage regeneration. Mechanical properties of the scaffold, such as stiffness play a critical role in supporting proliferation, migration and differentiation into a specific tissue. Collins et al. [19] and Murphy et al. [94] elucidated the influence of CS and HA incorporated within COL-based scaffolds as well as the mechanical properties of finished constructs on MSCs. Their *in vitro* tests with MSCs suggested that the fate of the cells is dependent on the mechanical properties of COL+GAG scaffolds. Murphy et al. [94] demonstrated that by varying the stiffness of COL+CS and COL+HA scaffolds, the MSCs could be directed towards either chondrogenic (lowest stiffness) or osteogenic (highest stiffness) lineage. Their *in vitro* cell differentiation test results revealed that scaffolds with the lowest stiffness (0.5 kPa) directed MSCs towards a chondrogenic lineage, whereas in the stiffest scaffolds (1.5 kPa) MSCs were differentiating towards an osteogenic lineage. Furthermore, it turned out that within the COL+HA scaffolds (compared to the COL+CS scaffolds) it was HA that further influenced MSCs towards chondrogenic differentiation, whereas in the COL+CS scaffolds (compared to the COL+HA scaffolds) CS on MSC differentiation suggested an osteogenic influence. [94] Matsiko et al. [89] had similar kinds of results with their COL+HA/CS scaffolds. In their *in vitro* cell culture and gene expression tests the COL+HA scaffolds showed greater levels of MSC infiltration compared to the COL+CS scaffolds. Also, the COL+HA scaffolds showed significant acceleration of early stage gene expression of type II COL and cartilage matrix production compared to the COL+CS scaffolds. [89]

3.5 Processing of porous scaffolds

Highly porous structure is a necessity for a tissue engineering scaffold in order it to be fully replaced by living tissue after implantation *in vivo*. Interconnected pores enable cells to infiltrate within the scaffold matrix *in vivo* [72] as well as the diffusion of nutrients and waste products. [22] Moreover, it must provide sufficient temporary mechanical support and match the mechanical properties of the host tissue as closely as possible in order to bear *in vivo* stresses and loading. Therefore, the selection of materials together with suitable processing methods, is the key factor for producing applicable scaffolds. [111] Numerous processing techniques have been developed for the manufacture of porous tissue

engineering scaffolds. Most commonly employed processing techniques are gathered in Table 3.1 and presented in short in the following paragraph.

Electrospinning is a broadly used technique, which utilizes electrical forces to fabricate electrostatic nanofibers and fabrics from polymer solutions or melts. In electrospinning polymer solution is placed in a capillary tube, where it becomes subjected to an electric field. The repulsive electrical forces overcome the liquid surface tension forces and a charged solution is ejected from the capillary tip in form of thin fibers. The process can be set up vertically or horizontally; both presented in Figure 3.1. [4]

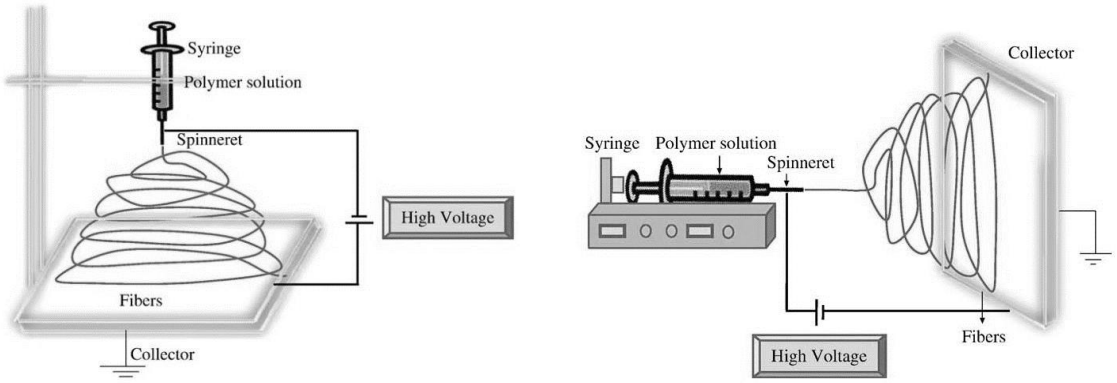

(a) (b)

Figure 3.1. *Typical vertical (a) and horizontal (b) set-ups of electrospinning process. Modified from [4].*

Rapid prototyping is a group of techniques (examples presented in Table 3.1) that are used to fabricate a scale model of a physical part or assembly utilizing 3D computer aided design (CAD) data. It has been referred to as layered manufacturing, solid free-form manufacturing and computer automated manufacturing. [24] *Porogen leaching* and *super critical fluid technology* [19] both exploit porogens to create a porous structure. Porogen leaching involves mixing suitable porogen (usually inorganic salts) with a solution of polymer, after which the porogen is leached out during a casting procedure in order to form porous sponges. [129] *Super critical fluid technology*, in turn, uses gas that is dissolved in a polymer at high pressures. Porous structure is formed, when gas molecules are homogenously nucleated and thermodynamic driving force produce gas bubbles throughout the polymer. Polymer solution can be induced in several different ways with *phase separation*: non solvent induced phase separation, chemically induced phase separation and thermally induced phase separation (TIPS). The basic principle is, however, similar in all of them: solvent is removed by extraction, evaporation or sublimation, while the polymer in the polymer-rich phase solidifies and the space occupied by the solvent becomes porous. There are several *micro pattering* techniques (examples shown in Table 3.1), which are capable of producing 3D scaffolds with tailored microstructural properties. As an example of such tailoring is a femtosecond laser two photon polymerization

(TPP) technique that can produce 3D submicron patterns on hydrogel scaffolds with precise control of geometry. [19] *Freeze-drying*, which was the method of choice in the present study, is presented in more detail in the next chapter.

Table 3.1. *Various fabrication and processing techniques that produce porous 3D scaffolds. UNS = unspecified. Modified from [19].*

Processing technology	Processing method	Obtained porosity (%)	Pore architecture	Advantages	Disadvantages	Reference
Electro-spinning	Needling	< 95	Nanofibers	3D scaffolds and fabrics	Limited control of pore size an shape, poor mechanical properties	[19, 4]
Rapid prototyping	Solid free form fabrication Layer by layer deposition Bioprinting	UNS	Interconnected macro (various shapes), incorporation of biological molecules	Controllable pore geometry and size scaffolds	Difficult processing	[19, 24]
Porogen leaching	Casting and particulate leaching	20-60	Spherical	3D scaffolds	Limited control of pore size an shape	[19, 129]
Phase separation	Casting	< 97	Interconnected micropore structure	3D scaffolds	Limited control of pore size and shape	[19]
Super critical fluid technology	Casting	< 95	Non-interconnected micro structure with interconnected macrostructure	UNS	UNS	[19]
Micro pattering	Casting and femtosecond laser induced TPP Lithography Nanoimprinting	> 90	Spherical	Geometry control chemical cues in nanoscale topography, controlled degradation	Slow processing	[19]
Freeze-drying	Casting	< 97	Interconnected micropore structure	Easy processing, 3D scaffolds	Expensiveness, limited control of porosity	[19, 7, 143]

Scaffold should possess over 90% porosity with a highly porous surface and microstructure in order to allow *in vitro* cell adhesion, ingrowth and reorganization. Different pore architectures (i.e. microenvironments) are required for different tissues and their regeneration. [111] All of the above-mentioned processes generate scaffolds with interconnected pore structure [20] with varying degrees of porosity, pore size and architecture. With phase separation, salt leaching, freeze-drying and electrospinning it is possible to fabricate 3D models. Freeze-drying is often used because of the easy processing it involves [7].

3.5.1 Freeze-drying

Freeze-drying, or lyophilisation [143] is a form of casting, which produces interconnected macro structure with pores size less than 200 µm and porosity less than 97% [19]. The general process in short is following: a solvent is removed from a frozen material or solution by sublimation and by desorption, usually under reduced pressure (a vacuum). Freeze-drying can be divided into three stages: freezing, primary and secondary drying (Figure 3.2). [7]

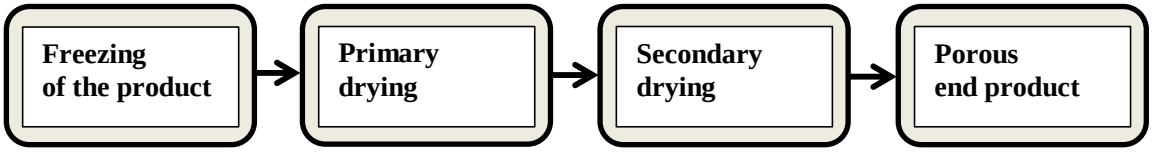

Figure 3.2. *The steps of freeze-drying process. Modified from [7].*

During the first step (freezing) the material in hydrogel form is cooled down to a temperature below the solidification. During freezing the water in the solution forms dense pockets (ice crystals) throughout the structure [19], which are then removed by sublimation and heat addition during the second stage (primary drying period). [7, 143] Heating of the product removes the unfrozen bound water and leaves behind a porous sponge network [19]. The last stage (secondary drying) clears the solvent from the sample chamber, while a small amount of sorbed water is removed by desorption. The performance of the overall process depends significantly on the stage and rate of the freezing as well as the processed material. Pore size, shape, distribution and connectivity depend on the ice crystals formed during the freezing stage [7], which can be controlled by exposing the material to different freezing conditions (e.g. -20°C and -80°C) [19]. [7]

There are many advantages in freeze-drying. First, it involves easy processing and porous 3D scaffold formation. Secondly, the process preserves the original polymer structure of the material, while a fast transition of the moisture product minimizes several degradation reactions. Thirdly, a reduced pressure enables processing at low temperatures, which is beneficial especially for the processing of thermosensitive polymers. The downsides of freeze-drying are limited control of porosity [19] and expensiveness [7]. The process also generates several freezing and drying stresses to the material such as formation of dendritic ice crystals, phase separation and pH changes [143].

The described process correspond a conventional freeze-drying method, where variable cooling rates (utilized throughout the scaffold during freezing) produce a heterogeneous matrix pore structure with a large variation in average pore diameter at different locations throughout the scaffold. This has been shown to lead to variable cell adhesion and to affect the ability of the cell to produce a uniform distribution of ECM proteins. [99] O'Brien et al. [99] have created a modified version of the process. In their study the scaffold synthesis was modified to produce more homogeneous freezing by controlling of the rate of freezing during fabrication. The COL+CS scaffolds fabricated on constant cooling

rate technique produced more homogenous solid scaffolds and did not show notable special variation in pore size. In addition, the pores appeared to be more equiaxed than with scaffolds fabricated by the conventional quenching technique. The significant variations on the end results between both techniques can be observed in Figure 3.3.

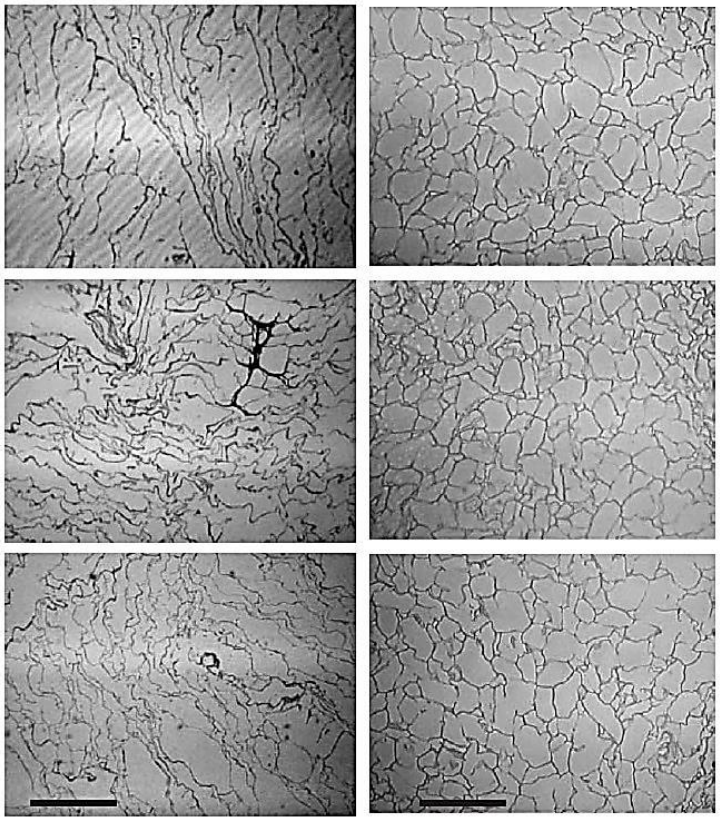

Figure 3.3. *A series of longitudinal images taken via the fixed selection protocol from a single sheet of scaffold produced using the conventional, quenching freeze-drying technique (a) and the modified, constant cooling rate technique. Scale bar = 300 µm. Modified from [99].*

Freeze-drying has been the traditional fabrication method for numerous COL, HA and/or CS composite scaffolds. With this technique it is possible to produce 3D scaffolds in various shapes and sizes, and the freezing rate and final freezing temperature can be manipulated to affect scaffold pore size and uniformity. [11] Numerous COL+CS-based 3D scaffolds of varying designs have been reported such as membrane shaped scaffolds for skin scaffolds and wound dressings [56] and cylindrical shaped scaffolds for tendon tissue engineering [10, 11]. In addition, fiber-reinforced scaffolds have been designed for tissue engineering in general [21] and for soft tissue and cartilage regeneration [117]. Furthermore, COL+CS chambers have been fabricated for peripheral nerve regeneration [41]. The majority of reported freeze-dried COL+HA 3D scaffolds have been disk shaped; in general for tissue engineering purposes [126], for cartilage and bone tissue engineering [59, 140] and for dermal restoration [106]. Other freeze-dried COL+HA scaffolds reported include membrane shaped for tissue regeneration in general [107], sponge-like for

brain tissue engineering [142], antibiotic bi-layered matrices as skin substitutes [105] and microspheres developed for drug delivery as cell/tissue carriers and bone grafting [13]. COL+CS+HA 3D scaffolds have been fabricated by freeze-drying into cylindrical shaped [36, 147] as well as sponge-like [63]; all designed for cartilage tissue engineering.

Overall, especially for cartilage tissue engineering purposes following freeze-dried COL+CS/HA/CS+HA scaffolds have been fabricated: disk [59, 140, 106, 128, 31], cylindrical [36, 147, 10, 11, 47] and membrane [94, 107, 23] shaped, fiber reinforced [117] and sponge-like scaffolds [63, 142]. Details concerning all of the above mentioned researches can be found in the Appendices 9-12. In the present study Telfon® molds, especially designed for fabricating 3D disk shaped scaffolds were used. This shape was considered beneficial for the purposes of the present study; i.e. easily achievable and suitable for testing of compression, swelling and water uptake. Furthermore, changes in the original shape could be easily seen just by visual observation.

4 CROSS-LINKING METHODS FOR NATURAL POLYMERS

Due to their polymeric nature most natural polymers have weak mechanical properties and poor durability against enzymatic degradation [104] that limit their usefulness for orthopedic applications. These issues can be solved e.g. by adding a second stiffer phase to the scaffold matrix or through various cross-linking mechanisms, which produce mechanically and chemically robust materials. [20, 19] Cross-linking methods differ in the extent of cross-linking and in use of different cross-linking agents [130]. Various cross-linking methods include for example physical, chemical, auto- and photo-cross-linking [19]. Examples of chemical methods include the use of glutaraldehyde, carbodiimides and genipin, whereas common biophysical methods include the use of ultraviolet light and dehydrothermal cross-linking (DHT) [20]. With all crosslinkers, the degree of cross-linking can be varied by controlling the duration, concentration and pH of the incubation [141].

In most cases, a chemical cross-link refers to a covalent structure between molecules. However, in some cases the term has also been used in a context of weaker chemical interactions. [53] An attachment between two functional groups on a single protein creates intramolecular cross-links (Figure 4.1 (a)), whereas the attachment between groups on two different proteins creates intermolecular cross-links (Figure 4.1 (b)) that stabilize a protein-protein interaction [130].

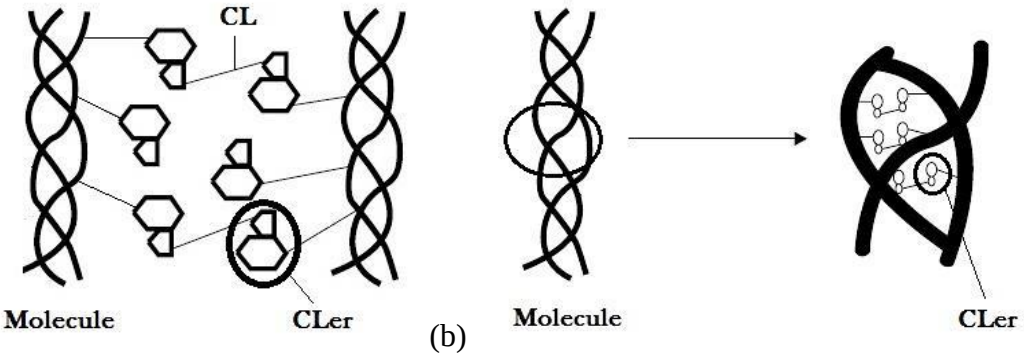

Figure 4.1. *A schematic presentation of intermolecular (a) and intramolecular (b) cross-links. CL stands for cross-link, and CLer stands for crosslinker. Modified from [14].*

Cross-linking reagents or crosslinkers are molecules that contain two or more reactive ends capable of chemically attaching to specific functional groups (e.g. primary amines, sulfhydryls, carboxyls) on proteins or other molecules [130]. Generating reactive sites for the chemical modification (i.e. covalent bonds) of the original molecule involves cleaving or attaching functional groups by for example hydrolysis, esterification, oxidation [131]. This process may alter significantly physicochemical properties of the native molecule,

but most derivatives retain their biocompatibility and biodegradability [19]. In principle, different crosslinkers can be divided into two groups. First are agents (e.g. glutaraldehyde, epoxy compounds and genipin) that can be used to bridge amino groups of lysine or hydroxylysine residues of different polypeptide chains by monomeric or oligomeric cross-links. Second group (carbodiimides) forms direct cross-linking of the polypeptide chains. After a nucleophilic attack by free amino groups of lysine or hydroxyline residues, they result as amide-type cross-links. [123]

Numerous cross-linking techniques, methods and cross-linking degrees have been shown to cause differing impacts on cellular response. The matter has been investigated for example by Vickers et al. [140] with porous 3D DHT and EDC/NHS cross-linked COL+HA scaffolds and MSCs. In their research they demonstrated the effects of various levels of the aforementioned cross-linking treatments on cellular condensation and chondrogenesis. The results indicated an increase in cell number densities and enhanced chondrogenesis with lower cross-linking densities compared to more highly cross-linked densities. [140]

In the present study the two chemical cross-linking methods applied to the scaffolds were EDC/NHS and genipin cross-linking. Compared to the well-established EDC cross-linking agent, genipin is a novel addition to the more natural and less toxic crosslinkers. In the results part the EDC/NHS and genipin cross-linked scaffolds are compared and their possible differences assessed according to the mechanical, visual and microstructural properties of the scaffolds. The next two chapters provide theoretical information on these two crosslinkers.

4.1 1-ethyl-3-(3-dimethylaminopropyl)-carbodiimide hydrochloride / N-hydroxysuccinimide cross-linking

1-ethyl-3-(3-dimethylaminopropyl)-carbodiimide hydrochloride (EDC, EDAC or EDCI [119]) is a representative of a chemical cross-linking agent [33]. It belongs to the class of zero-length crosslinkers (carbodiimides) that modify specific side-groups to permit cross-link formation but do not become part of that linkage [75]. In contrast to conventional chemical agents such as bifunctional [75] glutaraldehyde or polyfunctional [75] polyepoxides, carbomiidies are simply converted to water-soluble 1-ethyl-3-(3-dimethyl-aminopropyl)-urea that have very low cytotoxicity [107, 146].

In proteins like COL, EDC cross-linking process modifies the primary amine ($-NH_2$) and carboxyl (-COOH) side-groups of amino acids making them reactive with other side groups [75]. EDC has reportedly coupled groups that are located within 1.0 nm from each other, and thus has potential to form both intra- and intermolecular cross-links within or between tropocollagen molecules. However, carboxylic acid and amino groups located on two adjacent COL microfibrils are supposedly too far in order to be bridged. [123] Figure 4.2 shows the two reactive sites in the basic amino acid structure of proteins.

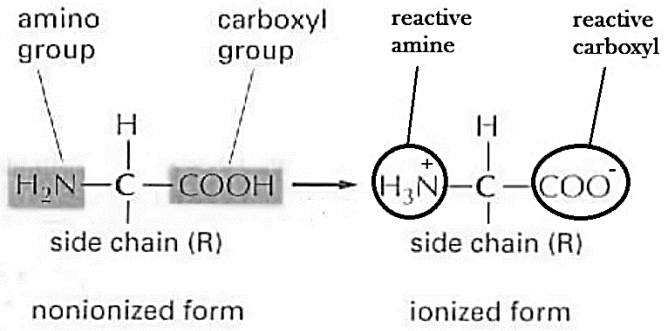

Figure 4.2. *The two reactive sites in the amino acid structure of proteins. Modified from [1].*

EDC reacts with a carboxyl group to form an amine-reactive *O*-acylisourea intermediate that facilitates bonding with an amine near-by. If *O*-acylisourea intermediate does not encounter an amine, it will hydrolyze and regenerate the carboxyl group. The conjugation reaction between *O*-acylisourea and an amine causes two protein molecules to become cross-linked with each other via an amide bond, while releasing EDC reagent as an isourea by-product. [131] Figure 4.3 illustrates the conjugation reaction of carboxylic acid to primary amines that EDC establishes in protein molecules.

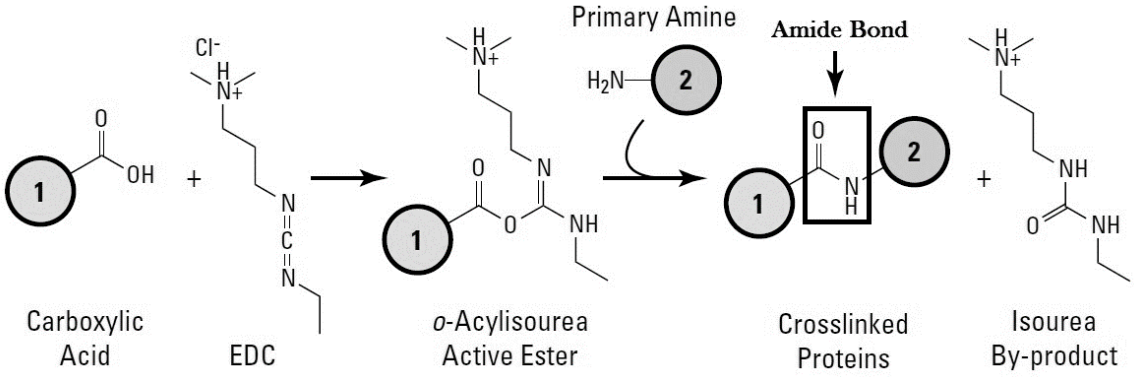

Figure 4.3. *The EDC facilitated conjugation reaction of carboxyl-to-amine cross-link between protein molecules. Molecules (1) and (2) stand for peptides, proteins or any chemicals that have respective carboxylate and primary amine groups. Modified from [131].*

Polysaccharides, such as HA and CS can be chemically cross-linked to form hydrogels because of their abundant functional groups. In GAGs like HA and in CS EDC targets the hydroxyl and carboxyl groups. [70, 97] EDC converts carboxyl groups into amides and mediates acid anhydride formation between two carboxyl groups belonging to the same or different HA/CS molecules. The resultant acid anhydride may readily react with hydroxyl groups of HA/CS to yield an ester bond, which functions as a covalent cross-link between molecules. [107] Figure 4.4 shows the two reactive sites on HA.

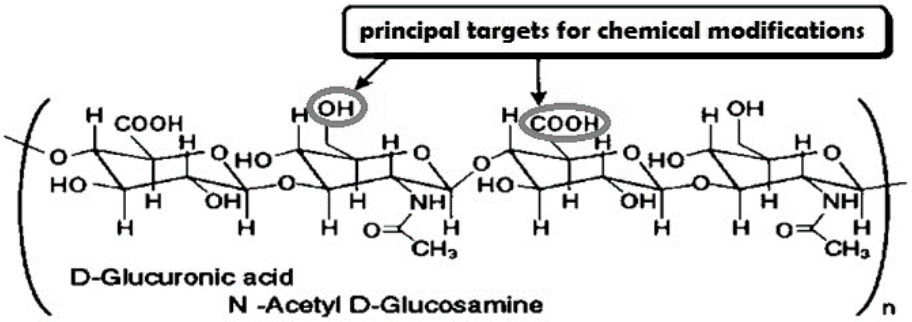

Figure 4.4. *Principal reactive sites for chemical modification in HA. Similar sites are found in the structure of CS. Modified from [19].*

EDC is commonly used in combination with N-hydroxysuccinimide (NHS). It acts as a catalyst that intensifies the mechanism of EDC cross-linking. By suppressing side reactions like hydrolysis, NHS induces more effective and stabilized reaction. [146] In the presence of NHS, EDC converts carboxylic groups to form activated NHS-esters that are considerably more stable than O-acylisourea intermediates (in Figure 4.3) [131]. Olde Damink et al. [101] have claimed that the addition of NHS to the EDC containing solution is a very effective way to increase the number of cross-links. This was determined by monitoring the free amino group content, which was significantly decreased with EDC/NHS present and thereby considered as a proof of higher degree of cross-linking. [101]

The cross-linking with EDC/NHS has been reported to increase the mechanical strength [13, 108, 11, 117] and to decrease the swelling and water uptake [13, 142, 140, 22, 127] of freeze-dried COL+HA or COL+CS scaffolds. In the studies by Wang et al. [142] and Chang et al. [13] the water uptake capacity has been reported to decrease in connection with increased cross-linking degree. Furthermore, with the increase of EDC/NHS cross-linking level the degradation ratio of similar scaffolds have shown to decrease [11, 61, 108, 117]. The effect of EDC/NHS cross-linking on the mechanical durability has also been widely studied. In most cases, the cross-linking has enhanced the mechanical durability of composite scaffolds. Caliari et al. [11] and Shepherd et al. [117] have reported increase in tensile strength with greater cross-linking degree, while Pek et al. [108] have had similar results on compression strength. The degradation ratio has evidently been shown to slow down after cross-linking according to investigations by Want et al. [142], Kim et al. [61], Pek et al. [108], and Kangjian et al. [56]. Moreover, Vickers et al. [140] studied the effects of EDC/NHS cross-linking treatment with COL+HA scaffolds on cell number densities. They discovered that scaffolds with low-crosslink densities resulted in an increase of cell number densities and in a greater degree of chondrogenesis compared to more highly cross-linked that seemed to resists cellular contraction. [140]

Determining the effects of EDC/NHS cross-linking on porosity, pore size and structure of freeze-dried COL+HA/CS scaffolds, following observations and results have been made. Numerous studies reported on freeze-dried COL+HA scaffolds [140, 22, 142, 106,

107, 105] and COL+CS scaffolds [138, 117] that maintained an open, interconnected pore structure after EDC/NHS cross-linking. A histologic examination by Vickers et al. [140] on COL+HA scaffolds revealed that the scaffolds of highest cross-link densities had the best looking porous structure (open and interconnected). Another study on similar scaffolds reported interconnected pore structure with total porosity of ~85% and no signs of COL denaturation during cross-linking treatment [22].

Carbodiimides utilizing chemical cross-linking of proteins, polysaccharides and other biomolecules is a well-established procedure. However, this reaction is known to be non-selective and to produce insignificant or very low chemical modification of the polysaccharide, which is why researches are currently investigating alternative crosslinkers as well. [48]

4.2 Genipin cross-linking

Genipin is a natural cross-linking agent extracted as a hydrolytic product from geniposide (Figure 4.5 (a)), found in the fruits of *Gardenia jasminoides* ELLIS. Genipin itself is colorless but forms blue particles by spontaneous reaction with amino acid residues and proteins. [145] The structure of genipin, shown in Figure 4.5 (b), was discovered in the 1960s. But since there were other more commonly used and inexpensive cross-linking agents available, such as synthetic glutaraldehyde (GTA) [123] it was not until the recent decade that genipin became a subject of extensive investigations. It was mainly the toxicity concerns associated with GTA [123] that led to the search for other less toxic and more natural crosslinkers [137] like genipin. Recent investigations include genipin cross-linked gelatin for the use as a bioadhesive, wound dressing, bone substitutes [137] and cartilage tissue engineering scaffolds [80].

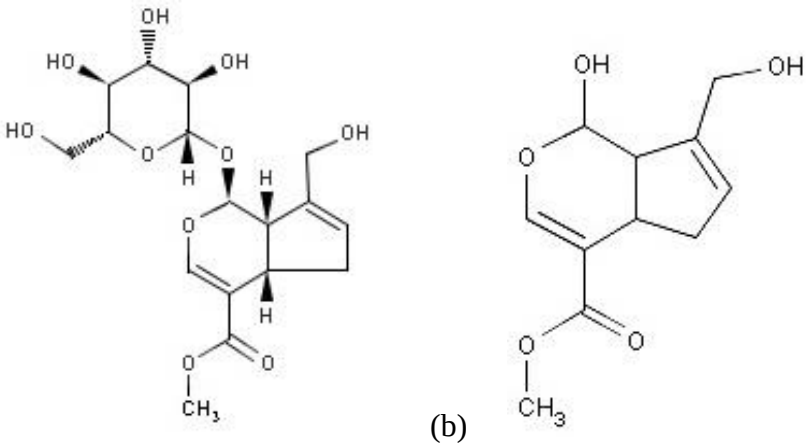

(a) (b)

Figure 4.5. *The structure of geniposide (a) and its hydrolytic product, genipin (b). [145]*

Genipin has been used to cross-link for example COL gels [141], chitosan, proteins [145] and biological tissues [82]. It has been shown to affect the mechanical properties of COL II, bovine pericardium [124] and porcine tendon by increasing their tensile strength. In

addition, genipin has been studied for anti-inflammatory effects *in vitro* (directly to different cell lines) and *in vivo* (oral administration to animals). [82]

As a crosslinker genipin can bridge amino groups of lysine or hydroxylysine residues of different polypeptide chains by monomeric or oligomeric cross-links but only via another genipin molecule [123]. The cross-linking mechanism between a primary amine group and genipin still remains unclear in detail but Chang et al. [14] suggested following reaction shown in Figure 4.6 (a). Furthermore, the presumable reaction between genipin and the primary amine groups of COL is illustrated in Figure 4.6 (b).

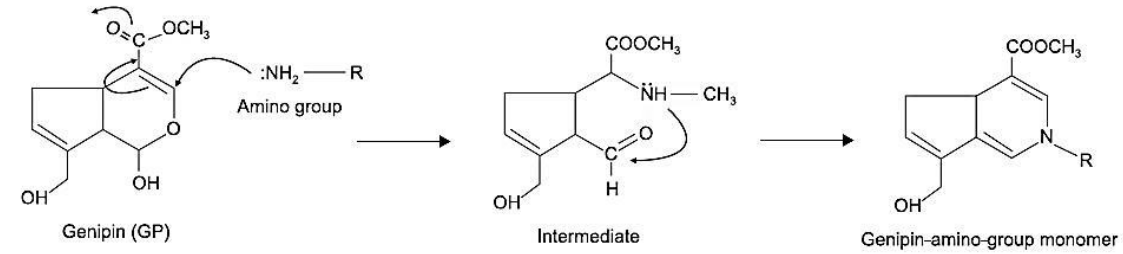

(a)

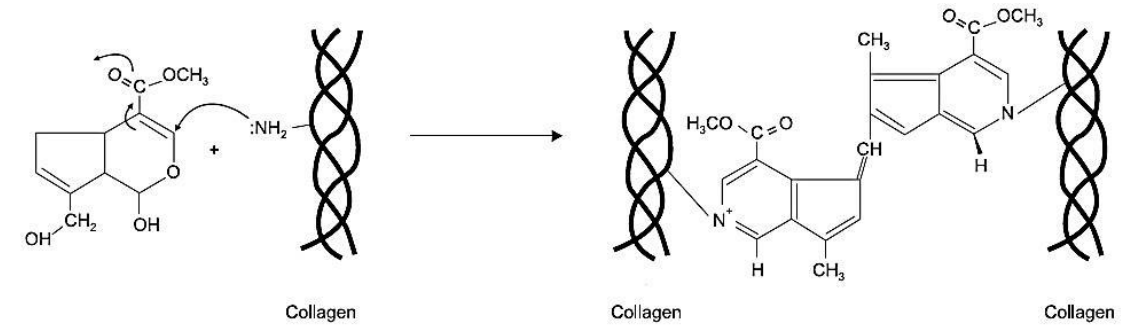

(b)

Figure 4.6. *The presumable mechanism of amino group with genipin (a), and genipin cross-linking with COL molecules (b). Modified from [14].*

With COL genipin forms intra- and intermolecular cross-links of the amino residues on tropocollagen or proteoglycan molecules [82]. As opposed to EDC, genipin can form additional intermicrofibrillar cross-links [123], which result in better biostability of COL [144]. Genipin can reside stably as a modified cyclic form within the ECM by adding bridges across adjacent COL fibers [82]. When free amino groups of different COL molecules become cross-linked with each other, they form an interpenetrating polymeric network (IPN) that lead to better biostability of COL [144]. Figure 4.7 shows a schematic presentation that illustrates the presumable genipin cross-links formed with tropocollagen molecules.

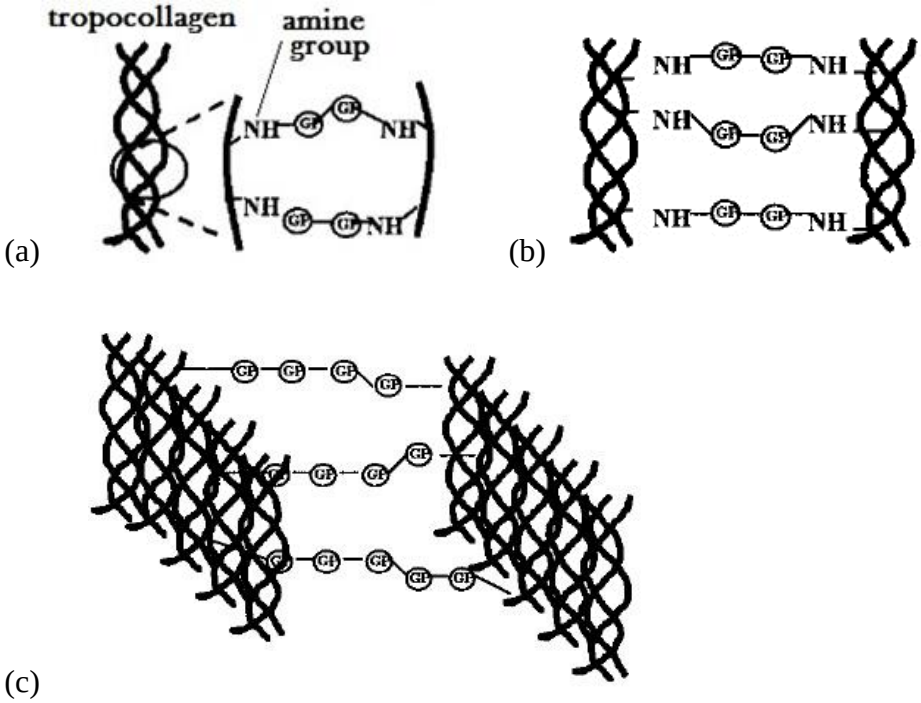

Figure 4.7. *Genipin can form both intramolecular (a), intermolecular (b) and intermicrofibrillar (c) cross-links between tropocollagen molecules. Modified from [14].*

In the field of tissue engineering only a few studies (since 2009) have been reported on genipin (GP) cross-linked composite scaffolds composed of COL, HA and/or CS [147, 63, 64, 36]; details found in the Appendix 12. In fact, the GP cross-linked composite scaffolds have invariably been COL+CS+HA composites. From their results following findings can be concluded: a greater degree of GP cross-linking has resulted in a slight increase of compression strength [147], lower water uptake and swelling tendency [147, 64] and decreased degradation rate [147, 63]. In these studies, the purpose of GP cross-linking was specifically to improve the physical and chemical performance of the scaffolds such as compressive strength, water uptake, degradability, pore size and pore architecture. Zhang et al. [147] reported that with increased GP concentration following improvements could be achieved: a significant decrease in pore size (c_{GP}: 0 → 0.75 mM), a slight increase in compressive strength, lower water uptake (c_{GP}: up to 1 mM) and slower degradation. Ko et al. [63] had similar degradation results as Zhang et al. [147].

Many research groups have revealed positive results concerning the effects of GP cross-linking on pore architecture. For instance, Zhang et al. [147] fabricated COL+CS+HA scaffolds that maintained interconnected and homogenously distributed pore structure after freeze-drying and GP cross-linking. Ko et al. [63] reported an interconnected pore structure and porosities of 92-95% after GP cross-linking in similar kinds of composite scaffolds. Ko et al. [64] provided varying porosity results on cross-linked COL+CS+HA scaffolds, cross-linked COL scaffolds and non-cross-linked scaffolds. The pore structure stayed intact in all of the variations; with the exception of surface pores collapsing slightly.

The effect of GP cross-linking on the degree of porosity has also been investigated. Ko et al. [64] reported that the porosity in GP cross-linked plain COL scaffolds was 95%, in GP cross-linked COL+CS+HA scaffolds 90% and in non-cross-linked COL scaffolds 96%. Scaffolds for tissue regeneration purposes should possess over 90% porosity in order to allow *in vitro* cell adhesion, ingrowth and reorganization. However, increased porosity (well over 90%) causes the scaffold to lose significantly its mechanical strength. In addition to the necessity of a certain porosity degree, the size and microstructure of the pores is equally important. Increased pore size causes decrease in the internal surface area. On the other hand, when pore diameter is too small, cells may provoke pore occlusion and prevent cellular penetration within the scaffold, which leads to an ingrowth of smaller pores and eventually fibrous tissue. Scaffold microstructure allow *in vitro* cell adhesion, ingrowth and reorganization, and ultimately result in the success or failure of the scaffold construct. [111]

Currently there is no standard GP cross-linking procedure established. Many researchers have reported several more or less different practices; in terms of the concentration and the amount of GP cross-linking solution per scaffold, solvent in which the solid GP powder is dissolved, cross-linking time and temperature, washing procedures etc. The GP cross-linking procedure in the present study was carried out based on results collected from various sources (shown in the Appendix 8) and is explained in more detail in the Materials and Methods.

5 AIMS OF THE PRESENT STUDY

- To study how to fabricate freeze-dried composite scaffolds from collagen, hyaluronic acid and/or chondroitin sulfate that mimic natural cartilage composition.
- To study the suitability of the fabricated scaffolds for cartilage engineering with compressive and microstructural testing.
- To characterize water uptake, swelling and dimensional changes of the fabricated scaffolds.

6 MATERIALS AND METHODS

6.1 Materials

6.1.1 Collagen, hyaluronic acid, chondroitin sulfate

COL solution (Type I, purified bovine dermal COL, PureCol®) with the COL concentration of 3.0 mg/ml used in the present study was purchased from Nutacon B.V. (Leimuiden, the Netherlands). Table 6.1 provides the product information of the used COL, HA and CS. HA sodium salt from Streptococcus equi and CS sodium salt from shark cartilage were purchased from Sigma-Aldrich Finland Oy (Helsinki, Finland).

Table 6.1. *Materials used to fabricate composite scaffolds.*

Material	Product information	
Collagen	Trade mark Advanced Biomatrix PureCol® Purified bovine, Type I	Sterile solution in 0.01 N HCl, c_{col} = 3.0 mg/ml
Hyaluronic acid	Product number 53747 CAS no 9067-32-7	Sodium salt from Streptococcus equi, powder
Chondroitin sulfate	Product number C4384 CAS no 9007-28-7	Sodium salt from shark cartilage, powder

6.1.2 Cross-linking agents

Two different cross-linking agents were used in the present study: EDC/NHS and genipin. Detailed information concerning the crosslinkers is shown in Table 6.2. All crosslinkers were purchased from Sigma-Aldrich Finland Oy (Helsinki, Finland).

Table 6.2. *Crosslinkers used in the present study.*

Cross-linking agent	CAS number	M_W [g/mol]	Product number
N-(3-dimethylaminopropyl)-N'-ethylcarbodiimide hydrochloride	25952-53-8	191.70	E1769 – 10g
N-Hydroxysuccinimide	6066-82-6	115.09	130672 – 5g
Genipin	6902-77-8	226.23	G4796 – 125mg

6.2 Methods

6.2.1 Fabrication of scaffolds

Prior to the actual scaffold fabrication preliminary composite scaffolds with varying COL, HA and CS compositions were fabricated to determine the most applicable composite composition. Criteria for the selection of appropriate composition were: 1) scaffolds needed to hold their shape and size; 2) to endure cross-linking; and 3) testing. COL concentrations of 0.5 wt.% and 1.0 wt.% were blended separately in a ratio of 3:1 with either HA or CS of 0.05 wt.%, 0.5 wt.% and 1.0 wt.%. Detailed information about the preliminary composite scaffolds is shown in Table 6.3.

Table 6.3. *Preliminary composite scaffolds fabricated from COL, HA and/or CS.*

Scaffold composition and concentration
0.5 wt.% COL + 0.05 wt.% HA
0.5 wt.% COL + 0.05 wt.% CS
1.0 wt.% COL + 0.5 wt.% HA
1.0 wt.% COL + 0.5 wt.% CS

To study the effects of the different components/compositions as well as the two different cross-linking treatments on the scaffolds, 11 different test groups with a specific COL, HA and/or CS compositions were fabricated. Four scaffold groups were cross-linked with GP and seven with EDC/NHS. Each test group composed of 6 parallel scaffolds. Names of the groups varied according to their composition and cross-linking treatment. Table 6.4 shows detailed information of the scaffold groups, where C stands for “collagen”, H stands for “hyaluronic acid” and CS for “chondroitin sulfate”. E or G at the end stands for scaffolds cross-linked with “EDC/NHS” or “Genipin”, respectively. Numbers in the middle indicate the volume percentage of the blended components (0-100%, v/v).

Table 6.4. *Actual test scaffold groups and their composition; more detailed information can be found in the Notations.*

Notations of the test scaffolds groups	Interpretation of the abbreviations
C100E	1.0 wt.% COL; EDC/NHS
C100G	1.0 wt.% COL; GP
C80HE	1.0 wt.% COL + 1.0 wt.% HA | 80:20 wt.%; EDC/NHS
C80HG	1.0 wt.% COL + 1.0 wt.% HA | 80:20 wt.%; GP
C60HE	1.0 wt.% COL + 1.0 wt.% HA | 60:40 wt.%; EDC/NHS
C80CSE	1.0 wt.% COL + 1.0 wt.% CS | 80:20 wt.%; EDC/NHS
C80CSG	1.0 wt.% COL + 1.0 wt.% CS | 80:20 wt.%; GP
C60CSE	1.0 wt.% COL + 1.0 wt.% CS | 60:40 wt.%; EDC/NHS
C80CS15HE	1.0 wt.% COL + 1.0 wt.% CS + 1.0 wt.% HA | 80:15:5 wt.%; EDC/NHS
C80CS15HG	1.0 wt.% COL + 1.0 wt.% CS + 1.0 wt.% HA | 80:15:5 wt.%; GP
C60CS30HE	1.0 wt.% COL + 1.0 wt.% CS + 1.0 wt.% HA | 60:30:10 wt.%; EDC/NHS

The preliminary composite scaffolds were not cross-linked, and their suitability for testing was assessed only visually. Concentrations of 1.0 wt.% COL, 1.0 wt.% HA and/or 1.0 wt.% CS were chosen for the fabrication of the actual test scaffolds due to obvious reasons seen in Figure 7.3 (in the Results and Discussion).

6.2.1.1 Preparation of blends and freeze-drying

Fibrillogenesis buffer solution (pH 11.2) was used to process COL-HCl solution into a gel-like form. Sodium hydroxide (Product of EMD Millipore Corporation, USA) and 85% phosphoric acid (Product of J.T. Baker®, Netherlands) were used to prepare fresh fibrillogenesis buffer monthly. Specific information concerning these reagents can be found in Table 6.5. Both reagents were purchased from VWR International Oy (Helsinki, Finland).

Table 6.5. *Reagents used for fibrillogenesis buffer preparation.*

Reagent	CAS number	M_W [g/mol]	Molecular formula
Sodium hydroxide	12179-02-1	40.0	NaOH
Phosphoric acid, 85%	7664-38-2	98.0	H_3PO_4

For the gelation of COL, COL-HCl solution and fibrillogenesis buffer (0.2 M NaH_2 PO_4) were mixed in a ratio 10:1 and stirred gently with magnetic stirrer for 10-15 minutes. The

result was 0.3 wt.% COL gel from which the 1.0 wt.% Col-gel was prepared by centrifugation (CF-510-A device, Labsystems Oy, Helsinki, Finland). Centrifugation was performed at a rate of 5000 rpm at 20°C for 30 minutes, after which the correct amount of the clear solvent was removed with a pipette. The remaining COL pellet and remaining solvent was finally mixed with a spatula into a uniform COL gel. The pH of the Col-gel was adjusted to 7.2 with 1 M HCl or 1-10 M NaOH.

Prior to the blending of COL, HA and CS, COL was processed into a gel-like form and HA and CS were dissolved in deionized water. The initial components of all prepared blends were 1.0 wt.% COL-gel, 1.0 wt.% HA-solution and 1.0 wt.% CS-solution. It was noticed that the 100 mg of HA did not dissolve easily (under 24 hours) in regular deionized water (pH 7). Therefore, the dissolution to 1.0 wt.% HA-solution was performed according to Kim et al. [59]. CS seemed to dissolve easier in regular deionized water, but to ensure the same starting point, it was decided that both HA and CS was dissolved in deionized water (pH 3.2-3.5). The dissolution was performed in a magnetic stirrer (RT) at the maximum speed (1000-11000 rpm) for 1-1.5 hours.

After preparation of individual components, they were blended together gently with a spatula in a volume per volume ratios (%) of 80:20, 60:40, 80:15:5 and 60:30:10 (COL:HA/CS/CS:HA); COL being the most abundant component in all of the blends. The blends were then injected into polytetrafluoroethylene (Teflon®) molds (d = 8 mm, h = 2 mm, Figure 6.1) through an injection needle, placed into a freezer for 24 hours (-30°C) and finally freeze-dried for 24 hours. The freeze-dryer (Figure 6.2) used in the present study was Heto RYWINNER with Heto CT 110 Cooling Trap (Jouan Nordic A/S, AllerØd, Denmark), attached to ILMVAC Rotary Vane Pump, Type PK 4 Dp (ILMVAC, Ilmenau, Germany).

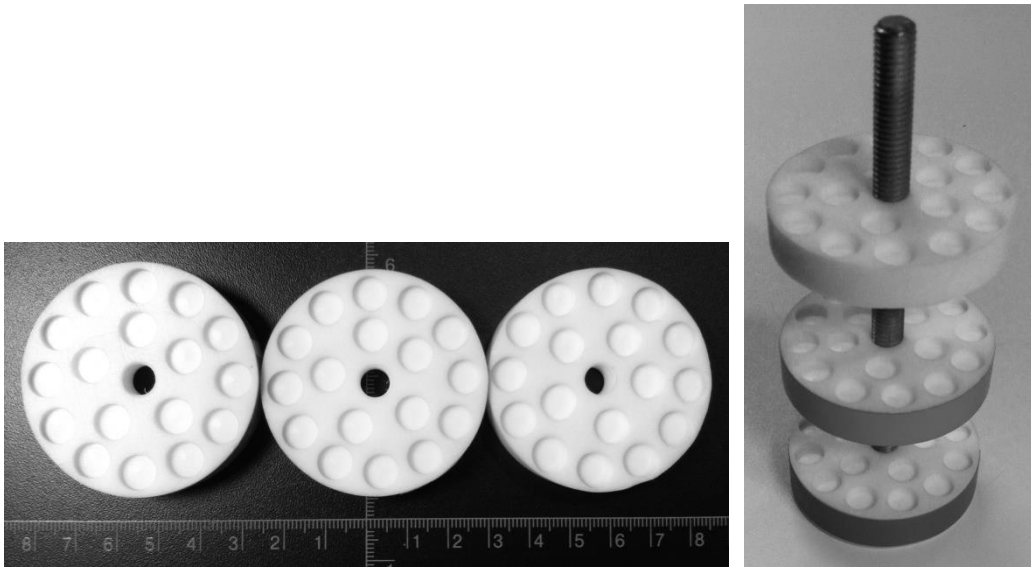

(a) (b)

Figure 6.1. *Polytetrafluoroethylene molds used in the present study; as disassembled (a) and as assembled (b).*

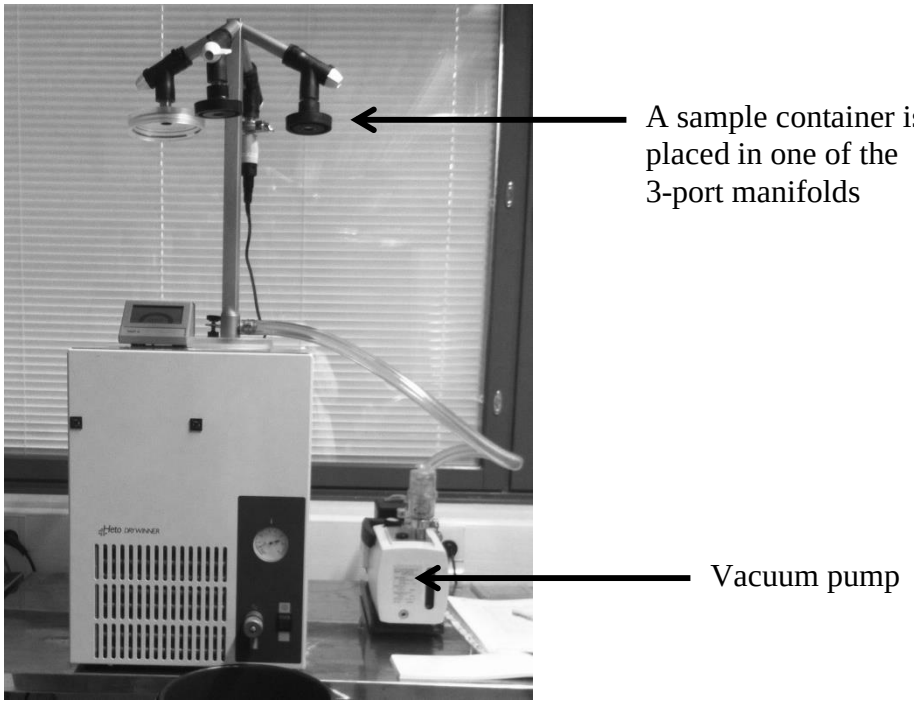

Figure 6.2. *The freeze-dryer used in the present study.*

6.2.1.2 Cross-linking

Freeze-dried scaffolds were cross-linked with either EDC/NHS or GP. The washing procedures after cross-linking, in both cases, were following: 5 minutes with 50% ethanol, 2 x 10 minutes with deionized water and 2 x 5 minutes in deionized water in an ultrasonic washer. The amount of ethanol or water was 10 ml (minimum) per scaffold at each stage of the washing. The EDC/NHS cross-linking solution was prepared by dissolving 14 mM EDC and 6 mM NHS in 95% ethanol. Each scaffold was immersed in 10 ml of EDC/NHS-solution for 4 hours in room temperature (RT). Immediately after washing scaffolds were placed in Teflon® molds, kept in the freezer (-30°C) for 24 hours and finally freeze-dried for 24 hours.

No standard GP cross-linking procedures is yet established in the literature, and therefore the GP cross-linking conditions were decided according to the amount of GP purchased and based on information collected from numerous sources (shown in the Appendix 8). In the present study 0.1 wt.% GP-solution was prepared by dissolving GP powder in 70% ethanol, and each scaffold was immersed in GP-solution (1.5 ml/scaffold) for 48 hours at 37°C.

After the EDC/NHS or GP cross-linking treatments, 6 scaffolds with the best structure from each group were selected by visual observation for the compression, swelling, FTIR and micro-CT testing. Prior and between the testing, all fabricated scaffolds were stored in a vacuum cabinet.

6.2.2 Characterization of scaffolds

For the characterization of the scaffolds, following methods were chosen: compression testing for dry and wet scaffolds (including study on the recovery from compression), water uptake and dimensional changes upon water uptake (swelling), FTIR spectroscopy and micro-CT imaging. All tests were carried out using 6 parallel scaffolds from each of the 11 different scaffold groups, with the exception of FTIR and micro-CT tests that were carried out on only one scaffold per group. EDC/NHS and GP cross-linked scaffolds grouped separately. For the names of the test groups see Table 6.4. Exceptionally, FTIR imaging was performed also for non-cross-linked scaffolds (one per each test group).

6.2.2.1 Water uptake and dimensional changes

The weights of the scaffolds were measured both in dry and wet conditions with a digital scale with an accuracy of 0.01 mg. For water uptake and dimensional changes upon water uptake characterization 6 parallel scaffolds from each scaffold group were soaked in 5 ml phosphate buffered saline solution (PBS) for 24 hours (37ºC). Two different methods were performed while weighing of the wet scaffolds (detailed descriptions on the next page). Fresh PBS (pH 7.4) was prepared every 2 weeks from reagents specified in Table 6.6 and according to the instructions seen in Table 6.7. All reagents in Table 6.6 are Products of J.T. Baker®, Netherlands and were purchased from VWR International Oy (Helsinki, Finland).

Table 6.6. *Reagents used for phosphate buffered saline solution.*

Reagent	CAS number	M_W [g/mol]	Molecular formula
Sodium hydrogen phosphate, anhydrous	7558-79-4	141.96	Na_2HPO_4
Sodium dihydrogenophosphate, monohydrous	10049-21-5	137.99	$Na_2HPO_4 * H_2O$
Sodium chloride	7647-14-5	58.44	NaCl

Table 6.7. *The instructions for the preparation of phosphate buffered saline solution.*

Reagent	5 liters of PBS (pH 7.4)
Na_2HPO_4	17.700 g
$Na_2HPO_4 * H_2O$	3.775 g
NaCl	29.500 g

The dimensions (diameter and height) of both dry and wet scaffolds were measured with a digital slide gauge with an accuracy of 0.01 mm. The comparable wet weight measurement was done to soaking wet scaffolds because filter drying causes the scaffolds to

shrink. The diameter and height change percentages were calculated with Equations 1 and 2.

$$Diameter\ change\ (\%) = \frac{d_{SW} - d_D}{d_D}, \quad (1)$$

where d_{SW} stands for the diameter measured from the scaffold in soaking wet condition and d_D for the diameter measured from the scaffold in dry condition.

$$Height\ change\ (\%) = \frac{h_{SW} - h_D}{h_D}, \quad (2)$$

where h_{SW} stands for the height measured from the scaffold in soaking wet condition and h_D for the height measured from the scaffold in dry condition.

Two different water uptake characterizations were performed on the wet scaffolds to assess their ability to absorb water. In the **first water uptake characterization** the scaffolds were lifted from PBS with tweezers, shaken gently to eliminate excess liquid drops and weighed soaking wet without drying (SW). With this method the ability of the scaffold structure to absorb water was determined as a whole (the material and the pores). After the first weighing, scaffolds were placed back in PBS (37ºC) for 1 hour. After 1 hour of recovery, the **second water uptake characterization** of the scaffolds was performed to determine the water absorption of the scaffold material itself (no excess water inside the pores). In this second method the same wet scaffolds were dried 15 seconds per side with filter paper and weighted again as filter dried (FD). The water uptake measurements were determined by calculating the change in weight between dry and wet condition of the scaffolds. The water uptake percentages were calculated by using Equations 3 and 4.

$$Water\ uptake\ of\ scaffold\ and\ pore\ system\ (\%) = \frac{w_{SW} - w_D}{w_D}, \quad (3)$$

where w_{SW} stands for the soaking wet weight and w_D for the dry weight of the scaffold.

$$Water\ uptake\ of\ scaffold\ only\ (\%) = \frac{w_{FD} - w_D}{w_D}, \quad (4)$$

where w_{FD} stands for the filter dried weight and w_D for the dry weight of the scaffold.

6.2.2.2 Compression strength

To determine compression properties, scaffolds were tested both dry and wet with Bose BioDynamic ElectroForce 5100 instrument (Figure 6.3). The manufacturer of the device is Bose (Minnesota, the United States) and the model is 5160 with a Bose 50 lbf load

transducer. Six parallel scaffolds from each scaffold group were tested to gain statistical value to the results. Scaffolds were placed between two compression platens shown in Figure 6.3. Tests parameters were: distance between compression platens (mm), compression speed (mm/min), preset value (N), scan time (s), and scan points (pcs). Compression was set to proceed up to 70% from the initial height, at the speed of 5 mm/min.

Due to the small size of the scaffolds, preset value was used to enable similar initial setting prior to compression. The machine lowered the upper compression platen by coming in contact with each scaffold to the point, where pre-determined preset value was reached. Preset value for dry scaffolds was set to 1.5 N and for wet scaffolds 0.7 N. The preset value for the wet scaffolds had to be adjusted into lower value because they were much softer compared to the dry scaffolds. After scaffold loading between the compression platens and presetting, distance of the platens was measured and used to calculate all the other parameter values. The scaffold became compressed by the lower platen moving up towards the stationary upper platen.

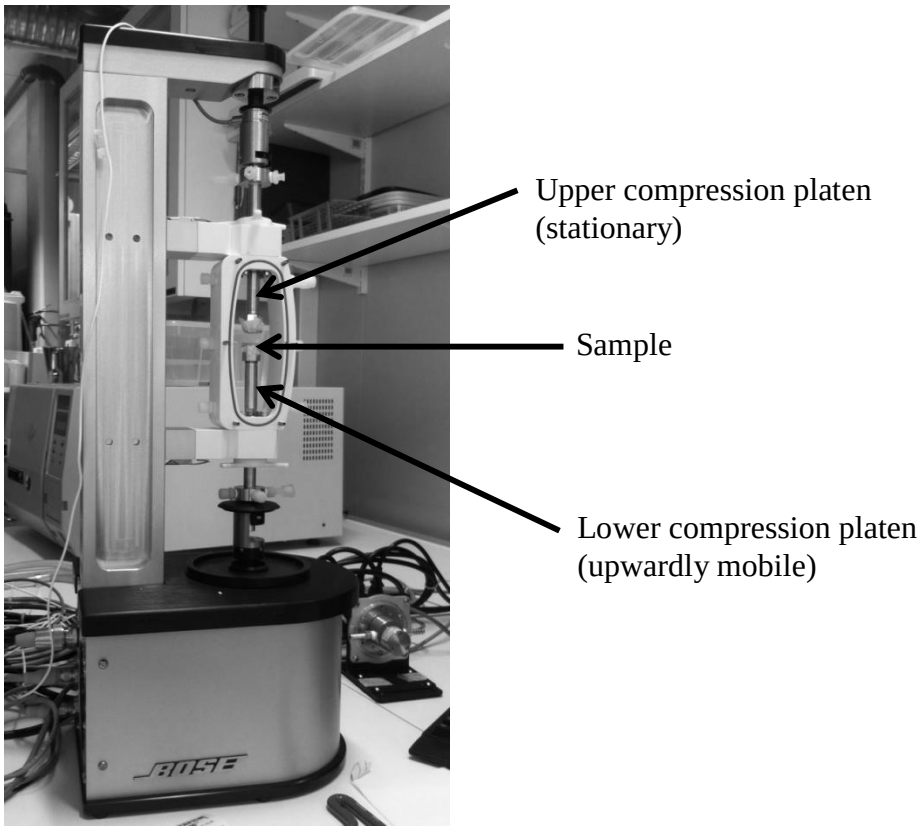

Figure 6.3. *Bose BioDynamic ElectroForce 5100 instrument for compression testing.*

Compression data (load and displacement values) was obtained from the software, and translated into stress-strain figures. The compressive modulus and compressive stiffness values were determined as mean ± standard deviation (SD) from 6 parallel scaffolds of each test group.

Compressive modulus, or elastic modulus equals the slope of the linear region of stress-strain diagram. The elastic region ranges up to the elastic limit, beyond which the

material breaks or no longer goes back to its original shape, when load is removed. It is also the maximum stress that can be applied to the material without permanent deformation. Equation 5 presents the relationship and direct proportionality of stress (σ), strain (ε) and compressive modulus (E). [112]

$$\sigma = E\varepsilon \tag{5}$$

The compressive modulus was defined as the slope of the linear region of each stress-strain curve. The linear region was defined as 7-11 % strain with dry scaffolds and 9 %-21 % strain with the wet scaffolds. The stress-strain curves of the wet scaffolds had a lot of interference (explained in more detail in the Results and Discussion). Therefore, the linear region of the wet scaffolds (from which the compressive modulus was obtained) was defined from a longer region to compensate the extensive interference. The compressive stiffness for each scaffold group was also determined from the compression data. Equation 6 shows that stiffness (k) is defined as load (or force, F) divided by displacement (x) caused by the load [3].

$$k = \frac{F}{x} \tag{6}$$

In connection with determining compression properties, scaffolds were tested for their ability to recover after the compression. Scaffold dimensions (d and h) were measured before and after the compression; recovery time being 10 minutes (RT) with the dry scaffolds and 1 hour in PBS (37ºC) with the wet scaffolds. Equations 6 and 7 were used to determine the ability of the scaffolds to return to their original size after the load had been removed.

$$Diameter\ change\ after\ recovery\ (\%) = \frac{d_{AC} - d_{BC}}{d_{BC}} \tag{7}$$

where d_{BC} stands for the diameter measured from the dry/wet scaffold before compression, and d_{AC} for the diameter measured from the dry scaffold after 10 minutes recovery (RT) or from the wet scaffold after 1 hour recovery in PBS (37°C).

$$Height\ change\ after\ recovery\ (\%) = \frac{h_{AC} - h_{BC}}{h_{BC}}, \tag{8}$$

where h_{BC} stands for the height measured from the dry/wet scaffold before compression, and h_{AC} for the height measured from the dry scaffold after 10 minutes recovery (RT) or from the wet scaffold after 1 hour recovery in PBS (37°C).

6.2.2.3 Fourier transform infrared spectroscopy and micro-computed tomography

FTIR spectroscopy was used to investigate the differences in the biochemical compositions of scaffolds before and after EDC/NHS and GP cross-linking. FTIR spectrum provides information on the molecular structure of materials. Assignment of the absorption peaks associated with major functional groups, such as amide, hydroxyl and carboxyl groups [132] help to identify specific chemical bonds, atoms and molecules as well as their movements relative to each other (e.g. bending, stretching [52]) [58].

A basic IR spectrum is presented as a diagram of either absorbance or transmittance percent on the vertical axis and frequency or wavelength on the horizontal axis. Absorbance is usually translated to transmittance, since the manual spectral libraries are provided in transmittance scale. Usually (and also in the present study) IR spectrum shows the intensity axis as transmittance per cents (0-100%). The analyzing of FTIR spectral data is further explained and discussed in the Results and Discussion. In the present study, the level of cross-linking was not analyzed from the FTIR diagrams, since it would have required additional methods (see the Results and Discussion).

FTIR spectroscopy imaging took place in the Department of Chemistry and Bioengineering at the Tampere University of Technology. Tests were performed with a potassium bromide (KBr) pellet method. The instrument used was Perkin Elmer Spectrum One FTIR Spectrometer (Waltham, MA, USA). 1-2 mg of each scaffold was milled, mixed with 200 mg of KBr powder and compressed (8.6 t, 10 min.) into a thin pellet. Each pellet was placed one by one into the spectrometer to obtain scaffold-specific spectral data. Types of the chemical bonds within the scaffolds were identified mainly according to the correlation tables by Tuure-Pekka Jauhiainen [52].

Micro-CT uses X-ray to produce image files that can be compiled to generate 3D images, from which quantitative analysis of material properties can be obtained without physically interfering with the scaffolds [81]. Micro-CT has been extensively used to image animal tissues (*in vitro*) [81], live animals (*in vivo*), metal etc. [45]. Micro-CT systems are typically optimized for spatial resolution to obtain an image that approaches histological microscopy as closely as possible. It provides images that retain information about 3D connectivity, density, topology and microarchitecture; with spatial resolution of 15–50 µm over a field view of 15-50 mm. [45]

The aim for micro-CT imaging in the present study was to obtain information on the inner pore structure and architecture and to see the possible differences that the different compositions and cross-linking treatments may have brought to the construct. Micro-CT scan and the reconstruction of the scaffolds were performed by M.Sc. Eng. Markus Hannula from Tampere University of Technology (Department of Electronics and Communications Engineering). Scanned area was 1 mm x 1 mm x 1 mm of each scaffold. Porosity and pore size data together with micro-CT images (available also in the Appendix 5) are presented in the Results and Discussion.

7 RESULTS AND DISCUSSION

7.1 Preliminary scaffolds

In cartilage tissue HA forms the backbone in complex proteoglycan structures immobilized in a COL network and CS chains attached to it [6]. COL II contributes 50-60% of cartilage's dry weight, proteoglycans 30-35% and non-collagenous proteins the rest [148]. In the adult cartilage GAGs form 15% of the cartilage's dry weight, from which approximately 85% consists of CS and 6% of HA [25]. The compositions of COL+HA/CS/CS+HA scaffolds in the present study were designed based on the aforementioned information on natural cartilage composition.

In the beginning it was unclear, what would be the most beneficial compositions the three components (COL, HA, CS) should be blended in. It was also necessary to study the individual concentrations in which the components should be mixed in order to produce a successful scaffold. There were several requirements that needed to be taken into account. First, COL, HA and CS solutions needed to be stiff enough to produce a scaffold construct that would stay in its 3D shape and simultaneously liquid enough to be blended homogenously. In addition, HA and CS powders had to be totally dissolved into the solvent (deionized water) within less than 24 hours.

After fabrication and prior to further steps (cross-linking and testing) the scaffolds were evaluated visually. Criteria for the selection were that the scaffolds should not contain separate phases, lumps, wrinkles etc., their shape and size should correspond to the molds they were fabricated in and the scaffolds should not collapse after removing them from the molds. Finally, they should be able to endure cross-linking and testing. All the different concentrations of the components of preliminary scaffolds, studied prior to actual scaffold fabrication are listed in Tables 7.1 and 7.2.

Table 7.1. *The concentrations of the components studied prior to blending.*

Component	Concentrations (wt.%)
COL	0.5, 1.0 (v/v)
HA	0.05, 0.5, 1.0 (m/v)
CS	0.05, 0.5, 1.0 (m/v)

Table 7.2. *The preliminary composite scaffolds.*

Blends	Concentrations (wt.%)	Mixing ratios (v/v)
COL + HA	0.5 + 0.05	3:1
	1.0 + 0.5	3:1
	1.0 + 1.0	3:1
COL + CS	0.5 + 0.05	3:1
	1.0 + 0.5	3:1
	1.0 + 1.0	3:1

HA solution was viscous with all the three different concentrations used. However, the 1.0 wt.% solution was notably more viscous than the other two making it difficult to blend HA homogenously with more liquid CS solution. When preparing 1.0 wt.% HA solution, deionized water (pH 7) turned out to be ineffective as a solvent. After adjusting the water to pH 3.2-3.5, 100 mg of HA powder was successfully dissolved in it. Plain HA and CS solutions were fabricated into freeze-dried scaffolds (Figures 7.1-7.2) in order to select the best concentration for further scaffold fabrication with COL.

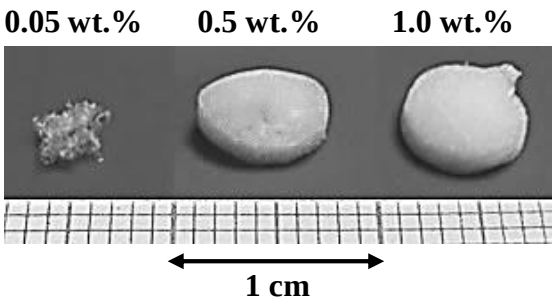

Figure 7.1. *Preliminary plain HA scaffolds after freeze-drying.*

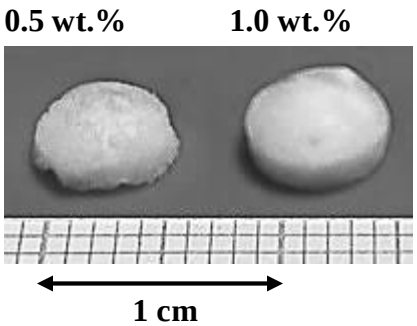

Figure 7.2. *Preliminary plain CS scaffolds after freeze-drying.*

CS solution turned out to be highly nonviscous with all three concentrations. Thus it was speculated, whether CS could be fabricated into freeze-dried scaffold without other components and whether it would withstand the cross-linking treatment. It turned out that with 0.05 wt.% CS there was no CS left in the Telfon® molds after freeze-drying, and

thus there are no 0.05 wt.% CS scaffolds to shown in Figure 7.2. However, with the concentrations of 0.5 wt.% and 1.0 wt.% the CS scaffolds could be fabricated (Figure 7.2).

From the Figures 7.1 and 7.2 it can be seen that the plain 1.0 wt.% HA and CS scaffolds turned out the best. Also the shape of the 1.0 wt.% scaffolds corresponded most the intended 3D matrix; having no obvious wrinkles, holes or twists. The extra peak on top of the 1.0 wt.% scaffold is caused due to excess solution material coming over from the mold. Furthermore, since there were no obvious separate phases detected in the freeze-dried scaffold, the 1.0 wt.% solution appeared to be distributed evenly, fulfilling the whole mold.

Next step was to test the scaffold fabrication with different concentrations. After gentle mixing to avoid air bubbles, blends were freeze-dried into 3D scaffolds to see the final outcome of different concentrations. The blending of 0.5 wt.% COL with 0.05 and 0.5 wt.% HA, or 0.05 and 0.5 wt.% CS was tested, but the fabricated composite scaffolds were too thin and coarse. Also, the highly liquid nature of the CS solution raised concerns about the scaffolds holding its shape after freeze-drying and cross-linking. Therefore, it was decided that 1.0 wt.% COL was used in all of the following blends as well as in the final (actual) scaffold fabrication. The concentrations and mixing ratios of the preliminary composite scaffolds are listed in Table 7.2. and Figure 7.3 shows photographs taken from some of the manufactured preliminary composite scaffolds.

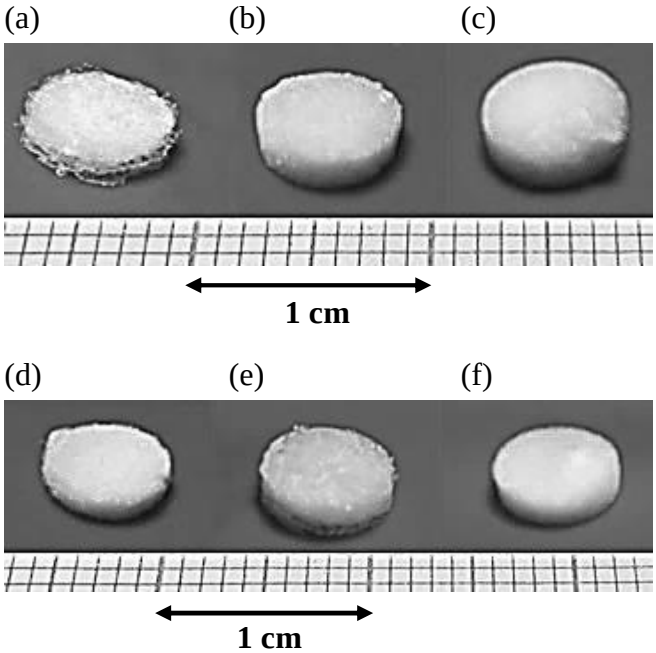

(a) 0.5 wt.% COL + 0.05 wt.% HA
(b) 1.0 wt.% COL + 0.5 wt.% HA
(c) 1.0 wt.% COL + 1.0 wt.% HA

(d) 0.5 wt.% COL + 0.05 wt.% CS
(e) 1.0 wt.% COL + 0.5 wt.% CS
(f) 1.0 wt.% COL + 1.0 wt.% CS

Figure 7.3. *Preliminary COL+HA/CS composite scaffolds.*

Based on visual characterization between freeze-dried scaffolds (Figures 7.1-7.3), the blend of 1.0 wt.% COL + 1.0 wt.% HA/CS appeared to produce the best scaffolds. The preliminary test scaffolds were cross-linked with EDC/NHS after freeze-drying in order

to evaluate their stability after processing. Their suitability for testing was assessed visually. All preliminary composite compositions appeared to endure the cross-linking treatment without collapsing or shrinking significantly.

Actual test scaffolds were composites of COL+HA, COL+CS and COL+CS+HA and the final compositions of the scaffolds were decided based on natural cartilage composition [137, 23]: COL as the predominant component (80 or 60 wt.%) and the rest of being either HA and/or CS. In COL+CS+HA composites COL was mixed together with more CS than HA, as they are in native cartilage tissue. The final compositions and concentrations of the actual test scaffolds are presented in Table 7.3.

Table 7.3. *The final blends, concentrations and component compositions of the actual test scaffolds.*

Blends	**Concentrations (wt.%)**	**Blend compositions (wt.%), i.e. (v/v)**	**Notations**
COL + HA	1.0 + 1.0 (v/v) + (m/v)	80:20 60:40	C80H C60H
COL + CS	1.0 + 1.0 (v/v) + (m/v)	80:20 60:40	C80CS C60CS
COL + CS + HA	1.0 + 1.0 + 1.0 (v/v) + (m/v) + (m/v)	80:15:5 60:30:10	C80CS15H C60CS30H

Scaffolds in Table 7.3 were freeze-dried after blending and cross-linked with either EDC/NHS or GP. Additional test group (a control group), not seen in the Table 7.3 was 1.0 wt.% COL (C100). Figure 7.4 shows some examples of the best and worst scaffolds after fabrication; additional photographs of the scaffolds are in the Appendix 1 (the photographs of the scaffolds before and after cross-linking).

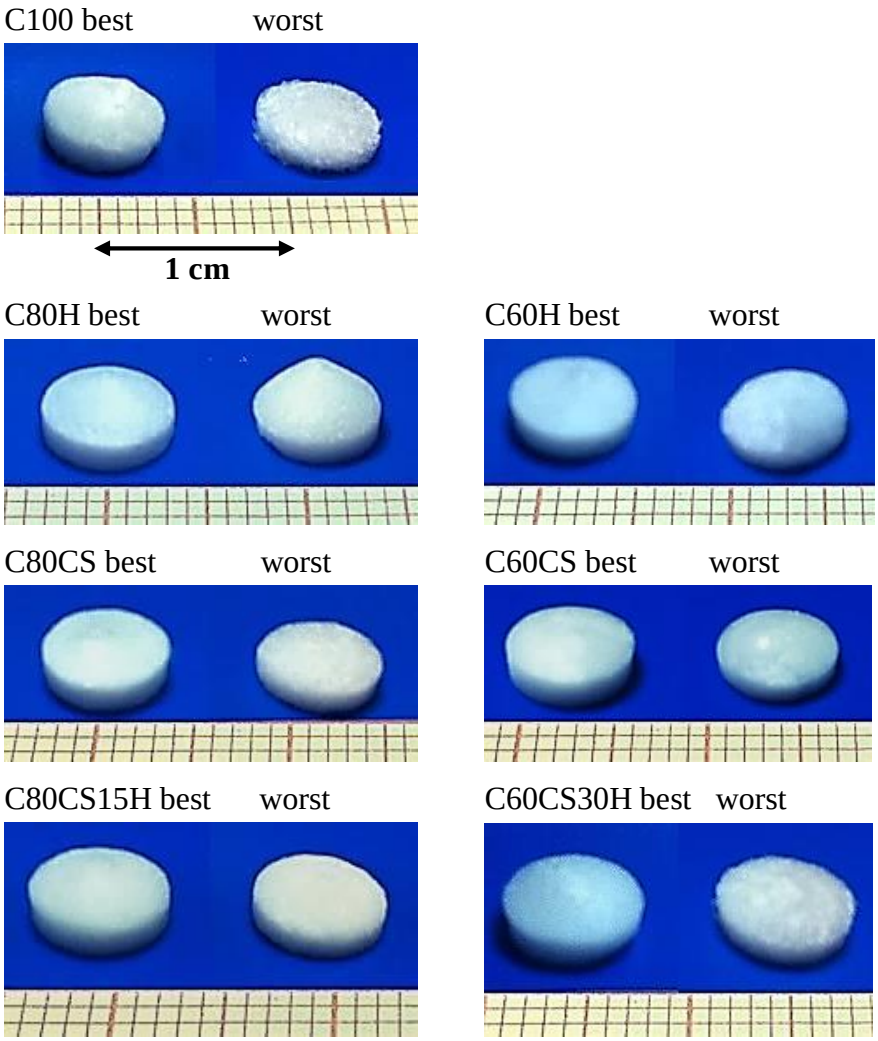

Figure 7.4. *The actual test scaffolds after fabrication by freeze-drying, including examples of the most (best) and the least (worst) successful scaffolds.*

Visual examination of the actual scaffolds after freeze-drying (Figure 7.4) revealed that all combinations and compositions produced rather similar looking scaffolds. When comparing the most successfully fabricated scaffolds (best in Figure 7.4), none of them seemed to be significantly better or worse than others. However, the differences became clearer when observing the least successful scaffolds. The compositions of C80H/CS, C80CS15H and C60CS produced the best overall looking scaffolds. These four groups maintained smooth surface as well as rounder and thicker shape even with the least successful scaffolds, whereas the C60H, C60CS30H and C100 scaffolds appeared thinner, more lumpy or coarse. These observations ultimately led to the decision that all groups with only 60 wt.% COL would be omitted from GP cross-linking. However, all the scaffolds were cross-linked with EDC/NHS.

7.2 Cross-linking

The actual test scaffolds were cross-linked after freeze-drying with either EDC/NHS or GP, after which they were freeze-dried for the second time. Since the visual characterization of the 80 wt.% COL containing composite scaffolds generally showed better structure than the 60 wt.% COL containing scaffolds; the former were chosen for the GP treatment. EDC/NHS cross-linking was carried out to all of the scaffold groups.

Figure 7.5 presents some of the photographs taken before and after EDC/NHS or GP cross-linking. Photographs taken after GP treatment revealed that GP colored the scaffolds dark grey. This is a common effect reported in the literature caused by GP reacting with free amino acid residues [145, 147]. The best scaffolds from each scaffold group are shown in Figure 7.5 as an example of the effect that the cross-linking treatments had on the scaffolds. The Appendix 1 shows the photographs of all the different scaffolds, taken before and after the cross-linking treatment.

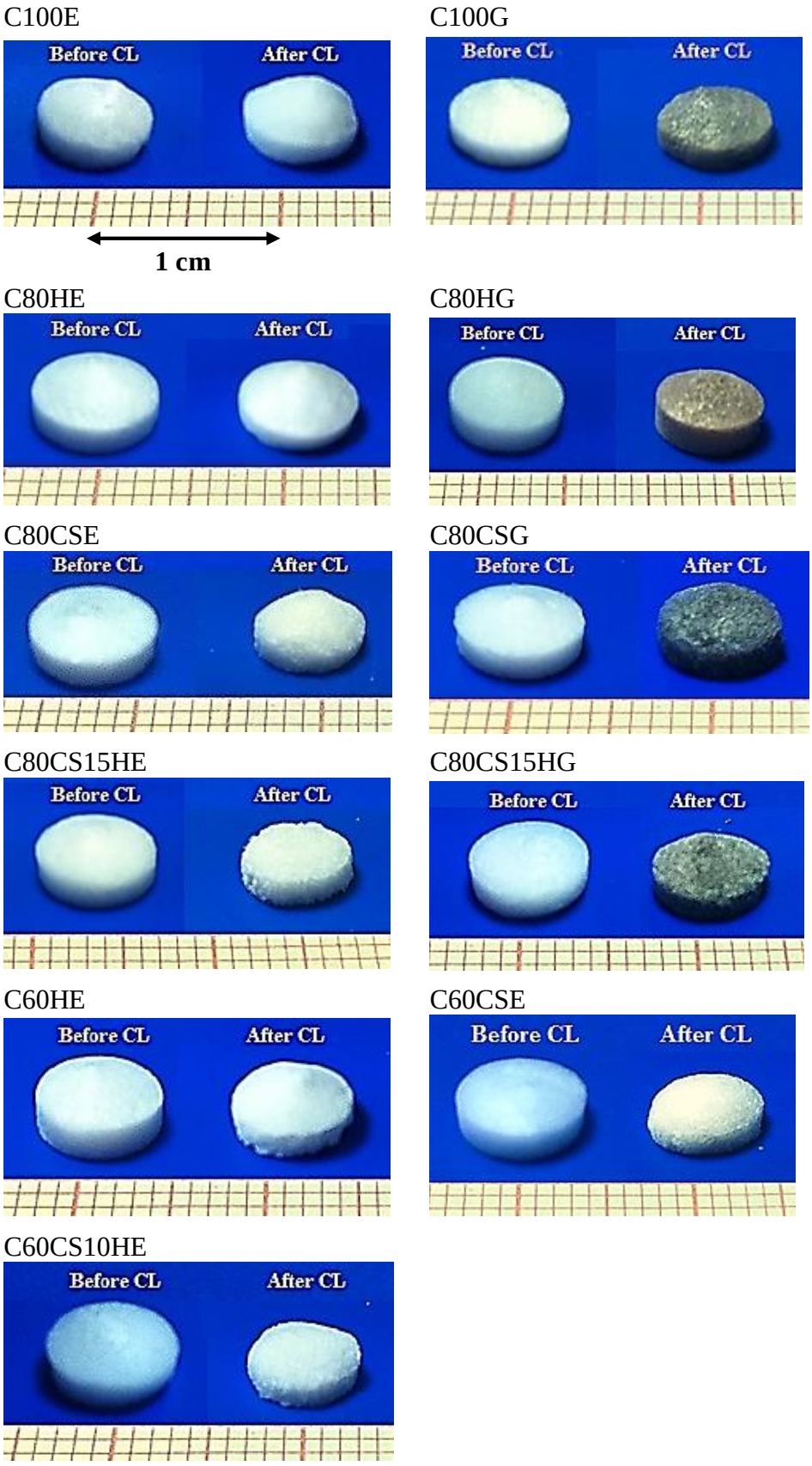

Figure 7.5. *Photographs of the scaffolds taken before and after EDC/NHS or GP cross-linking. Images show the most successful scaffold structure of each group. Note that the adjacent images are most likely taken from different scaffolds.*

All GP cross-linked scaffolds experienced approximately 0.5-1 mm shrinkage in diameter (data not shown), whereas the EDC/NHS treated scaffolds shrunk even less in diameter. In fact, some of the C100E and C80HE scaffolds managed to maintain their diameter intact and only maximum of 0.2 mm shrinkage was seen in other EDC/NHS treated scaffolds. However, the biggest shrinkage in diameter was seen with the EDC/NHS cross-linked CS containing scaffolds. Especially the C60CSE scaffolds shrunk noticeably; in some cases as much as 2 mm. The C60CSE as well as C80CS15HE and C60CS30HE scaffolds did not maintain their round and even shape but instead appeared as flatten and rough edged. The same phenomenon was seen with some of the C80CSG scaffolds and with the C100E and C80CS15HG scaffolds. It is noteworthy that even though the shape of the plain COL scaffolds suffered after EDC/NHS cross-linking treatment, their diameter remained close to the one measured before cross-linking. Note that the differences in diameter of the scaffolds are better seen in the photographs presented in the Appendix 1 as a contrast to the images shown in Figure 7.5.

After EDC/NHS treatment a majority of the scaffolds also showed shrinkage in height (data not shown), whereas GP made most of the scaffolds slightly thicker; evident especially with the C100G and C80HG scaffolds (Figure 7.5). Besides intramolecular and short-range intermolecular cross-links formed with EDC/NHS and GP, additional long-range intermolecular cross-links are formed in connection with GP cross-linking [77], resulting in scaffolds that hold their shape better. The C100G and C80HG scaffolds also seemed to have smoother surface after being treated with GP. However, the other two groups, i.e. C80CSG and C80CS15HG looked quite the opposite. In fact, the GP cross-linked C80CS and C80CS15H scaffolds did not only shrunk more in height but they also appeared significantly more uneven and rough. All in all, these two groups were the least successful scaffolds after GP cross-linking. In addition, especially the C80CSG and C80CS15HG scaffolds did not for some reason withstand the second freeze-drying, and/or the multiple washing procedures involving gentle shaking. During these steps some inner pores may have collapsed and/or some small pieces become detached from the scaffolds resulting in such poor appearance.

Scaffold groups that held their original shape and size the best after GP cross-linking were the C100 and C80H scaffolds. The most damaged groups after GP treatment were C80CS and C80CS15H. As a comparison, the groups that endured the EDC/NHS cross-linking the least, both in diameter and in height were the C60CS, C80CS15H and C60CS30H scaffolds. It seems that both cross-linking treatments caused especially CS containing composites to lose their round and even shape, in addition to their original thicker size. The fact that plain CS scaffolds dissolved entirely into the 50% ethanol during washing procedures, raised concerns that the washing steps might have dissolved some of the CS from the CS containing composites regardless of being cross-linked. This could be the reason, why the CS containing composites looked inferior after cross-linking treatments compared to the scaffolds without CS. Washing of plain CS scaffolds was furthermore tested with 95% ethanol, in which the scaffolds did not dissolve and with deionized water, in which the plain CS scaffolds dissolved totally.

When comparing the EDC/NHS and GP treated scaffolds, it is evident that both produced visually different looking scaffolds; in terms of size, shape and surface. Even though there has not been reported results between GP and EDC/NHS cross-linked freeze-dried scaffolds, Sung et al. [123] used GP comparatively with EDC for cross-linking of biological tissues. They found out that GP cross-linking was slower than carbodiimide cross-linking and that the tissue fixation with GP versus EDC may produce distinct cross-linking structures. [123] The different outcome of the GP treatment as opposed to EDC/NHS treatment is most likely due to the fact that GP forms additional intermicrofibrillar cross-links between COL molecules, whereas the EDC forms only intrahelical and interhelical cross-links. The additional intermicrofibrillar cross-links between adjacent COL microfibrils affect significantly on the mechanical properties such as shrinkage and ruptured pattern of the GP treated material [123]. However, in the present study there were only four GP cross-linked groups to compare between the seven EDC/NHS cross-linked groups. Therefore, in order to be certain which of the two crosslinkers could produce better looking or otherwise superior scaffolds it is recommendable to study this more widely in the future.

Regardless of being treated with either EDC/NHS or GP, all the scaffolds in every group shrunk in diameter; the GP cross-linked more than the EDC/NHS cross-linked scaffolds. The reason for this could be the cross-linking treatment itself and/or the second freeze-drying. The second time freeze-drying could have broken both the inner pore structure as well as the outer surface of some of the less successfully fabricated scaffolds causing them to shrink noticeably. Visually the most damaged scaffolds after EDC/NHS cross-linking were the CS containing scaffolds and after GP treatment the plain COL and C80CS15H scaffolds. Park et al. [107] reported results that support the assumption that a cross-linking treatment could be the reason for the shrinkage of freeze-dried scaffolds. A slight decrease in the porosity and pore size of the COL+HA membranes that Park et al. [107] fabricated by freeze-drying (at -20°C) was noticed; indicating shrinkage of the constructs. Furthermore, Sung et al. [123] stated that the shrinkage of EDC/NHS or GP cross-linked tissues are due to a contraction of the COL network, which may be associated with intrahelical, interhelical (EDC and GP) or intermicrofibrillar (GP) cross-links introduced into the COL fibers. These observations support the visual observations that the scaffolds can indeed shrink to some extent after either of the two cross-linking treatments.

Individual differences seen between the scaffolds of a same group are most likely due to different microstructures formed in the scaffolds during fabrication. This was due to the processing method (freeze-drying), where many different characteristics, such as temperature gradients during the procedure influenced to the final structure of the fabricated scaffolds. These could not have been avoided during selection of the scaffolds for cross-linking treatments, since the microstructure is not visible to the naked eye. In addition, some of the scaffolds were significantly smaller than others, which may have caused them to suffer more during the cross-linking.

7.3 Microstructure of the scaffolds

Scaffold microstructure effects the *in vitro* cell adhesion, ingrowth and reorganization and ultimately results in the success or failure of the scaffold construct [111]. TE scaffold should possess an interconnected pore structure with high porosity (usually exceeding 90%) [111] and with large surface/volume ratios in order to provide sufficient space for cell growth and proliferation [22]. Moreover, the pore interconnectivity directly influences to the diffusion of physiological nutrients and gases to cells as well as to the removal of metabolic waste and by-products from cells. [111] In the present study the porosity, pore size and structure of the different scaffolds were studied with micro-CT imaging. Figure 7.6 shows series of micro-CT images of the scaffolds. In addition, the material thickness, porosity and pore size data is presented in Table 7.4. Additional micro-CT images are available in the Appendix 5.

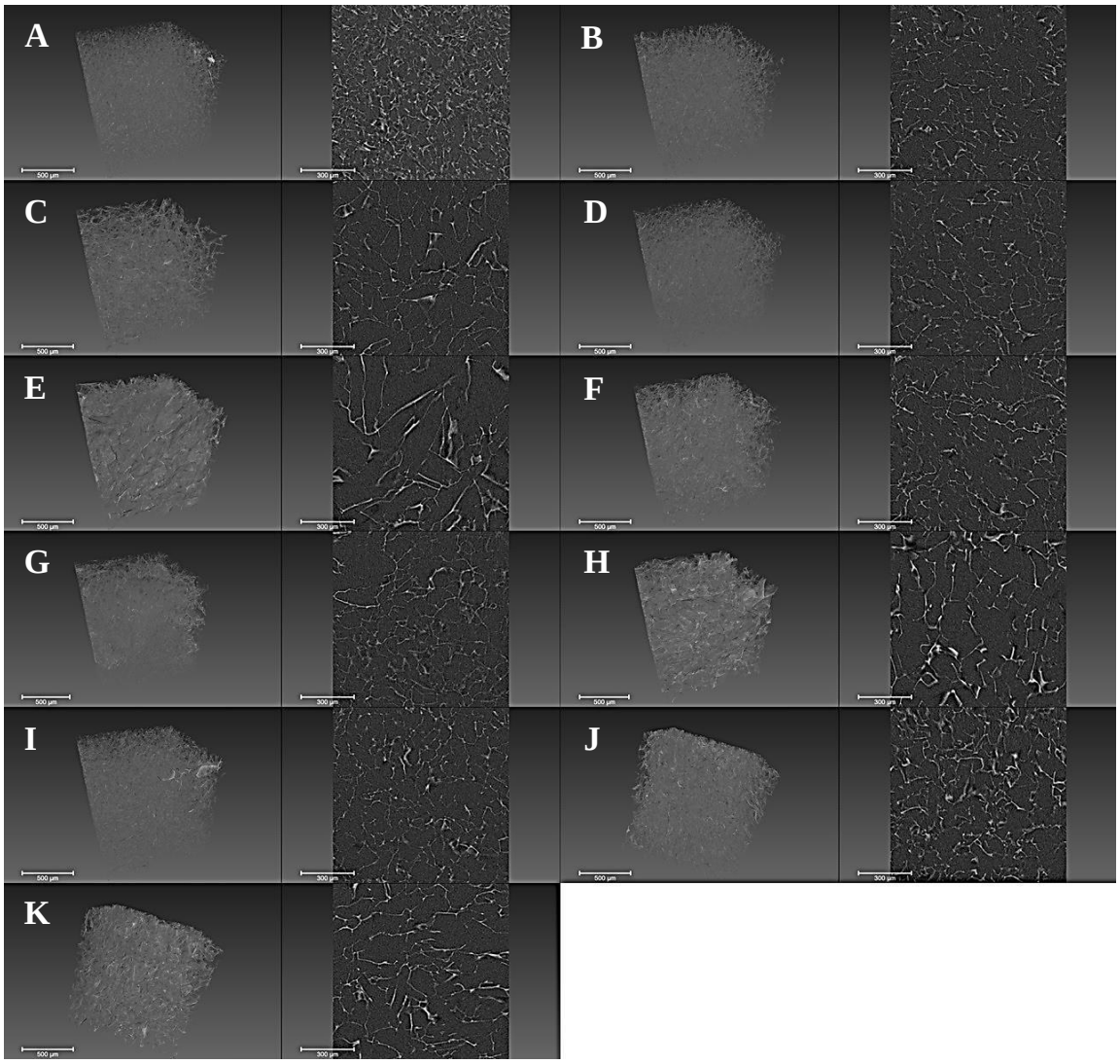

Figure 7.6. *Micro-CT images of the scaffolds: C100E (A), C100G (B), C80HE (C), C80HG (D), C80CSE (E), C80CSG (F), C60HE (G), C60CSE (H), C80CS15HE (I), C80CS15HG (J) and C60CS30HE (K). Scale bars are 500 µm on the left frame and 300 µm on the right frame.*

Table 7.4. *The porosity, material thickness and pore size data of the scaffolds obtained from micro-CT imaging.*

Scaffold group	Porosity [%]	Material data		Porosity data	
		Material thickness [μm] (mean ± SD)	Max. material thickness [μm]	Pore size [μm] (mean ± SD)	Max. pore size [μm]
C100E	88	7 ± 2	17	26 ± 10	70
C100G	92	7 ± 2	15	36 ± 10	78
C80HE	94	7 ± 2	17	54 ± 16	112
C80HG	91	7 ± 2	14	38 ± 12	83
C60HE	92	6 ± 2	16	40 ± 13	92
C80CSE	89	7 ± 2	19	57 ± 25	145
C80CSG	91	7 ± 2	17	41 ± 14	99
C60CSE	90	7 ± 2	17	54 ± 21	125
C80CS15HE	91	7 ± 2	15	40 ± 13	101
C80CS15HG	88	7 ± 2	23	37 ± 6	132
C60CS30HE	91	7 ± 2	15	57 ± 22	118

7.3.1 Porous structure of the scaffolds

The A-K images (in Figure 7.6) show a 3D reconstruction of each scaffold (on the left taken from 1 mm x 1 mm x 1 mm area) and a 2D cross-sectional view (on the right). Images E, F, H-K in Figure 7.6 represent the CS containing scaffolds. The inclusion of CS to COL may be the reason for greater voids seen in most of their microstructure; particularly visible in images E, H and K. The effect of CS on the microstructure of the scaffolds is also seen, when comparing the COL+CS scaffolds to the corresponding COL+HA scaffolds. Both EDC/NHS and GP cross-linked CS containing scaffolds had bigger pores compared to the CS containing scaffolds; evident from the data shown in Table 7.4. The plain COL scaffolds had the smallest pores. In a study by Douglas et al. [23] CS was reported to be the reason for COL fibrils to become thinner. The data in Table 7.4 demonstrate that the maximum material thickness in the COL+CS scaffolds is slightly bigger than in the COL+HA scaffolds. Obviously the inclusion of CS to COL did not have similar effect on the material thickness of the scaffolds fabricated in the present study.

In Figure 7.6 the images B, D, F and J represent the GP cross-linked scaffolds. When comparing the EDC/NHS cross-linked scaffolds to the GP cross-linked, the latter treatment seems to have produced scaffolds with a denser pore structure as well as smaller pore sizes (more clearly visible from the additional micro-CT images in the Appendix 5). In fact, this can be observed in all the images of the scaffolds with the exception of plain COL scaffolds, where the C100E (image A in Figure 7.6) scaffold appear significantly more compact and denser than the C100G (image B in Figure 7.6) scaffold. The data shown in Table 7.4 support the aforementioned observation by demonstrating smaller

pore sizes (and denser microstructure) in GP cross-linked scaffolds compared to corresponding EDC/NHS cross-linked scaffolds; only exception being, again the C100 scaffolds. The denser microstructure of the GP scaffolds could be explained by the intermicrofibrillar cross-links that GP creates between COL molecules pulling the adjacent COL microfibrils closer to each other. Similar cross-links are not known in connection with EDC treatment [123], therefore resulting in bigger voids seen in the EDC/NHS cross-linked scaffolds.

Even though the microstructure of all the scaffolds was demonstrated as highly porous and interconnected, some heterogeneity (i.e. presence of large pores, local regions of higher density etc.) is also visible in the micro-CT images. Some heterogeneity is seen in the microstructure of the C80CS15H/G scaffolds, whereas in the C80HE, C60HE and C80CSE/G scaffolds the heterogeneity is more dominant. In the case of COL+HA scaffolds this may be due to the relatively high concentration of COL or COL+HA suspension (1 wt.%) used in the scaffold fabrication. The viscous nature of the two solutions may have caused somewhat heterogeneous blending. Instead, with the groups containing CS the cause of heterogeneity may be due to the blending of the extremely liquid CS to much more viscous COL and/or HA solutions.

7.3.2 Porosity

The data in Table 7.4 shows that all the scaffolds had high porosity ranging from 88% to 94%. The lowest porosity (88-89%) was detected with the C80CS15HG, C100E and C80CSE scaffolds. The three scaffold groups with the highest porosities (92-94%) were the C80HE and C60HE and C100G scaffolds. Tissue engineered scaffolds should possess over 90% porosity in order to allow the infiltration and growth of cells. However, an increased porosity of well over 90% can cause the scaffold to lose significantly its compressive strength. [111] The compressive modulus result obtained from the C80HE scaffolds (Table 7.4) demonstrated that their well over 90% exceeding porosity (94%) did not affect their compressive properties negatively, when comparing their compressive modulus to the scaffolds with a lower porosity (Figures 7.9-7.10).

GP cross-linked scaffolds have been reported to exhibit porosities as high as 90-95% [64, 63]. In the present study the porosity of GP cross-linked scaffolds ranged from 88% to 92%. The porosities obtained from EDC/NHS cross-linking were between 88% and 94%. As a conclusion, both treatments showed optimal porosity values without being significantly better or worse over the other.

Further comparison between the corresponding EDC/NHS and GP cross-linked scaffolds revealed that the C100G and C80CSG scaffolds had higher porosities than the C100E and C80CSE scaffolds, whereas the C80HG and C80CS15HG scaffolds had lower porosities than the C80HE and C80CS15HE scaffolds. In study by Ko et al. [64] the porosity was reported lowest in cross-linked COL+CS+HA scaffolds (90%) compared to cross-linked plain COL scaffolds (95%) and to non-cross-linked COL scaffolds (96%). Based on the results of Ko et al. and on the results of the present study, the porosity of the scaffolds may rather be affected by the varying compositions of the raw materials than

the cross-linking treatment. By analyzing the COL+HA and COL+CS compositions, it appears that in the GP cross-linked scaffolds HA could rather be the reason for the slight decrease in the porosity of the composites than CS. However, despite of the different cross-linking methods and scaffold compositions the porosity values of all the scaffolds were rather similar. Thus, these minor differences can also be due to the fabrication process.

7.3.3 Pore size and material thickness

In addition to a sufficient degree of porosity, generating a specific pore size and pore structure must be taken into account in order to produce a successful tissue engineered scaffold. Pores must be large enough to allow migration and ingrowth of the cells towards the center of the scaffolds. At the same time pores should be sufficiently small in order to provide adequate ligand density for cellular attachment. [22] When pores become too large, the internal surface area of the scaffold decreases. On the other hand, when the pore size is too small (pore diameter less than ~10 µm), it can prevent cellular penetration within the scaffold and eventually result in ingrowth of fibrous tissue. [111] The ideal pore size depends not only on the purpose of the scaffold but is also defined based on whether it should endure high mechanical strength or not. In addition, different cell and tissue types may need different amount of space when reorganizing the scaffold matrix.

In the present study the pore sizes of the fabricated scaffold ranged from 26 µm to 57 µm (Table 7.4). The biggest pores (over 50 µm) were detected in the C80HE, C80CSE, C60CS30HE and C60CSE scaffolds. Scaffolds with the smallest pores (under 40 µm) were C100E, C100G, C80CS15HG and C80HG. A study by Griffon et al. [35] support the idea that larger (70-120 µm) interconnective pores improve the cellularity and matrix content within the scaffold and potentially produce a larger construct in less time. On the other hand, pores smaller than 50 µm in diameter are recommended in order to improve mechanical strength of engineered constructs. Furthermore, small pores (supposedly ranging from 2.5 to 6.5 nm) are naturally present in the native cartilage matrix. [65] Based on these two arguments, scaffolds with small pores may nevertheless be the best choice towards successful chondrogenesis [35].

Matsiko et al. [89] have reported results, in which the addition of HA to COL caused a significant reduction in scaffold mean pore size compared to COL+CS and plain COL scaffolds. The results of the present study suggest otherwise. Plain COL (both EDC/NHS and GP treated) as well as the C80CS15HG scaffolds demonstrated smaller pore sizes compared to any of the COL+HA scaffolds. In fact, the pores in the C100E scaffolds were significantly smaller compared to all other scaffolds. The image A in Figure 7.6 as well as the data in Table 7.4 support this. Not much can be deduced based on the micro-CT images taken from one scaffold, but one explanation to this could also be that the selected plain COL scaffold could simply have had smaller pores than other fabricated COL scaffolds.

In the study by Ko et al. [64] the researchers cross-linked type II COL (COL2) and COL2+HA+CS scaffolds with GP and demonstrated that CS and HA decreased the porosity of the scaffolds compared to plain COL (cross-linked and non-cross-linked) scaffolds. Similar results were obtained also in the present study, since the porosity of all COL+CS+HA scaffolds were smaller than the GP cross-linked plain COL scaffolds. However, it should be noted that the EDC/NHS cross-linked C100 scaffolds had lower porosity than the C60CS30HE and C80CS15HE (and C100G).

In general, the pore sizes differed more than the material thickness between the scaffolds. In fact, the wall thickness of the scaffolds remained roughly the same regardless of the composition or the cross-linking treatment (Table 7.4). The data in Table 7.4 shows that the four scaffolds with the thickest pore walls all contained CS to some extent. This is an interesting remark, since the CS solution in the blending phase seemed almost too liquid to be fabricated into a solid construct. It may be that the inclusion of highly liquid CS to more viscous plain COL or COL+HA solution diluted the blend and caused bigger pores. Furthermore, when the total amount of polymer in the blend is the same in all of the scaffolds, the end result is seen as thicker pore walls.

It should be noted that the micro-CT images were taken from one visually selected scaffold per each group. Therefore, the selected scaffolds could have contained inner defects (collapsed pores, separate phases) that have affected the results.

7.4 Compression testing

A tissue engineered scaffold should have sufficient mechanical strength during the whole *in vitro* culturing in order to maintain the open pore structure required for cell ingrowth and matrix formation. With sufficient compressive strength and compressive stiffness, ability to recover etc. the structural integrity of the scaffold is possible to retain until the newly grown tissue is able to support loads and stresses and can assure its structural role. [111] In the present study the mechanical properties of the scaffolds were evaluated by performing compression tests separately on both dry and wet scaffolds. The small size of some of the scaffolds, especially from groups C60CS, C80CS15H and C60CS30H made it difficult to measure the compression properties of the scaffolds accurately. Compressive modulus of the different scaffolds are shown in Figures 7.9-7.10. Compressive modulus results of relatively similar scaffolds of other studies are shown in the Appendix 7 for comparison. However, varying fabrication and cross-linking methods, scaffold sizes and shapes as well as any additional processing steps should be taken into account when comparing the results.

7.4.1 Compressive modulus

The compressive stress-strain curves of the scaffolds are shown in Figure 7.7 (dry scaffolds) and in Figure 7.8 (wet scaffolds). The curves present one scaffold from each group, chosen as the best representative scaffold from each group. Additional stress-strain dia-

grams are available in the Appendices 3 (dry) and 4 (wet). Figures 7.9 show the compressive modulus of the dry scaffolds and Figure 7.10 the compressive modulus of the wet scaffolds.

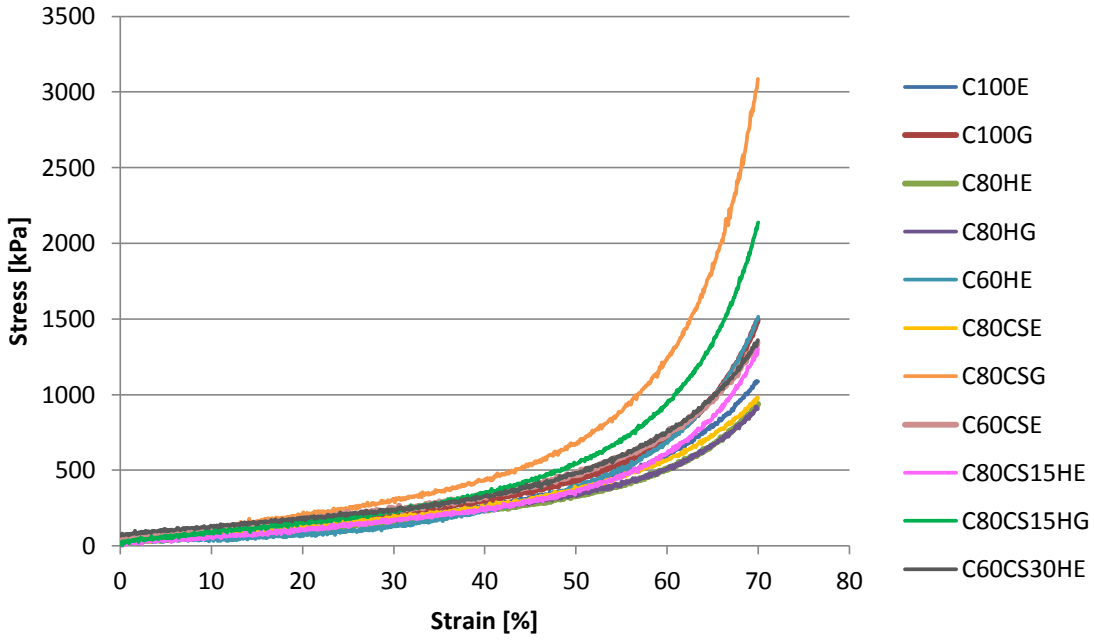

Figure 7.7. *The compressive stress-strain curves obtained from the dry scaffolds.*

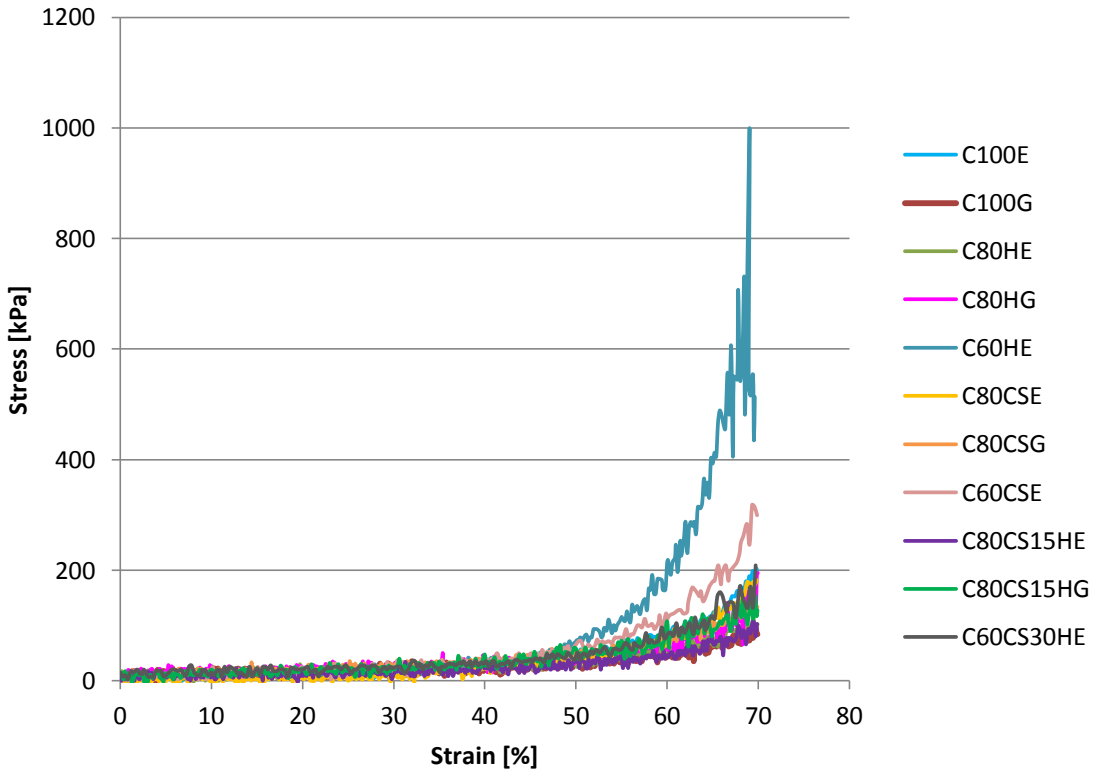

Figure 7.8. *The compressive stress-strain curves obtained from the wet scaffolds.*

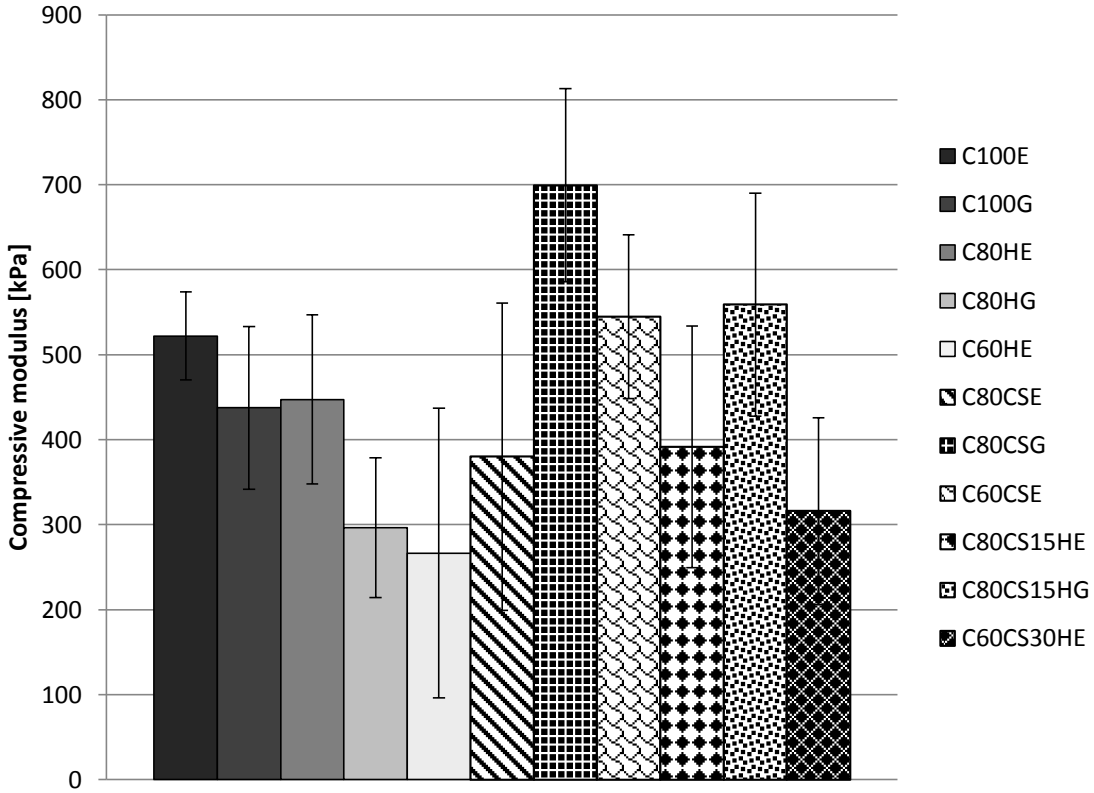

Figure 7.9. *Compressive modulus results of the dry scaffolds. Results shown as mean ± SD.*

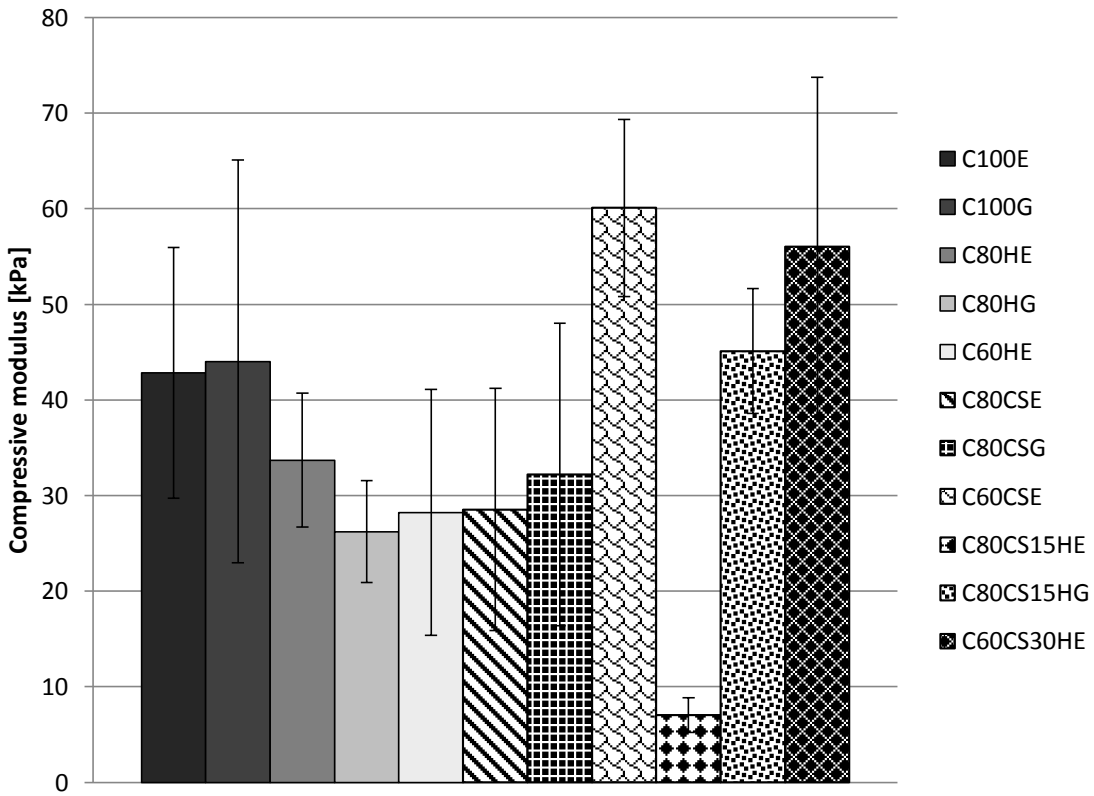

Figure 7.10. *Compressive modulus results of the wet scaffolds. Results shown as mean ± SD.*

As it can be seen from the compressive stress-strain curves in Figure 7.7, the stress values of the dry scaffolds rose steadily after the linear region (approximately up until 15% of strain). Instead, in the stress-strain curves of the wet scaffolds (Figure 7.8) the stress values stayed relative low until 40% of strain. In both cases the slope of the curves increased rapidly after 50-60% of strain, demonstrating the final densification regime [87]. Due to the lower stress values and the higher interference seen in the stress-strain curves of the wet scaffolds (Figure 7.8), the area of linear region (from which their compressive modulus values were determined) was longer than the linear region of the dry scaffolds.

Comparison between Figures 7.9 and 7.10 show the difference in compressive modulus of the dry and wet scaffolds. As it was expected, the dry scaffolds had significantly higher compressive modulus than the corresponding wet scaffolds. The compressive modulus values of the dry EDC/NHS cross-linked scaffolds were approximately 6-13 times higher compared to the corresponding wet scaffolds. The difference between the dry and wet scaffolds was even greater when comparing the groups of GP cross-linked scaffolds. The dry GP-scaffolds exhibited approximately 10-22-fold compressive modulus values compared to the similar wet scaffolds.

The three dry scaffold groups that had the highest compressive modulus (C80CSG, C80CS15HG and C60CSE) all contained CS. Similarly, the three groups that had the highest compressive modulus of the wet scaffolds (C60CSE, C60CS30HE and C80CS15HG) also contained CS. From these results it can be deduced that that the inclusion of CS to plain COL and COL+HA could have a positive effect on compression properties. Kangjian et al. [56] have reported somewhat similar results. According to them CS was the reason for the increase in the tensile strength of COL+Chi+CS scaffolds (compared to COL+Chi scaffolds). However, from the results of the present study it should be noted that one of the CS containing scaffolds (wet C80CS15HE) showed the lowest compressive modulus. Other two scaffold groups with the lowest compressive modulus were wet C80HG and C60HE scaffolds.

From the results presented in Figure 7.10 it should be noted that the compressive modulus obtained from wet C80CS15HE scaffolds is partially controversial. Due to this is the fact that half of the scaffolds (3/6) gave values that needed to be excluded from the mean calculations. Moreover, the three abandoned values differed from each other to the extent that it is recommended to perform similar measurements with similar scaffolds in the future to get more reliable results for this combination. There was no obvious reason that could explain why half of the measurements of the C80CS15HE scaffolds failed. However, one explanation could be the small size of the scaffolds that caused too much interference to the measurements.

In summary, the biggest compressive modulus values measured from the dry scaffolds were C80CSG, C80CS15HG and C60CSE, and from the wet scaffolds C60CSE, C60CS30HE and C80CS15HG. Lowest compressive modulus values were obtained in terms of both dry and wet scaffolds from the C60HE and C80HG scaffolds. From these results it can be deduced that the compositions of either COL+CS or COL+HA effected

more on the compressive properties of the scaffolds than the different cross-linking treatments. In general, both dry and wet CS containing composites exhibited higher compressive modulus than the HA containing composites.

It should be noted that the compression machinery used in the present study is very sensitive. Thus some unintentional shaking of the table (where the equipment was on) could have caused some high individual peaks in the stress-strain curves. Especially the wet compression testing was extremely challenging due to the small size and softness of the scaffolds. This caused extensive interference; seen as clusters of high peaks throughout the stress-strain curves of the wet scaffolds (in the Appendix 4). Moreover, couple of the smallest wet scaffolds did not reach the 70% compression because the two compression platens came too close to each other, causing the machine to abort prematurely. However, this did not affect the overall compressive modulus and compressive stiffness results, since any exceptional values were excluded from the mean calculations.

7.4.2 Compressive stiffness

The compressive stiffness values were determined form the compression data. Figures 7.11 and 7.12 show the compressive stiffness of the dry and wet scaffolds. The particularly high SDs seen with some of the wet scaffold results (Figure 7.12) are caused by the small size of the scaffolds that complicated the measurements.

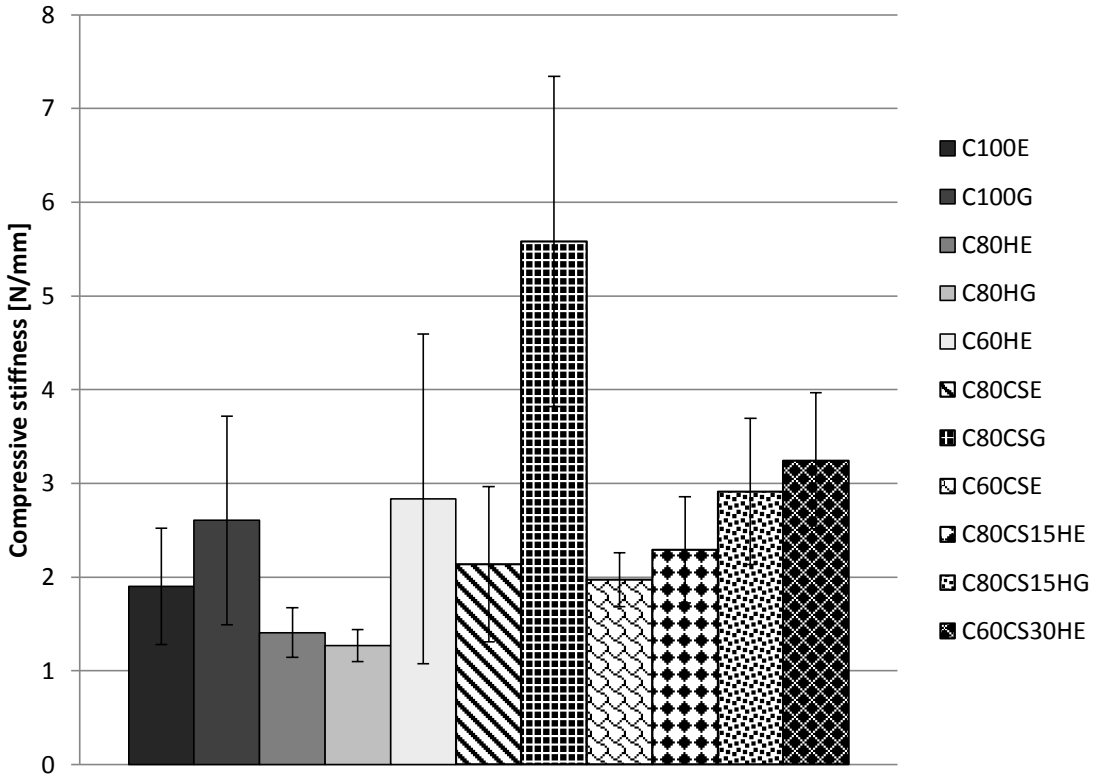

Figure 7.11. *Compressive stiffness results of the dry scaffolds. Results shown as mean ± SD.*

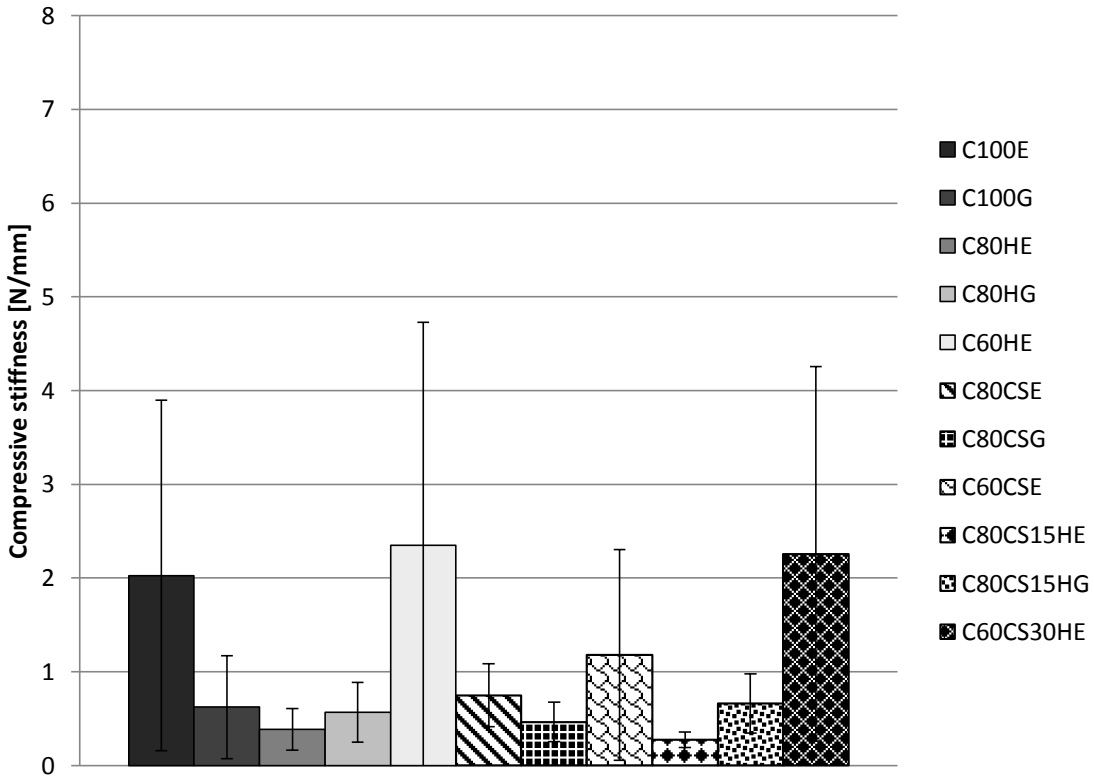

Figure 7.12. *Compressive stiffness results of the wet scaffolds. Results shown as mean ± SD.*

In most cases the difference between the compressive stiffness of the dry and wet scaffolds was not as significant as expected. All the 60 wt.% COL containing composites demonstrated roughly the same compressive stiffness in both dry and wet states. The rest of the dry scaffolds were approximately 3-4 times stiffer than the corresponding wet scaffolds. The two most notable differences in the compressive stiffness results were seen with the C80CSG and C80CS15HE scaffolds; the C80CSG scaffolds demonstrated over 12-fold greater compressive stiffness and the C80CS15HE scaffolds 8.5-fold greater compressive stiffness in dry versus wet state.

From the Figures 7.11 and 7.12 it can be stated that in general all three 60 wt.% COL containing scaffolds demonstrated higher stiffness than the C100E and C80HE/G scaffolds. However, in this context the notably high SDs related to the C60-scaffolds should be noted, and therefore these results are not to be considered as 100% accurate. The high SDs are most definitely caused by the exceptionally small size of the C60-scaffolds that caused severe interference to the stress-strain curves.

From the results of the wet scaffolds, the stiffest were the C60HE, C60CS30HE and C100E scaffolds, whereas the C80CS15HE, C80HE and C80CSG scaffolds were the least stiff. However, the extremely high SD values has to be considered when observing the results of the wet scaffolds, and therefore these results are somewhat open to interpretations. As a comparison, the three stiffest dry scaffolds were C80CSG, C80CS15HG and C80CS15HE, and the three dry scaffold groups with the lowest compressive stiffness were C80HG, C80HE and C100E. In the case of the C80CSG and C80CS15HE scaffolds interesting remarks can be made from these results: in wet state the two groups exhibited the lowest compressive stiffness values, whereas in dry state these groups were the stiffest. Similarly, but with opposite results can be noticed from the C80HE scaffolds: in dry state they were among the stiffest, whereas in wet state they were among the least stiff. It should be noted that all the compressive stiffness results of the wet C60-scaffolds as well as the dry results of the C80CSG scaffolds had significantly high SDs.

When a porous scaffold is highly hydrophilic and absorbs lots of water, it becomes softer and thus the compressive stiffness of the scaffold usually decreases. In fact, this assumption is supported by the water uptake results (Figure 7.16 and 7.17) versus the compressive stiffness results (Figure 7.11) of the corresponding scaffolds. The most clear correlation of compressive stiffness with water uptake is seen with the results of the 60 wt.% COL containing scaffolds.

7.4.3 Recovery from compression

Compression testing involved additional investigation on the ability of the scaffolds to recover after the compression. The dimensions of all the scaffolds were measured prior to the compression and re-measured after a defined recovery time. The recovery time for the dry scaffolds was 10 minutes in RT and 1 hour in PBS (37°C) for the wet scaffolds. Figure 7.13 shows the diameter change and Figure 7.14 the height change of both dry and wet scaffolds after the recovery from compression.

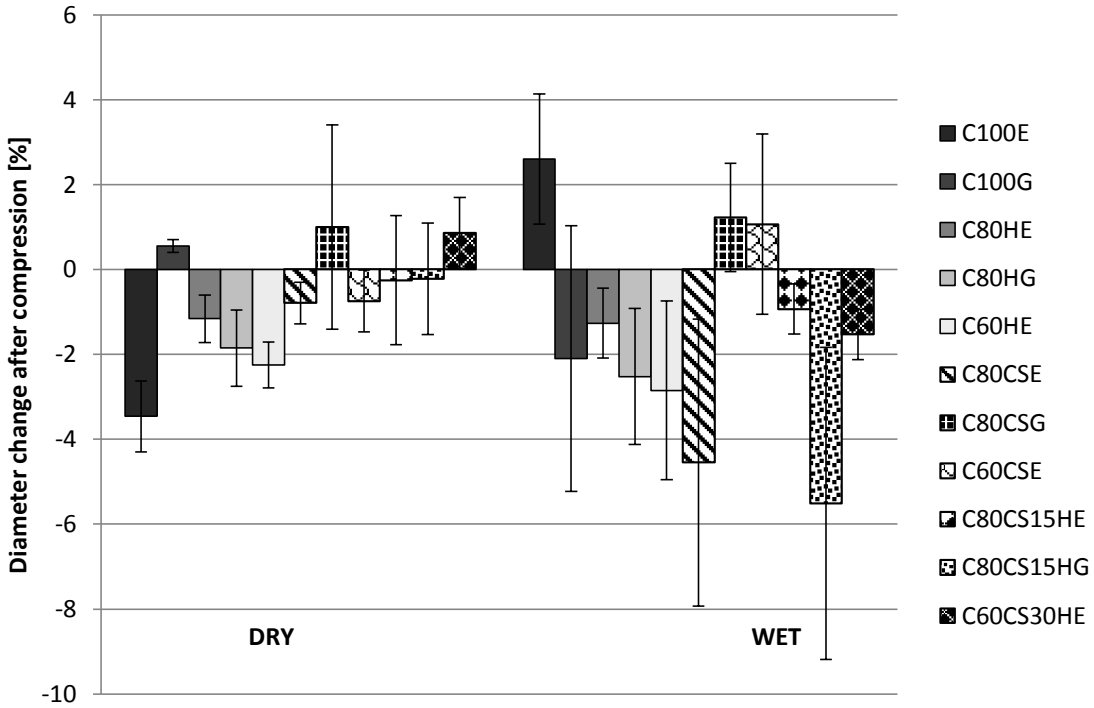

Figure 7.13. *The diameter change of the scaffolds after compression. The recovery times after compression were 10 minutes (RT) for the dry scaffolds and 1 hour for the wet scaffolds (PBS, 37°C). Results shown as mean ± SD.*

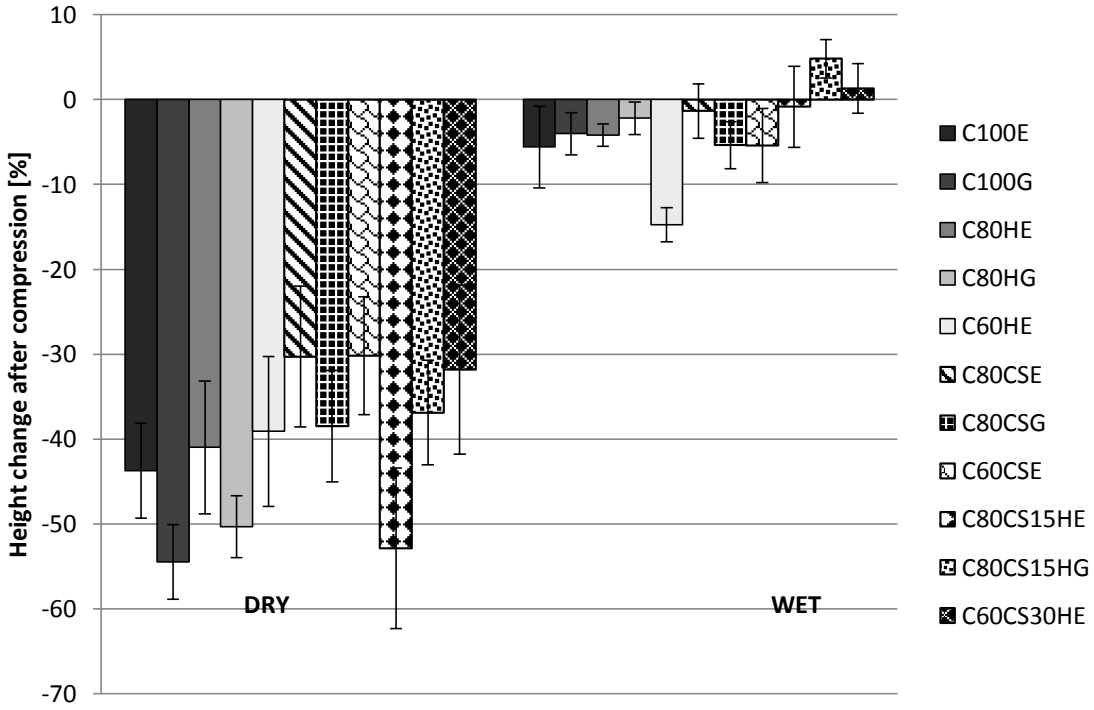

Figure 7.14. *The height change of the scaffolds after compression. The recovery times after compression were 10 minutes (RT) for the dry scaffolds and 1 hour for the wet scaffolds (PBS, 37°C). Results shown as mean ± SD.*

First, it should be noted that the results shown in Figures 7.13 and 7.14 have exceptionally high SDs. Therefore, even though the values presented in Figures 7.13 and 7.14 vary widely between the individual scaffolds, the relative high variation in SDs indicates somewhat similar values between the scaffolds. And thus, especially the axial recovery of the dry scaffolds as well as the radial recovery of both dry and wet scaffolds, respectively are not significantly different between the different scaffold types. The smallest SDs are seen with the axial recovery results of the wet scaffolds (Figure 7.14). Therefore, from Figure 7.14 it can be stated more certainly that the scaffolds that demonstrate the least recovery in height are the C60HE scaffolds. Moreover, it can be stated that most of the COL+HA scaffolds recovered overall better than the COL+CS scaffolds, when the exceptionally high SDs of the latter scaffold groups are taken into account.

Overall, the wet scaffolds managed to recover as well as 85-99% of the initial height and 85-100% from their initial diameter. The dry scaffolds recovered up to 46-70% from their initial height and 97-100% from their initial diameter. These results show that the recovery between the dry and wet scaffolds was relatively similar. The biggest difference was that the axial recovery of the dry scaffolds was somewhat poorer compared to the other results.

Interestingly some of the wet scaffolds demonstrated an increase in height after the recovery from compression, whereas all the dry scaffolds showed only decrease in height. In terms of height recovery (and when taking the result-specific SDs into account) the C80CSE, C60CSE and C60CS30HE scaffolds seemingly recovered the best from the dry scaffolds. As to diameter, some groups of both dry and wet scaffolds showed also increase in dimension. However, since most of the radial results of the wet scaffolds have notably high SDs, these results are somewhat controversial.

Exceptionally high SDs were noticed in most of the diameter change results of both dry and wet scaffolds and with some of the height change results of the wet scaffolds. This is explained by the fact that some of the parallel scaffolds experienced shrinkage while some of them experienced expansion upon recovery. Furthermore, it is highly possible that the measuring of the small and soft scaffolds with a slide gauge could have created some error to the results. The biggest challenge was to maintaining the measuring procedure identical for every scaffold. The height and diameter were measured from the highest and widest part of each scaffold, but the re-measuring of the dimensions after the recovery may have been performed on a slightly different place than initially. In addition, the soft and sponge-like nature of the scaffolds made it difficult to avoid any squishing of the scaffolds during the measurements. Finally, it should be noted that the recovery results obtained from only one measuring place in the scaffold may not represent the overall recovery of the scaffold. Since not all of the scaffolds were perfectly even, round and homogenous, their recovery to the original shape might not have happened similarly in all directions causing some regions of the scaffold recover more while others remained more unchanged.

7.5 Water uptake

The water uptake ability is an important property of a tissue engineering scaffold, since it relates to the diffusion of signaling molecules, nutrients and waste products [111]. In the present study the water uptake characterization was performed by two weighting methods. The first wet weighting method (first water uptake characterization) was to determine the ability of the scaffold structure as a whole, i.e. the pores and the material itself. The second wet weighting method (second water uptake characterization) evaluated the water uptake of the scaffold alone without the water being inside the pores.

As an example, Figure 7.15 shows one scaffold from the C100E group and one from the C100G group in dry, soaking wet (SW) after immersion in PBS for 24 hours and filter dried (FD) states. The rest of the photographs taken from other groups in similar states are shown in the Appendix 3. The first water uptake characterization results are presented in Figure 7.16 and the second characterization results in Figure 7.17.

(a)

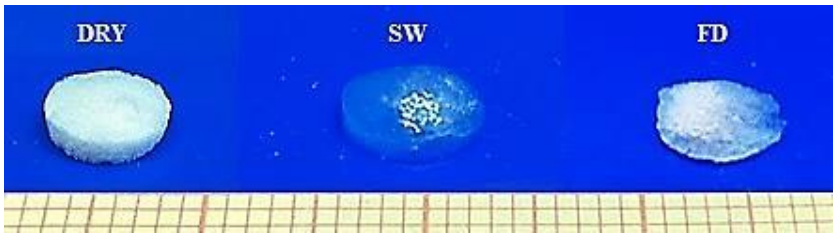

(b)

Figure 7.15. *EDC/NHS (a) and GP (b) cross-linked plain COL scaffolds in dry, soaking wet (SW) and filter dried (FD) states. SW shows the scaffold after immersion in PBS (pH 7.4) for 24 hours and FD after being dried between filter papers.*

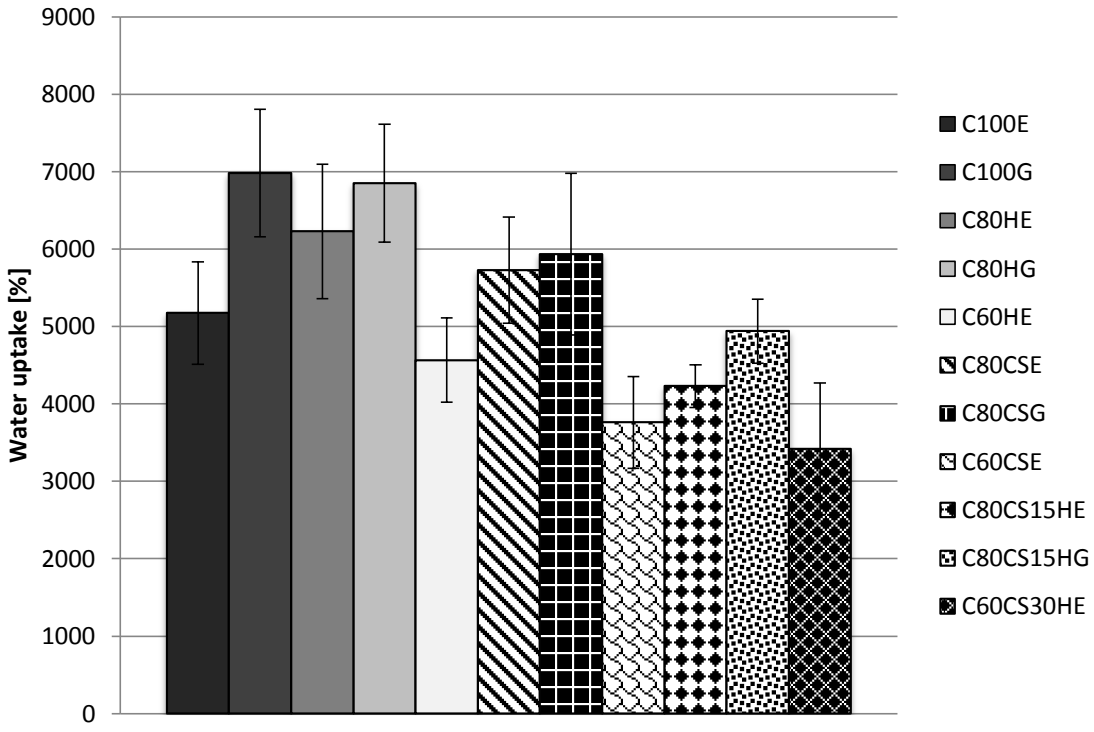

Figure 7.16. *The water uptake of the scaffold and the pore systems. Values obtained from the first wet weighting. Results shown as mean ± SD.*

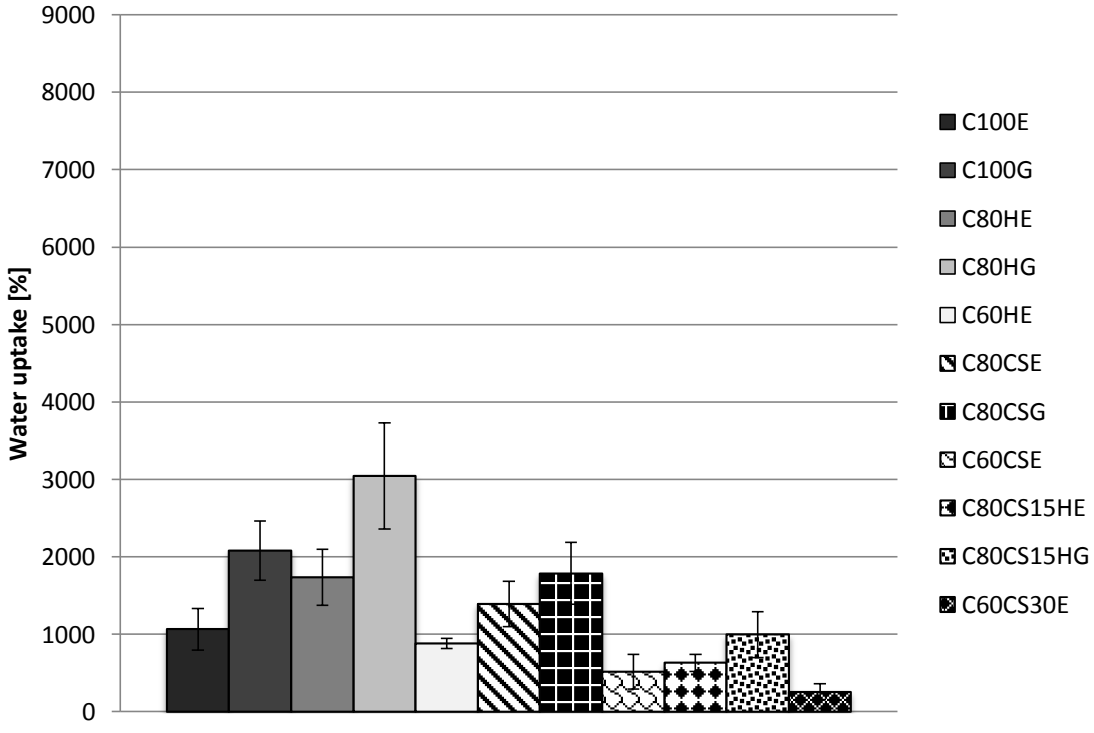

Figure 7.17. *The water uptake of the scaffolds only. Values obtained from the second wet weighting. Results shown as mean ± SD.*

Figures 7.16 and 7.17 show the difference between the different wet states (first and second weighting) of the scaffolds. In both Figures the four scaffold groups with the highest water uptake abilities were C100G, C80HG, C80HE and C80CSG; demonstrating a difference only in the order of these groups between the two weighting methods. In the first water uptake characterization the C100G scaffolds showed the highest water absorption ability, C80HG being the second, C80HE the third and C80CSG the fourth. In the second water uptake characterization the C80HG scaffolds absorbed water the most, C100G as the second, C80CSG as the third and C80HE as the fourth. After the first four groups, rest of the groups were consistently in the same order in both Figures 7.16 and 7.17. Both water uptake characterization tests revealed that the C60CS30HE, C60CSE, C80CS15HE and C60HE scaffolds were the four least water absorbing groups. The slight variation in the results could be due to individual microstructural differences between the scaffolds as well as possible unintentional errors upon filter drying.

It is evident from both Figures (7.16 and 7.17) that the compositions containing only 60 wt.% of COL absorbed water the least. The lower water uptake capacity of the C60HE, C60CSE and C60CS30HE may be directly related to the amount of COL they contain. Both water uptake results demonstrate the higher water absorption of the 80 wt.% COL containing scaffolds compared to the 60 wt.% COL containing scaffolds, which supports the aforementioned assumption. Also, a study by Chang et al. [13] showed that the fabricated COL+HA scaffolds had increased water holding capacity with a higher concentration of COL. On the other hand HA has also been demonstrated having the ability to increase water uptake capacity of EDC/NHS cross-linked COL+HA scaffolds as opposed to plain COL scaffold [142, 127, 22]. In the present study an evidence of such effect is seen, again, in both water uptake characterization results. When comparing the second water uptake results of similarly cross-linked COL+HA scaffolds versus plain COL scaffolds, the C80HE scaffolds clearly show higher water uptake than the C100E scaffolds. Corresponding results was obtained from the first water uptake results (the scaffold and pore system) between the C80HE and C100E scaffolds. However, in the first water uptake characterization test the C80HG scaffolds demonstrated a slightly lower water uptake than the C100G scaffolds. The SDs of the two are relatively similar indicating that the results might not be because of the non-homogeneity of the parallel scaffolds. One reason to this could simply be that that the plain COL construct absorbs more water as a scaffold and pore system as opposed to scaffold only system.

In general, the GP cross-linked scaffolds demonstrated a higher water uptake ability compared to most of the EDC/NHS cross-linked scaffolds; 3/4 of the GP scaffolds being on top four together with the C80HE group and only C80CS15HG being among the five least water absorbing groups. The higher water uptake ability of GP treated scaffolds is evident also from the photographs (shown in the Appendix 3) taken before and after immersion in PBS. The highest water uptake capacity, based on the first wet weighting method was seen in the C100G scaffolds, and based on the second method in the C80HG scaffolds. According to a study by Aramwit et al. [2] GP has the ability to enhance water absorption capacity (and swelling) of scaffolds.

When comparing the results between the HA and CS containing scaffolds, the C80-scaffolds absorbed more water with the presence of HA than with CS. The 60 wt.% COL containing composite scaffolds showed similar results: C60HE/G scaffolds absorbed more water than C60CSE/G scaffolds. As GAGs, both HA and CS are known to attract water. HA needs water to hold its structure, whereas the water attracting properties of CS are based on the sulfate chains that ensure the water uptake of PGs in the cartilage. [50] Based on both of the water uptake results, CS also showed relatively promising water holding abilities; evident from the higher water uptake of all C80CS scaffolds versus plain EDC/NHS cross-linked COL scaffolds. Moreover, the difference between the C80HE and C80CSG scaffolds as well as between the C100E and C80CS15HG scaffolds was relatively small. This suggests that compared to the plain COL scaffolds, both CS and/or HA may be a potential choice in order to produce scaffolds for applications in need of high water uptake ability (such as cartilage scaffolds).

7.6 Dimensional change upon water uptake

In many times, water absorption lead to swelling of the material. Any absorption that causes a dimensional change (swelling) may have important clinical consequences. In general, it is desirable that the dimensional change of a tissue engineering scaffold remains relatively low. For example, a high water (meaning body fluid) absorption can generate significant pressure that may damage the tissue engineered material as well as constrain the natural healing of the tissue [90]. Figure 7.18 shows the dimensional change of the fabricated scaffolds upon water uptake.

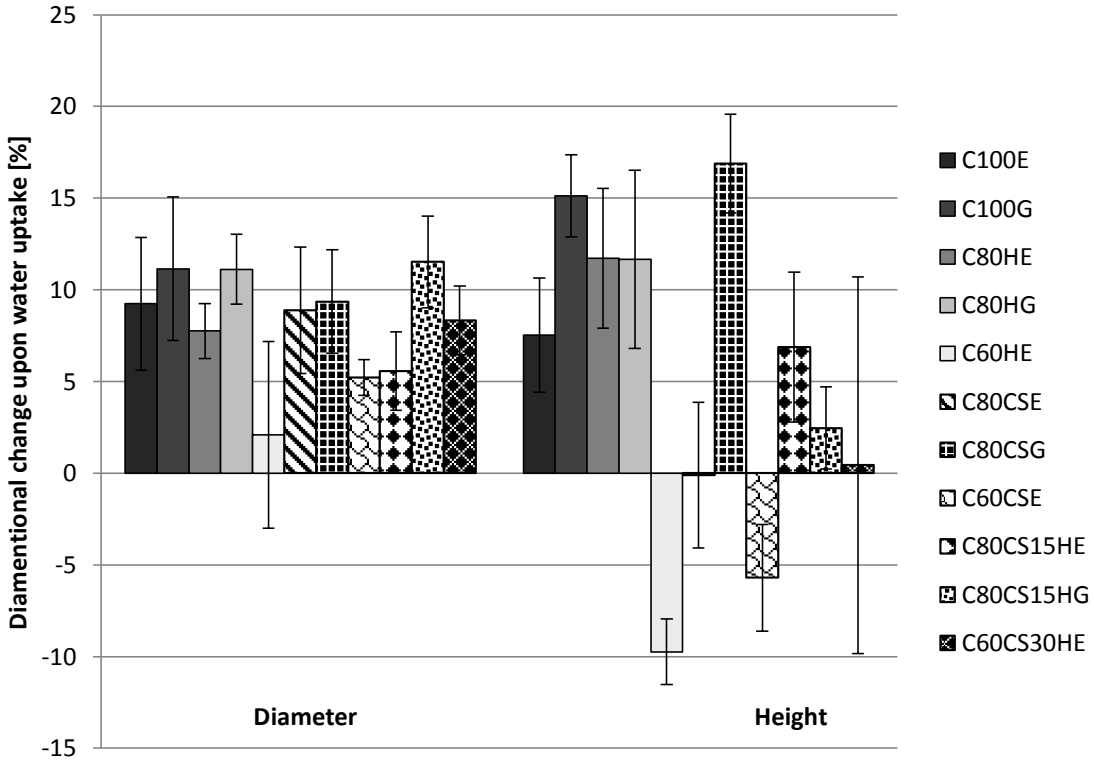

Figure 7.18. *Dimensional change percentages (change in diameter and change in height) of the different scaffolds upon water uptake. Diameter and height measured relative to the first wet weighting method. Results shown as mean ± SD.*

As it can be seen from Figure 7.18 most of the scaffolds swelled resulting in an increase in both diameter (2-12%) and in height (0-17%). However, all the scaffolds experienced notably different axial and radial swelling behavior. The C80CS15HG/E, C60CS30HE and C80CSE scaffolds swelled the least in height, while the C80CSG and C100G scaffolds swelled axially the most. Radial swelling was the least in the C60HE, C60CSE and C80CS15HE scaffolds, and the highest in the C80CS15HG, C100G and C80HG scaffolds. The C60HE and C60CSE scaffolds shrunk notably during wet conditions, whereas the C80CSE shrunk only marginally. The shrinking of the C60HE and C60CSE scaffolds during wet conditions may be due to a collapse of inner pores, caused by the penetrating of water and/or an inadequate cross-linking.

The majority of the dimensional change results differ notably between the EDC/NHS and GP cross-linked scaffolds. All the scaffolds treated with either of the two crosslinkers showed radial increase (2-12%) upon water uptake. However, all GP treated scaffolds swelled more in diameter (9-12%) as opposed to the EDC/NHS cross-linked scaffolds (2-9%). Partially corresponding results between the GP and EDC/NHS cross-linked scaffolds were obtained from the axial swelling behavior as well. All the GP treated scaffolds swelled in height; ranging from 3% to 17%, whereas the EDC-NHS treated scaffolds swelled only 0-12%. Moreover, three of the EDC/NHS cross-linked groups actually shrank in height (up to 10%).

In summary, all the different scaffolds swelled to some extent in diameter upon water uptake. Most scaffolds showed also swelling in height. However, the three groups that experienced shrinkage in height were C60HE (10%), C60CSE (6%) and C80CSE (±0%); probably caused by the collapsing of their inner porous structures upon water uptake. The C100G scaffolds were the group that swelled the most (d: 11%, h: 15%) as a whole and the C80CS15HE scaffolds the group that swelled the least (d: 6%, h: 7%). Corresponding to the water uptake results, the GP cross-linked scaffolds swelled overall more compared to the EDC/NHS cross-linked scaffolds. The more extensive swelling of the GP treated scaffolds is also visible from the photographs taken before and after immersion in PBS (see the Appendix 2). Finally, the swelling/shrinkage of all the scaffolds remained in all cases below 20%, and in most of the scaffolds it stayed around 10%. Dimensional changes of this magnitude can be considered as relatively small and acceptable for a cartilage tissue engineering scaffold.

7.6 Fourier transform infrared spectroscopy

Fourier transform infrared (FTIR) spectra was collected over a range of 450-4000 cm^{-1} to investigate differences in the biochemical compositions of scaffolds before and after cross-linking, demonstrating whether the cross-linking of the scaffolds was successful or not. FTIR measurements were performed by KBr pellet method on one scaffold per each EDC/NHS, GP treated and non-cross-linked scaffold group. FTIR spectra of untreated scaffolds were monitored to confirm the expected amide bond (cross-link) formation in the EDC/NHS and GP treated scaffolds. Figure 7.19 shows the FTIR spectra of all the scaffold groups. Additional spectral data is shown in the Appendix 6.

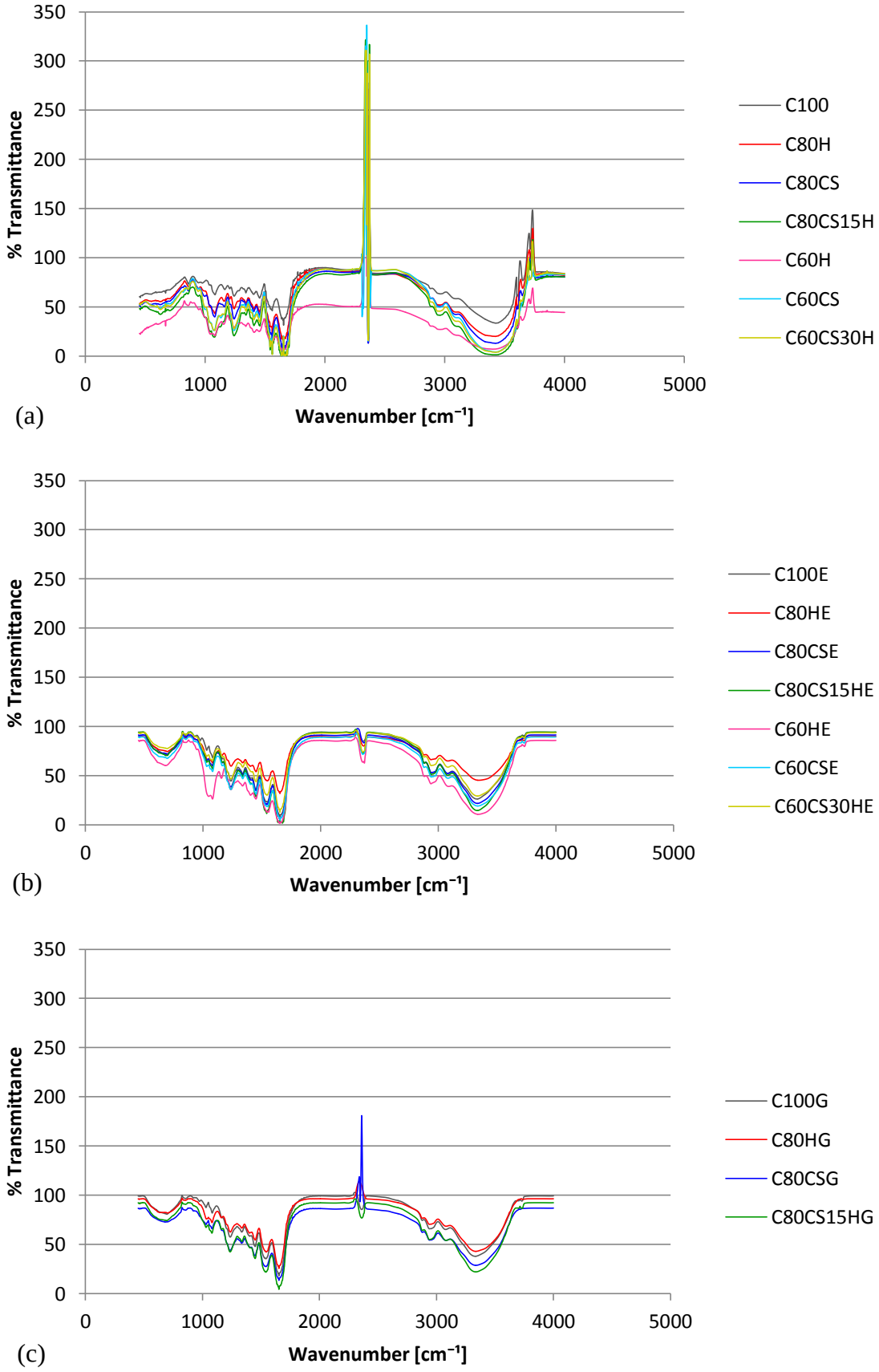

Figure 7.19. *FTIR spectral data of the non-cross-linked (a), EDC/NHS cross-linked (b) and GP cross-linked (c) scaffolds.*

EDC/NHS creates cross-links between molecules like COL, HA and CS by binding covalently carboxylic acids and amino groups to each other [87]. The cross-linking mechanism of GP is yet unknown in detail but presumably it forms cross-links between amino groups of polypeptides [123] via another GP molecule [185]. Thus, the formation of cross-links through both EDC/NHS and GP treatments was monitored by analyzing the primary (I) amide and secondary amide (II) bands; showing characteristic peaks at 1670-1620 cm^{-1} and 1570-1515 cm^{-1} [52]. These bands are assigned with the primary amines (NH_2) being converted to amide bonds (N-H) during the formation of cross-links [89]. In addition to amide bonds, EDC (and possibly GP as well) seems to mediate acid anhydride formation between two carboxyl groups belonging to the same or different polysaccharide molecules (in this case HA and CS). The resultant acid anhydride may readily react with a hydroxyl group of HA and CS to yield an ester bond, which functions as a cross-link in a polysaccharide molecule. [107]

Some of the peaks were clearly visible in the FTIR spectra of all of the scaffolds, and always around the same wavenumbers. The spectra of both cross-linked and non-cross-linked CS containing scaffolds included similar distinctive peaks at ~1240 cm^{-1} due to S=O stretching in CS molecules [132]. In all of the spectra of the different scaffolds, there were wide peaks at 3600-3200 cm-^{1} present. This band is assigned with primary amines (NH_2), and the prominent peaks are due to amide N-H stretching. [52] The spectra of both EDC/NHS and GP cross-linked scaffolds showed similar peaks at ~700 cm^{-1} due to out-of-plane bending of N-H; at 1670-1620 cm^{-1} due to bending of amide I bonds; at 1570-1515 cm^{-1} due to amide II bonds; and at around 1200 cm^{-1} due to C-O bonds [52]. Similar distinctive peaks between all the different scaffolds were detected with non-cross-linked scaffolds at 3750-3600 cm^{-1} due to free hydroxyl and carboxyl groups [52]; Figure 7.19 (a). These peaks are seen leveled down in the spectra of both cross-linked scaffolds due to associations with other molecules (cross-links).

Intermolecular cross-links formed between the carboxyl, hydroxyl and amino groups of the COL, HA and/or CS molecules were observed on all of the different scaffolds after both cross-linking treatments. In particular, the spectra of all the cross-linked scaffolds showed characteristic peaks at 1670-1620 cm^{-1} (amide I band) and 1570-1515 cm^{-1} (amide II band), indicating formation of amide bonds (cross-links) [52]. The amide I band of COL is sensitive to the change of secondary structure. The shifts of characteristic amide I band positions (at 1690-1640 cm^{-1}) in the spectra of C80CS15HE scaffolds could suggest a conformational change of COL and the existence of interactions between COL, HA and CS. [132]

The bands corresponding to ester cross-links between COL, HA and/or CS molecules are present on the FTIR spectra of all the different scaffolds. Specifically, several peaks can be detected at 970-1300 cm^{-1} in the spectra of all cross-linked scaffolds suggesting ester bonds between carboxyl and hydroxyl groups [89] of COL, HA and/or CS molecules. Some of the peaks observed especially at 1440-1210 cm^{-1} may also be due to the carboxyl groups of COL, HA and/or CS. The stretching of C-O combined with the bending of C-OH is known to generate distinctive peaks at the aforementioned band [52].

Unfortunately, between 1300-970 cm^{-1} there are several peaks in the spectra of the scaffolds and some peak positions are very close to each other. As a result it is difficult to identify all individual bands.

A noticeable difference seen between the spectra of non-cross-linked (Figure 7.19 (a)) and cross-linked scaffolds (Figure 7.19 (b) and (c)) was a cluster of peaks at 3750-3600 cm^{-1}; visible only in the spectra of non-cross-linked scaffolds. They result from free hydroxyl (-OH) and carboxyl groups (-COOH) or more specifically from the stretching of O-H involved [52]. Since the carboxyl and hydroxyl groups become associated (instead of remaining free) during cross-linking, these peaks are leveled in the cross-linked spectra. It should be noted that the distinctive peaks at 2300-2400 cm^{-1} seen in all of the spectra were caused by the FTIR measuring device and are not associated with the molecular composition of the scaffolds.

In summary, spectra of the different scaffolds all demonstrated characteristic peaks corresponding to amide bond formation (at 1670-1620 cm^{-1} and 1570-1515 cm^{-1}). Furthermore, in the spectra of the non-cross-linked scaffolds peaks assigned to free hydroxyl (-OH) and carboxyl groups (-COOH) (at 3750-3600 cm-1) were seen leveled down in the spectra of the cross-linked scaffolds due to the forming of cross-links. These observations supported the conclusion that both crosslinkers (EDC/NHS and GP) produced successfully cross-linked scaffolds and that the different compositions/components of the scaffolds did not affect the cross-linking mechanisms.

The degree of cross-linking was not analyzed in the present study because it would have required additional methods. Possibilities for a subsequent analysis on the degree of cross-linking is to use DSC and/or TG measurements to study the denaturation temperature (T_d) of the scaffolds [22, 63] or to use an equation by Aramwit et al. [2] exploiting absorbance values of FTIR measurements. In addition, it is possible to calculate a D value between intensities of deformation vibration and amide, which reflects the content of the primary amine [56].

CONCLUSIONS

In the present study COL-based scaffolds with HA and/or CS were successfully fabricated by freeze-drying and cross-linked with EDC/NHS and GP. The best looking COL+HA/CS/CS+HA scaffolds were fabricated with the blends of 1.0 wt.% COL, HA and/or CS. In general, the 80 wt.% COL containing scaffolds endured the fabrication and cross-linking procedures better than the 60 wt.% COL containing scaffolds. The GP cross-linked plain COL and the EDC/NHS cross-linked COL+HA scaffolds maintained their original size and shape the best after the cross-linking treatment, whereas the least successful cross-linked scaffolds were the CS containing composite scaffolds.

The FTIR spectra of all the scaffolds demonstrated that the varying compositions/components did not affect the cross-linking mechanism and that successful cross-linking was established in all of the scaffolds with both cross-linking treatments. The micro-CT images showed highly porous and interconnected microstructure in all of the scaffolds. COL+HA scaffolds demonstrated higher porosity (91-94%) compared to COL+CS scaffolds (89-91%). In general, GP treated scaffolds had smaller pores (less than 40 µm) compared to EDC/NHS cross-linked scaffolds.

The 60 wt.% COL containing scaffolds absorbed water the least. The GP treated scaffolds had higher water uptake capacity compared to the corresponding EDC/NHS scaffolds. This suggests that GP could possibly be particularly favorable choice as a cross-linker as opposed to the conventional EDC/NHS treatment; in terms of increasing the water uptake capacity of COL-based scaffolds. Furthermore, the results from both water uptake characterizations demonstrated that with the inclusion of HA and/or CS into COL the water uptake capacity of the scaffolds could be increased as opposed to plain COL scaffolds.

Corresponding to the water uptake results, the GP cross-linked scaffolds generally swelled more compared to the EDC/NHS cross-linked scaffolds. The swelling/shrinkage of all the scaffolds remained below 20%, and in most cases it was only around 10%. In general, the COL+HA scaffolds recovered slightly better from the compression than the COL+CS scaffolds. All the scaffolds recovered very well after the compression (up to 85-100% to their initial size); only the dry scaffolds recovered slightly poorer in terms of height. All the dimensional change results were considered acceptable for a tissue engineering cartilage scaffold.

In general, in terms of both dry and wet measurements the COL+CS scaffolds demonstrated superior compressive properties compared to the corresponding COL+HA scaffolds. Supposedly the presence of either CS or HA in the composite affected more on the compressive properties of the scaffolds than either of the cross-linking treatments. Furthermore, there was no clear correlation between the compressive modulus and the two cross-linking treatments; both demonstrated low and high values, respectively. All the 60 wt.% COL containing scaffolds demonstrated similar compressive stiffness in both dry

and wet states, while rest of the dry scaffolds demonstrated approximately 3-4 times higher stiffness compared to the corresponding wet scaffolds. The compressive stiffness results showed a strong correlation with the water uptake results; the scaffolds that demonstrated low water absorption exhibited in high compressive stiffness and vice versa.

In general, the results obtained from the microstructure, dimensional changes upon water uptake, recovery from compression and FTIR characterizations did not differ significantly between the scaffold groups. However, based on the results obtained from fabrication, cross-linking and water uptake characterization, the 80 wt.% COL containing composite scaffolds showed superior properties over the 60 wt.% containing composite scaffolds. It should be noted that the small size and soft nature of the fabricated scaffolds as well as the vast variety of non-homogenous scaffolds per each test group challenged the characterization and resulted in high SDs of some of the results.

The composition of COL+CS+HA was considered particularly interesting because in theory it mimics closest the composition of a native cartilage matrix. On the other hand, as a product a COL+CS+HA scaffold might be difficult to implement, since its fabrication involves inclusion of three individual components. So far there has been only a small amount of studies reported concerning this particular combination, but the results from those studies have been promising and encourage towards further studies. Also, in the present work the results obtained from the compression, water uptake (scaffold and the pore system), recovery from compression, FTIR, micro-CT and dimensional change upon water uptake tests of the C80CS15HE/G scaffolds were promising.

Further *in vitro* and *in vivo* studies are recommended for the 80 wt.% COL containing composite scaffolds. Following tests are suggested to be added to the ones performed in the present study: degradation studies, scanning electron microscope imaging (SEM) and *in vitro* cell tests as well at some point. The novel cross-linker GP proved to be a promising alternative for the conventional EDC/NHS cross-linker; GP did not only produce successfully cross-linked scaffolds but it also increased the water absorption ability of the scaffolds. Furthermore, the fact that GP is a natural cross-linking agent makes its use even more beneficial in order to produce tissue engineered scaffolds with the best possible biological properties. Finally, the use of COL type II instead of COL type I (used in the present study) is suggested for further studies on the COL-based CS and/or HA scaffolds. Since the native cartilage tissue is composed of type II COL, this approach could possibly further support chondrogenesis, and ultimately lead to better results with future *in vivo* experiments.

REFERENCES

[1] Alberts, B., Bray, D., Hopkin, K., Johnson, A., Lewis, J., Raff, M., Roberts, K. & Walter, P. Essential cell biology: Chemical components of cells. Second edition. New York 2003, Garland Science. pp. 39-82.

[2] Aramwit, P., Siritientong, T., Kanokpanont, S. & Srichana, T. Formulation and characterization of silk sericin-PVA scaffold cross-linked with genipin. International Journal of Biological Macromolecules, 47(2010), pp. 668-675.

[3] Baumgart, F. Stiffness – an unknown world of science? Injury, International Journal of the Care of the Injured, 31(2000)2, S-B14-S-B23.

[4] Bhardwaj, N. & Kundu, S.C. Electrospinning: A fascinating fiber fabrication technique. Biotechnology Advances, 28(2010)3, pp. 325-347.

[5] Bigi, A., Cojazzi, G., Panzavolta, S., Roveri, N. & Rubini, K. Stabilization of gelatin films by crosslinking with genipin. Biomaterials, 23(2002)24, pp. 4827-4832.

[6] BioCell Technology LLC. BioCell collagen benefits. [WWW]. [accessed on: 02.03.2015]. Available at: http://www.biocelltechnology.com/products/biocell-collagen

[7] Boss, E.A., Filho, R.M. & de Toledo, E.C.V. Freeze drying process: Real time model and optimization. Chemical Engineering and Processing: Process Intensification, 43(2004)12, pp. 1475-1485.

[8] Buckwalter, J.A. & Mankin, H.J. Articular cartilage: Tissue design and chondrocyte-matrix interactions. Instructional Course Lectures, 47(1998), pp. 477-486.

[9] Burdick, J.A. & Prestwich, G.D. Hyaluronic acid hydrogels for biomedical applications. Advanced Materials, 23(2011)12, pp. H41-H56.

[10] Caliari, S.R. & Harley, B.A. The effect of anisotropic collagen-GAG scaffolds and growth factor supplementation on tendon cell recruitment, alignment, and metabolic activity. Biomaterials, 32(2011)23, pp. 5330-5340.

[11] Caliari, S.R., Ramirez, M.A., & Harley, B.A.C. The development of collagen-GAG scaffold-membrane composites for tendon tissue engineering. Biomaterials, 32(2011)34, pp. 8990-8998.

[12] Cen, L., Liu, W., Cui, L., Zhang, W. & Cao, Y. Collagen tissue engineering: Development of novel biomaterials and applications. Pediatric Research, 63(2008)5, pp. 492-496.

[13] Chang, S.J., Kuo, S.M., Manousakas, I., Niu, G.CC. & Chen, J.P. Preparation and characterization of hyaluronan/collagen II microspheres under an electrostatic field system with disc electrodes. Acta Biomaterialia, 5(2009), pp. 101-114.

[14] Chang, Y., Tsai, CC., Liang, HC. & Sung, HW. Reconstruction of the right ventricular outflow tract with a bovine jugular vein graft fixed with a naturally occurring crosslinking agent (genipin) in a canine model. Journal of Thoracic Cardiovascular Surgery, 122(2001)6, pp. 1208-1218. **[118]**

[15] Chemical Land21. Chondroitin sulfate. [WWW]. [accessed on 02.03.2015]. Available at: http://www.chemicalland21.com/lifescience/foco/CHONDROITIN%20SULFATE.htm

[16] Chen, W.Y. & Abatangelo, G. Functions of hyaluronan in wound repair. Wound Repair and Regeneration, 7(1999)2, pp. 79-89.

[17] Cheng, NC., Estes, B.T., Young, TH. & Guilak, F. Genipin-crosslinked cartilage-derived matrix as a scaffold for human adipose-derived stem cell chondrogenesis. Tissue Engineering Part A, 19(2013)3-4, pp. 484-496.

[18] Chung, E.J., Jakus, A.E. & Shah, R.N. In situ forming collagen–hyaluronic acid membrane structures: Mechanism of self-assembly and applications in regenerative medicine. Acta Biomaterialia, 9(2013)2, pp. 5153-5161.

[19] Collins, M.N. & Birkinshaw, C. Hyaluronic acid based scaffolds for tissue engineering: A review. Carbohydrate Polymers, 92(2013)2, pp. 1262-1279.

[20] Cunniffe, M.G. & O'Brien, F.J. Collagen scaffolds for orthopedic regenerative medicine. JOM, 63(2011)4, pp. 66-73.

[21] Daamen, W.F., van Moerkerk, H.Th.B., Hafmans, T., Buttafoco, L., Poot, A.A., Veerkamp, J.H. & van Kuppevelt, T.H. Preparation and evaluation of molecularly-defined collagen–elastin–glycosaminoglycan scaffolds for tissue engineering. Biomaterials, 24(2003)22, pp. 4001-4009.

[22] Davidenko, N., Campbell, J.J., Thian, E.S., Watson, C.J. & Cameron, R.E. Collagen-hyaluronic acid scaffolds for adipose tissue engineering. Acta Biomaterialia, 6(2010)10, pp. 3957-3968.

[23] Douglas, T., Heinemann, S., Mietrach, C., Hempel, U., Bierbaum, S., Scharnweber, D. & Worch, H. Interactions of collagen types I and II with chondroitin sulfates A-C and their effect on osteoblast adhesion. Biomacromolecules, 8(2007)4, pp. 1085-1092.

[24] eFunda Inc. Rapid Prototyping: An Overview. [WWW] [accessed on: 02.03.2015]. Available at: http://www.efunda.com/processes/rapid_prototyping/intro.cfm

[25] Elliott, R.J. & Gardner, D.L. Changes with age in the glycosaminoglycans of human articular cartilage. Annals of the Rheumatic Diseases, 38(1979)4, pp. 371-377.

[26] Engel, E., Castaño, O., Salvagni, E., Ginebra, M.P. & Planell, J.A. Biomaterials for tissue engineering of hard tissues. In: Santin, M. Strategies in regenerative medicine. [eBook]. 2009, Springer Science. [accessed on 12.02.2015]. Available at: http://link.springer.com/book/10.1007%2F978-0-387-74660-9

[27] Englert, C., Blunk, T. Müller, R., Schulze von Glasser, S., Baumer, J., Fierlbeck, J., Heid, I.M., Nerlich, M. & Hammer, J. Bonding of articular cartilage using a combination of biochemical degradation and surface cross-linking. Arthritis Research and Therapy, 9(2007)3, R47.

[28] Eppley, B.L., Dadvand, B. Injectable soft-tissue fillers: clinical overview. Plastic and Reconstructive Surgery, 118(2006)4, pp. 98-106.

[29] Ernst, S., Langer, R., Cooney, C.L. & Sasisekharan, R. Enzymatic degradation of glycosaminoglycans. Critical Reviews in Biochemistry and Molecular Biology, 30(1995)5, pp. 387-444.

[30] Fakhari, A. & Berkland, C. Applications and emerging trends of hyaluronic acid in tissue engineering, as a dermal filler and in osteoarthritis treatment. Acta Biomaterialia, 9(2013)7, pp. 7081-7092.

[31] Fischer, R.L., McCoy, M.G. & Grant, S.A. Electrospinning collagen and hyaluronic acid nanofiber meshes. Journal of Material Science: Materials in Medicine, 23(2012), pp. 1645-1654.

[32] Gelse, K., Pöschl, E. & Aigner, T. Collagens—structure, function, and biosynthesis. Advanced Drug Delivery Reviews, 55(2003)12, pp. 1531-1546.

[33] Gomes, M., Azavedo, H., Malafaya, P., Silva, S., Oliveira, J., Silva, G., Sousa, R., Mano, J. & Reis, R. Natural polymers in tissue engineering applications. In: van Blitterswijk, C., Thomsen, P., Hubbell, J., Cancedda, R., de Bruijn, J., Lindahl, A., Sohier, J., Williams, D.F. Tissue engineering. 2008, Elsevier Inc. pp. 145-192.

[34] Gorczyca, G., Tylingo, R., Szweda, P., Augustin, E., Sadowska, M. & Milewski, S. Preparation and characterization of genipin cross-linked porous chitosan-collagen-gelatin scaffolds using chitosan-CO2 solution. Carbohydrate Polymers, 102(2014), pp. 901-911.

[35] Griffon, D.J, Sedighi, M.R., Schaeffer, D.V., Eurell, J.A. & Johnson, A.L. Chitosan scaffolds: Interconnective pore size and cartilage engineering. Acta Biomaterialia, 2(2006), pp. 313-320.

[36] Guo, Y., Yuan, T., Xiao, Z., Tang, P., Xiao, Y., Fan, Y. & Zhang, X. Hydrogels of collagen/chondroitin sulfate/hyaluronan interpenetrating polymer network for cartilage tissue engineering. Journal of Material Science: Materials in Medicine, 23(2012)9, pp. 2267-2279.

[37] Haaparanta, AM., Järvinen, E., Cengiz, I.F., Ellä, V., Kokkonen, H.T., Kiviranta, I. & Kellomäki, M. Preparation and characterization of collagen/PLA, chitosan/PLA, and collagen/chitosan/PLA hybrid scaffolds for cartilage tissue engineering. Journal of Material Science: Materials in Medicine, 25(2014)4, pp. 1129-1136.

[38] Habermehl, J. Development and validation of a collagen-based scaffold for vascular tissue engineering: Introduction. [WWW]. [accessed on: 02.03.2015]. Available at: http://theses.ulaval.ca/archimede/fichiers/23201/ch01.html

[39] Hardingham, T. Solution Properties of Hyaluronan. In: Garg, H.G., Hales, C.A. Chemistry and Biology of Hyaluronan. UK 2004, Elsevier Ltd. pp. 1–16.

[40] Hanson, John. Introduction to interpretation of infrared spectroscopy. [WWW]. [accessed on: 19.03.2015]. Available at: http://www2.ups.edu/faculty/hanson/Spectroscopy/IR/IRInterpretation.htm

[41] Harley B.A., Spilker M.H., Wu J.W., Asano K., Hsu HP., Spector M. & Yannas I.V. Optimal Degradation Rate for Collagen Chambers Used for Regeneration of Peripheral Nerves over Long Gaps. Cells Tissues Organs 176(2004)1-3, pp. 153-165.

[42] Harley, B.A., Leung, J.H., Silva, E.C.C.M. & Gibson, L.J. Mechanical characterization of collagen–glycosaminoglycan scaffolds. Acta Biomaterialia, 3(2007)4, pp. 463-474.

[43] Haugh, M.G., Jaasma, M.J. & O'Brien, F.J. The effect of dehydrothermal treatment on the mechanical and structural properties of collagen-GAG scaffolds. Journal of Biomedical Material Research A, 89(2008), pp. 363-369.

[44] He, X., Wang, Y. & Wu, G. Layer-by-layer assembly of type I collagen and chondroitin sulfate on aminolyzed PU for potential cartilage tissue engineering application. Applied Surface Science, 258(2012)24, pp. 9918-9925.

[45] Holdsworth, D.W. & Thornton, M.M. Micro-CT in small animal and specimen imaging. Trends in Biotechnology, 20(2002)8, S34-S39.

[46] Holzapfel, G.A. Biomechanics of soft tissue. [WWW]. [accessed on: 02.03.2015]. Available at: biomechanics.stanford.edu/me338/me338_project02.pdf

[47] Hortensius, R.A. & Harley, B.A.C. The use of bioinspired alterations in the glycosaminoglycan content of collagen–GAG scaffolds to regulate cell activity. Biomaterials, 34(2013)31, pp. 7645-7652.

[48] Huerta-Angele, G., Šmejkalová, D., Chládková, D., Ehlová, T., Buffa, R. & Velebný, V. Synthesis of highly substituted amide hyaluronan derivates with tailored degree of substitution and their crosslinking via click chemistry. Carbohydrate Polymers, 84(2011), pp. 1293-1300.

[49] Hyaluronic acid: History, chemical structure, and its benefits for the body. Hyalogic [WWW]. [accessed on 19.01.2015]. Available at: http://www.hyalogic.com/main/about_hyaluronic_acid

[50] Glucosamine and chondroitin sulfates. Invista [WWW]. [accessed on 13.03.2015]. Available at: http://www.innvista.com/health/ailments/arthritis/glucosamine-and-chondroitin-sulfates/

[51] Ishida, O., Tanaka, Y., Morimoto, I., Takigawa, M. & Eto, S. Chondrocytes are regulated by cellular adhesion through CD44 and hyaluronic acid pathway. Journal of Bone and Mineral Research, 12(1997)10, pp. 1657-1663.

[52] Jauhiainen, TP. Organic spectroscopy – Correlation tables of infrared- and NMR-spectroscopy. Finland 2010. The University of Joensuu, Department of Chemistry.

[53] Jenkins, A.D., Kratochvíl, P., Stepto, R.F.T. & Suter, W. Glossary of basic terms in polymer science (IUPAC Recommendations 1996). Pure and Applied Chemistry 68(1996)12, pp. 2287–2311.

[54] Jo, S., Kim, D., Woo, J., Yoon, G., Park Y.D., Tae, G. & Noh, I. Development and physicochemical evaluation of chondroitin sulfate-poly(ethylene oxide) hydrogel. Macromolecular Research, 19(2011)2, pp. 147-155.

[55] Johansson, J.A., Halthur, T., Herranen, M., Söderberg, L., Elofsson, U. & Hilborn, J. Build-up of collagen and hyaluronic acid polyelectrolyte multilayers. Biomacromolecules, 6(2005)3, pp. 1353-1359.

[56] Kangjian, W., Nianhua, D., Shiwei, X., Yichun, Y. & Weihua, D. Preparation and characterization of collagen-chitosan-chondroitin sulfate composite membranes. Journal of Membrane Biology, 245(2012)11, pp. 707-716.

[57] Kanungo, B.P. & Gibson, L.J. Density–property relationships in collagen–glycosaminoglycan scaffolds. Acta Biomaterialia, 6(2010)2, pp. 344-353.

[58] Keinonen, N. Recycling of the Plastic Waste in Grocery Shops. Bachelor's thesis. Finland 2014. Tampere University of Applied Sciences, Degree Programme in Chemical Engineering, Chemical Engineering. 49 p.

[59] Kim, H.J., Kim, K.K., Park, I.K., Choi, B.S., Kim, H.K. & Kim, M.S. Hybrid scaffolds composed of hyaluronic acid and collagen for cartilage regeneration. Tissue Engineering and Regenerative Medicine, 9(2012)2, pp. 57-62.

[60] Kim, I.L., Mauck, R.L. & Burdick, J.A. Hydrogel design for cartilage tissue engineering: A case study with hyaluronic acid. Biomaterials, 32(2011)34, pp. 8771-8782.

[61] Kim, T.G., Chung, H.J. & Park, T.G. Macroporous and nanofibrous hyaluronic acid/collagen hybrid scaffold fabricated by concurrent electrospinning and deposition/leaching of salt particles. Acta Biomaterialia, 4(2008)6, pp. 1611-1619.

[62] Kirkland Science Labs. Chondroitin sulfate. [WWW]. [accessed on 12.02.2015]. Available at: http://www.kirklandsciencelabs.com/info/chondroitin_sulfate

[63] Ko, CS., Huang, JP., Huang, CW. & Chu, IM. Type II collagen-chondroitin sulfate-hyaluronan scaffold cross-linked by genipin for cartilage tissue engineering. Journal of Bioscience and Bioengineering, 107(2009)2, pp. 177-182.

[64] Ko, CS., Wu, CH., Huang, HH. & Chu, IM. Genipin cross-linking of type II collagen-chondroitin sulfate-hyaluronan scaffold for articular cartilage therapy. Journal of Medical and Biological Engineering, 27(2007)1, pp. 7-14.

[65] Kon M., de Visser A.C. A poly (HEMA) sponge for restoration of articular cartilage defects. Plastic Reconstruction Surgery, 67(1981)3, pp. 288–94.

[66] Kubo, M., Ando, K., Mimura, T., Matsusue, Y. & Mori, K. Chondroitin sulfate for the treatment of hip and knee osteoarthritis: Current status and future trends. Life Sciences, 85(2009)13–14, pp. 477-483.

[67] Kumari, R. & Dutta, P.K. Physicochemical and biological activity study of genipin-crosslinked chitosan scaffolds prepared by using supercritical carbon dioxide for tissue engineering applications. International Journal of Biological Macromolecules, 46(2010)2, pp. 261-266.

[68] Lakshmi, S.N. & Cato, T.L. Polymers as biomaterials for tissue engineering and controlled drug delivery. Advanced Biochemical Engineering/Biotechnology, 102(2006), pp. 47-90.

[69] Lau, T.T., Wang, C. & Wang, DA. Cell delivery with genipin crosslinked gelatin microspheres in hydrogel/microcarrier composite. Composites Science and Technology, 70(2010)13, pp. 1909-1914.

[70] Lauder, R.M. Chondroitin sulphate: A complex molecule with potential impacts on a wide range of biological systems. Complementary Therapies in Medicine, 17(2009)1, pp. 56-62.

[71] Laurent, T.C. & Fraser, J.R.E. Hyaluronan. The FASEB Journal, 6(1992), pp. 2397-2404.

[72] Lee, C.H., Singla, A. & Lee, Y. Biomedical applications of collagen. International Journal of Pharmaceutics, 221(2001)1–2, pp. 1-22.

[75] Lee, J.M., Edwards, H.H.L., Pereira, C.A. & Samii, S.I. Cross-linking of tissue-derived biomaterials in 1-ethyl-3-(3-dimethylaminopropyl)-carbodiimide (EDC). Journal of Materials Science: Materials in Medicine, 7(1996), pp. 531-541.

[76] Levene, P.A. & La Forge, F.B. On Chondroitin Sulphuric Acid. Journal of Biological Chemistry, 15(1913), pp. 69–79.

[77] Liang, HC., Chang, WH., Liang, HF., Lee, MH. & Sung, HW. Crosslinking structures of gelatin hydrogels crosslinked with genipin or a water-soluble carbodiimide. Journal of Applied Polymer Science, 91(2004)6, pp. 4017-4026.

[78] Liang, HC., Chang, Y., Hsu, CK., Lee, MH. & Sung, HW. Effects of crosslinking degree of an acellular biological tissue on its tissue regeneration pattern. Biomaterials, 25(2004)17, pp. 3541-3552.

[79] Liang, WH., Kienitz, B.L., Penick, K.J., Welter, J.F., Zawodzinski, T.A. & Baskaran, H. Concentrated collagen-chondroitin sulfate scaffolds for tissue engineering applications. Journal of Biomedical Material Research A, 94(2010)4, pp. 1050-1060.

[80] Lien, S., Li, W. & Huang, T. Genipin-crosslinked gelatin scaffolds for articular cartilage tissue engineering with a novel crosslinking method. Materials Science and Engineering: C, 28(2008)1, pp. 36-43.

[81] Lilje, O., Lilje, E., Marano, A.V. & Gleason, F.H. Three dimensional quantification of biological samples using micro-computer aided tomography (microCT). Journal of Microbiological Methods, 92(2013)1, pp. 33-41.

[82] Lima, E.G., Tan, A.R., Tai, T., Marra, K.G., DeFail, A., Ateshian, G.A. & Hung, C.T. Genipin enhances the mechanical properties of tissue-engineered cartilage and protects against inflammatory degradation when used as a medium supplement. Journal of Biomedical Material Research A, 91(2009)3, pp. 692-700.

[83] Liu, Y., Ren, L. & Wang, Y. Crosslinked collagen–gelatin–hyaluronic acid biomimetic film for cornea tissue engineering applications. Materials Science and Engineering: C, 33(2013)1, pp. 196-201.

[84] Lopowitz, A.J. & Newton, C.D. Degenerative joint disease and traumatic arthritis. [WWW]. [accessed on: 02.03.2015]. Available at: http://cal.vet.upenn.edu/projects/saortho/chapter_87/87mast.htm

[85] Madhavan, K., Belchenko, D. & Tan, W. Roles of genipin crosslinking and biomolecule conditioning in collagen-based biopolymer potential for vascular media regeneration. Journal of Biomedical Material Research A, 97(2011)1, pp. 16-26.

[86] Madhavan, K., Belchenko, D., Motta, A. & Tan, W. Evaluation of composition and crosslinking effects on collagen-based composite constructs. Acta Biomaterialia, 6(2010)4, pp. 1413-1422.

[87] Mark, H.F. Encyclopedia of Polymer Science and Technology. Third edition. USA 2013. John Wiley & Sons. 1350 p.

[88] Martin, T.A., Caliari, S.R., Williford, P.D., Harley, B.A. & Bailey, R.C. The generation of biomolecular patterns in highly porous collagen-GAG scaffolds using direct photolithography. Biomaterials, 32(2011)16, pp. 3949-3957.

[89] Matsiko, A., Levingstone, T.J., O'Brien, F.J. & Gleeson, J.P. Addition of hyaluronic acid improves cellular infiltration and promotes early-stage chondrogenesis in a collagen-

based scaffold for cartilage tissue engineering. Journal of the Mechanical Behavior of Biomedical Materials, 11(2012), pp. 41-52.

[90] McCabe, J.F., Rusby, S. Water absorption, dimensional changes and radial pressure in resin matrix dental restorative materials. Biomaterials, 25(2004), pp. 4001-4007.

[91] MeSH. National Library of Medicine – Medical Subject Headings: Chondroitin sulfates. [WWW]. [accessed on 03.03.2015]. Available at: http://www.nlm.nih.gov/cgi/mesh/2011/MB_cgi?mode=&index=2689&view=expanded

[92] Mishra, D. Collagen: Predominant extra cellular matrix component. [WWW, PP-presentation]. [accessed on 02.03.2015]. Available at: http://www.slideshare.net/DrDebashis/collagen-drdeb

[93] Muir, H. Proteoglycans of cartilage. Journal of Clinical Pathology, s3-12(1978)1, pp. 67-81.

[94] Murphy, C.M., Matsiko, A., Haugh, M.G., Gleeson, J.P. & O'Brien, F.J. Mesenchymal stem cell fate is regulated by the composition and mechanical properties of collagen–glycosaminoglycan scaffolds. Journal of the Mechanical Behavior of Biomedical Materials, 11(2012), pp. 53-62.

[95] Muzzarelli, R.A.A. Genipin-crosslinked chitosan hydrogels as biomedical and pharmaceutical aids. Carbohydrate Polymers, 77(2009)1, pp. 1-9.

[96] Muzzarelli, R.A.A., Greco, F., Busilacchi, A., Sollazzo, V. & Gigante, A. Chitosan, hyaluronan and chondroitin sulfate in tissue engineering for cartilage regeneration: A review. Carbohydrate Polymers, 89(2012)3, pp. 723-739.

[97] Nair, L.S. & Laurencin, C.T. Biodegradable polymers as biomaterials. Progress in Polymer Science 32(2007)8–9, pp. 762-798.

[98] Nair, L.S. & Laurencin, C.T. Polymers as biomaterials for tissue engineering and controlled drug delivery. Advanced Biochemical Engineering/Biotechnology. 102(2006), pp. 47-90.

[99] O'Brien, F.J., Harley, B.A., Yannas, I.V. & Gibson, L. Influence of freezing rate on pore structure in freeze-dried collagen-GAG scaffolds. Biomaterials, 25(2004)6, pp. 1077-1086.

[100] O'Brien, F.J., Harley, B.A., Yannas, I.V. & Gibson, L.J. The effect of pore size on cell adhesion in collagen-GAG scaffolds. Biomaterials, 26(2005)4, pp. 433-441.

[101] Olde Damink, L.H.H., Dijkstra, P.J., van Luyn, M.J.A., van Wachem, P.B., Nieuwenhuis, P. & Feijen, J. Cross-linking of dermal sheep collagen using a water-soluble carbodiimide. Biomaterials, 17(1996)8, pp. 765-773.

[102] Osborne, C.S., Reid, W.H. & Grant, M.H. Investigation into the biological stability of collagen/chondroitin-6-sulphate gels and their contraction by fibroblasts and keratinocytes: The effect of crosslinking agents and diamines. Biomaterials, 20(1999)3, pp. 283-290.

[103] Paramonov S.E., Gauba V. & Hartgerink J.D. Synthesis of collagen-like peptide polymers by native chemical ligation. Macromolecules 38(2005), pp. 7555–7561.

[104] Parenteau-Bareil, R., Gauvin, R. & Berthod, F. Collagen-based biomaterials for tissue engineering applications. Materials, 3(2010)3, pp. 1863-1887.

[105] Park, SN., Kim, J.K. & Suh, H. Evaluation of antibiotic-loaded collagen-hyaluronic acid matrix as a skin substitute. Biomaterials, 25(2004)17, pp. 3689-3698.

[106] Park, SN., Lee, H.J., Lee, K.H. & Suh, H. Biological characterization of EDC-crosslinked collagen–hyaluronic acid matrix in dermal tissue restoration. Biomaterials, 24(2003)9, pp. 1631-1641.

[107] Park, SN., Park, JC., Kim, H.O., Song, M.J. & Suh, H. Characterization of porous collagen/hyaluronic acid scaffold modified by 1-ethyl-3-(3-dimethylaminopropyl)carbodiimide cross-linking. Biomaterials, 23(2002)4, pp. 1205-1212.

[108] Pek, Y.S., Spector, M., Yannas, I.V. & Gibson, L.J. Degradation of a collagen–chondroitin-6-sulfate matrix by collagenase and by chondroitinase. Biomaterials, 25(2004)3, pp. 473-482.

[109] Prestwich, G.D. Hyaluronic acid-based clinical biomaterials derived for cell and molecule delivery in regenerative medicine. Journal of Controlled Release, 155(2011)2, pp. 193-199.

[110] Prestwich, G.D & Vercruysse, K.P. Therapeutic applications of hyaluronic acid and hyaluronan derivates. Pharmaceutical Science and Technology Today, 1(1998)1, pp. 42-43.

[111] Puppi, D., Chiellini, F., Piras, A.M. & Chiellini, E. Polymeric materials for bone and cartilage repair. Progress in Polymer Science 35(2010), pp. 403-440.

[112] [Romel Verterra. Stress-strain diagram. [WWW]. [accessed on: 02.03.2015]. Available at: http://www.mathalino.com/reviewer/mechanics-and-strength-of-materials/stress-strain-diagram

[113] Saladin, K.S. Anatomy and physiology: The unity of form and function. Third edition. USA 2003, The McGraw-Hill Companies. 1192 p.

[114] Schneiders, W., Reinstorf, A., Biewener, A., Serra, A., Grass, R., Kinscher, M., Heineck, J., Rehberg, S., Zwipp, H. & Rammelt, S. In vivo effects of modification of hydroxyapatite/collagen composites with and without chondroitin sulphate on bone remodeling in the sheep tibia. Journal of Orthopedic Research, 27(2009)1, pp. 15-21.

[115] Schneiders, W., Rentsch, C., Rehberg, S., Rein, S., Zwipp, H. & Rammelt, S. Effect of chondroitin sulfate on osteogenetic differentiation of human mesenchymal stem cells. Materials Science and Engineering C, 32(2012), pp. 1926-1930.

[116] Segura, T., Chung, P.H. & Shea, L.D. DNA delivery from hyaluronic acid-collagen hydrogels via a substrate-mediated approach. Biomaterials, 26(2005)13, pp. 1575-1584.

[117] Shepherd, J.H., Ghose, S., Kew, S.J., Moavenian, A., Best, S.M. & Cameron, R.E. Effect of fiber crosslinking on collagen-fiber reinforced collagen-chondroitin-6-sulfate materials for regenerating load-bearing soft tissues. Journal of Biomedical Material Research A, 101(2013)1, pp. 176-184.

[118] Shu, X.Z., Liu, Y., Luo, Y., Roberts, M.C. & Prestwich, G.D. Disulfide cross-linked hyaluronan hydrogels. Biomacromolecules, 3(2002), pp. 1304-1311.

[119] Sigma Aldrich Co. LLC. N-(3-Dimethylaminopropyl)-N′-ethylcarbodiimide hydrochloride (Material safety data sheet). [WWW]. [accessed on 02.03.2015]. Available at: http://www.sigmaaldrich.com/catalog/product/sial/e6383?lang=fi&region=FI

[120] Singla, S.K. Nomenclature of hyaluronic acid. Biochemical Journal, 242(1987), p. 623.

[121] Staveley, B. Principles of cell biology (BIOL2060): Extracellular structures. [WWW]. [accessed on 02.03.2015]. Available at: http://www.mun.ca/biology/desmid/brian/BIOL2060/BIOL2060-17/CB17.html

[122] Sundararaghavan, H.G., Monteiro, G.A., Lapin, N.A., Chabal, Y.J., Miksan, J.R. & Shreiber, D.I. Genipin-induced changes in collagen gels: Correlation of mechanical properties to fluorescence. Journal of Biomedical Material Research A, 87(2008)2, pp. 308-320.

[123] Sung, HW., Chang, WH., Ma, CY. & Lee, MH. Crosslinking of biological tissues using genipin and/or carbodiimide. Journal of Biomedical Material Research Part A, 64(2003)3, pp. 427-438.

[124] Sung, HW., Chang, Y., Chiu, CT., Chen, CN. & Liang, HC. Crosslinking characteristics and mechanical properties of a bovine pericardium fixed with a naturally occurring crosslinking agent. Journal of Biomedical Material Research, 47(1999)2, pp 116-126.

[125] Sung, HW., Liang, IL., Chen, CN., Huang, RN. & Liang, HF. Stability of a biological tissue fixed with a naturally occurring crosslinking agent (genipin). Journal of Biomedical Material Research, 55(2001)4, pp. 538-546.

[126] Suri, S. & Schmidt, C.E. Photopatterned collagen–hyaluronic acid interpenetrating polymer network hydrogels. Acta Biomaterialia, 5(2009)7, pp. 2385-2397.

[127] Taguchi, T., Ikoma, T. & Tanaka, J. An improved method to prepare hyaluronic acid and type II collagen composite matrices. Journal of Biomedical Material Research, 61(2002)2, pp. 330-336.

[128] Tamaddon, M., Walton, R.S., Brand, D.D. & Czernuszka, J.T. (2013). Characterisation of freeze-dried type II collagen and chondroitin sulfate scaffolds. Journal of Material Science: Materials in Medicine, 24(2013)5, pp. 1153-1165.

[129] Tessmar, J.K.V., Holland, T.A. & Mikos, A.G. Salt leaching for polymer scaffolds: Laboratory-scale manufacture of cell carriers. In: Ma, P.X. & Elisseeff, J. Scaffolding in tissue engineering. USA 2009, Taylor & Francis Group. pp. 111-124.

[130] Thermo Fisher Scientific Inc. Chemistry of crosslinking. [WWW]. [accessed on 02.03.2015]. Available at: http://www.piercenet.com/method/chemistry-crosslinking

[131] Thermo Fisher Scientific Inc. Crosslinking technical handbook: Easy molecular bonding crosslinking technology. [WWW]. [accessed on 02.03.2015]. Available at: http://www.piercenet.com/method/chemistry-crosslinking

[132] Tian, H., Chen, Y., Ding, C. & Li, G. Interaction study in homogeneous collagen/chondroitin sulfate blends by two-dimensional infrared spectroscopy. Carbohydrate Polymers, 89(2012)2, pp. 542-550.

[133] Triche, R. & Mandelbaum, B.R. Overview of cartilage biology and new trends in cartilage stimulation. Foot and Ankle Clinics, 18(2013)1, pp. 1-12.

[134] Ulery, B.D., Nair, L.S. & Laurencin, C.T. Biomedical of biodegradable polymers: Review. Journal of Polymer Science Part B: Polymer Physics, 49(2011), pp. 832-864.

[135] University of Maryland Medical Center (UMMC). Chondroitin. [WWW]. [accessed on 02.03.2015]. Available at: http://umm.edu/health/medical/altmed/supplement/chondroitin

[136] Uquillas, J.A., Kishore, V. & Akkus, O. Genipin crosslinking elevates the strength of electrochemically aligned collagen to the level of tendons. Journal of the Mechanical Behavior of Biomedical Materials, 15(2012), pp. 176-189.

[137] Vaandering, B. Genipin. [WWW]. [accessed on: 02.03.2015]. Available at: https://www.wou.edu/las/physci/ch350/Projects_2006/Vaandering/Genipin.htm

[138] van Susante, J.L.C., Pieper, J., Buma, P., va Kuppevelt, T.H., van Beuningen, H., van Der Kraan, P.M., Veerkampf, J.H., van den Berg, W.B. & Veth, R.P.H. Linkage of chondroitin-sulfate to type I collagen scaffolds stimulates the bioactivity of seeded chondrocytes in vitro. Biomaterials, 21(2001)17, pp. 2359-2369.

[139] Vázquez, J.A., Rodríguez-Amado, I., Montemayor, M.I., Fraguas, J., González, M.P. & Murado, M.A. Chondroitin sulfate, hyaluronic acid and Chitin/Chitosan production using marine waste sources: Characteristics, applications and eco-friendly processes: A review. Mar. Drugs, 11(3), 747-774.

[140] Vickers, S.M., Gotterbarm, T. & Spector, M. Cross-linking affects cellular condensation and chondrogenesis in type II collagen-GAG scaffolds seeded with bone marrow-derived mesenchymal stem cells. Journal of Orthopaedic Research, 28(2010)9, pp. 1184-1192.

[141] Walters, B.D. & Stegemann, J.P. Strategies for directing the structure and function of three-dimensional collagen biomaterials across length scales. Acta Biomaterialia, 10(2014)4, pp. 1488-1501.

[142] Wang, TW. & Spector, M. Development of hyaluronic acid-based scaffolds for brain tissue engineering. Acta Biomaterialia, 5(2009)7, pp. 2371-2384.

[143] Wang, W. Lyophilization and development of solid protein pharmaceuticals. International Journal of Pharmaceutics, 203(2000)1–2, pp. 1-60.

[144] Yan, LP., Wang, YJ., Ren, L., Wu, G., Caridade, S.G., Fan, JB., Wang, LY., Ji, PH., Oliveira, J.M., Oliveira, J. T., Mano, J.F. & Reis, R.L. Genipin-cross-linked collagen/chitosan biomimetic scaffolds for articular cartilage tissue engineering applications. Journal of Biomedical Material Research Part A, 95(2010), pp. 465–75.

[145] Yoo, J.S., Kim, Y.J., Kim, S.H., & Choi, S.H. Study on genipin: A new alternative natural crosslinking agent for fixing heterograft tissue. Korean Journal of Thoracic Cardiovascular Surgery, 44(2011)3, pp. 197-207.

[146] Zeeman, R. Cross-linking of collagen-based materials. Doctoral thesis. Netherlands 1998. University of Twente. 199 p.

[147] Zhang, L., Li, K., Xiao, W., Zheng, L., Xiao, Y., Fan, H. & Zhang, X. Preparation of collagen–chondroitin sulfate–hyaluronic acid hybrid hydrogel scaffolds and cell compatibility in vitro. Carbohydrate Polymers, 84(2011)1, pp. 118-125.

[148] Zhu, J.J. Transport studies of chondroitin sulfate disaccharide through articular cartilage. Master's thesis. USA 1997. Massachusetts Institute of Technology, Department of Electrical Engineering and Computer Science. 57 p.

APPENDIX 1: SCAFFOLDS BEFORE AND AFTER CROSS-LINKING

The photographs below demonstrate the general impact that the cross-linking treatment had on each scaffold group. The scaffolds were photographed in mixed order before and after cross-linking, and therefore the before and after photographs should not be compared as scaffold per scaffold. Abbreviation 'CL' in the caption text stands for cross-linking.

C100 scaffolds *before* EDC/NHS CL

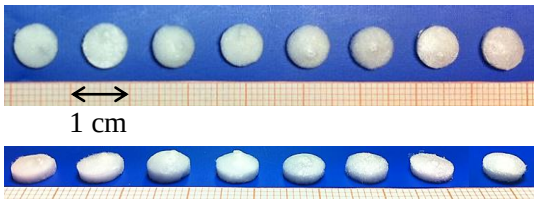

C100 scaffolds *after* EDC/NHS CL

C100 scaffolds *before* GP CL

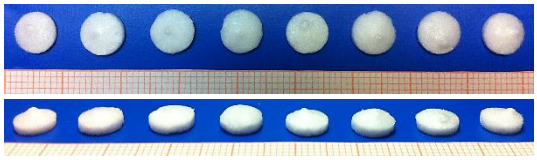

C100 scaffolds *after* GP CL

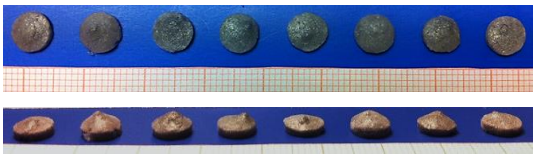

C80H scaffolds *before* EDC/NHS CL

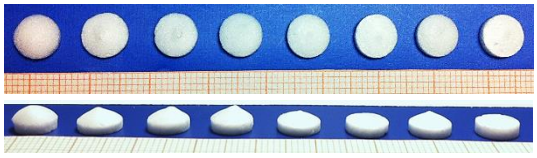

C80H scaffolds *after* EDC/NHS CL

C80H scaffolds *before* GP CL

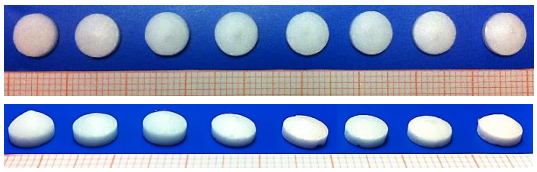

C80H scaffolds *after* GP CL

C60H scaffolds *before* EDC/NHS CL

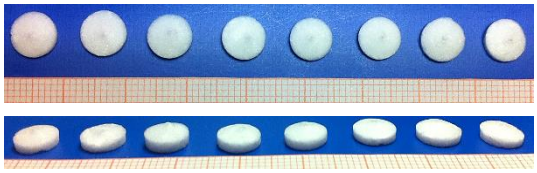

C60H scaffolds *after* EDC/NHS CL

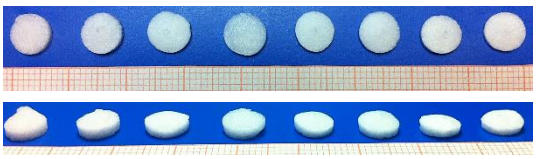

C80CS scaffolds *before* EDC/NHS CL

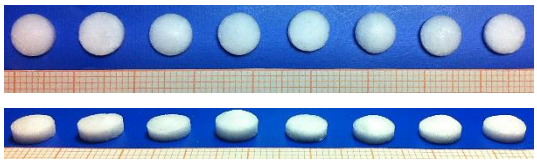

C80CS scaffolds *after* EDC/NHS CL

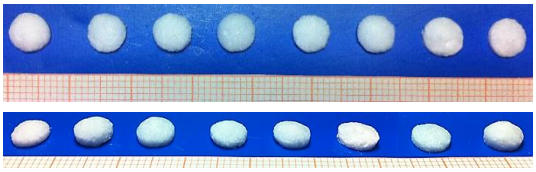

C80CS scaffolds *before* GP CL

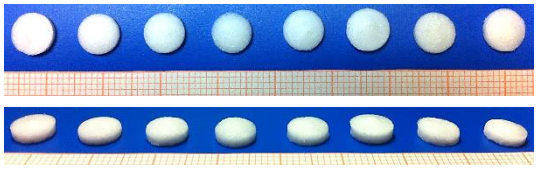

C80CS scaffolds *after* GP CL

C60CS scaffolds *before* EDC/NHS CL

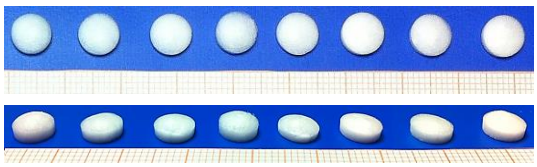

C60CS scaffolds *after* EDC/NHS CL

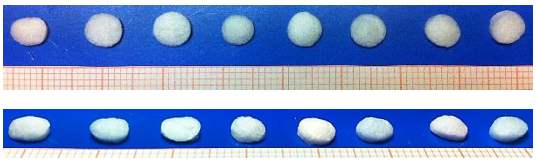

C80CS15H scaffolds *before* EDC/NHS CL

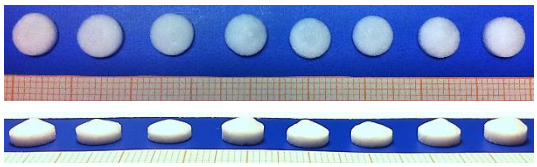

C80CS15H scaffolds *after* EDC/NHS CL

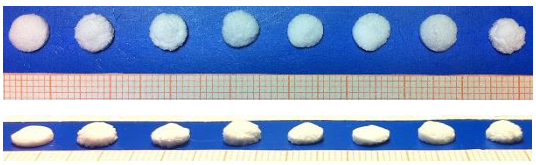

C80CS15H scaffolds *before* GP CL

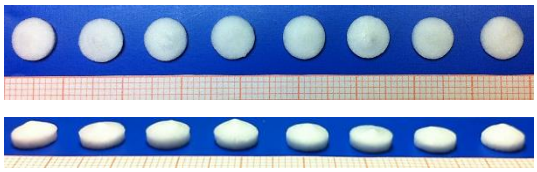

C80CS15H scaffolds *after* GP CL

C60CS30H scaffolds *before* EDC/NHS CL

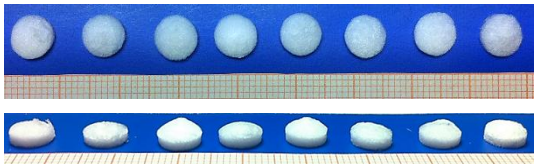

C60CS30H scaffolds *after* EDC/NHS CL

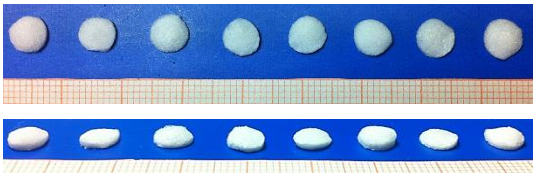

APPENDIX 2: PHOTOGRAPHS TAKEN FROM THE SCAFFOLDS IN DRY, SOAKING WET AND FILTER DRIED STATE

Adjacent images represent one scaffold from each scaffold group; photographed in dry, soaking wet (SW) and filter dried (FD) state. SW shows the scaffold after immersion in PBS (pH 7.4) for 24 hours and FD after drying between filter papers.

C100E

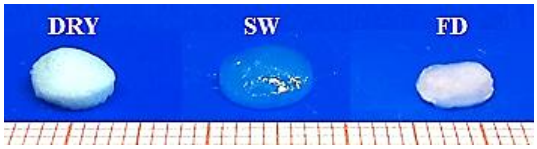

C100G

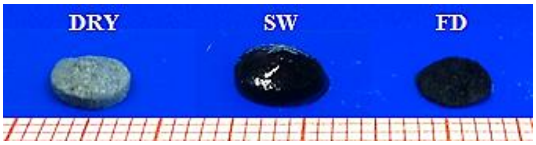

C80HE

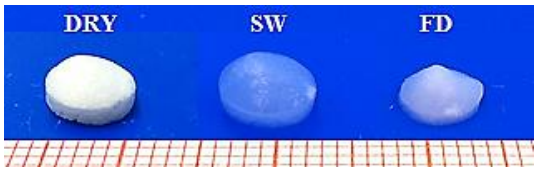

C80HG

C80CSE

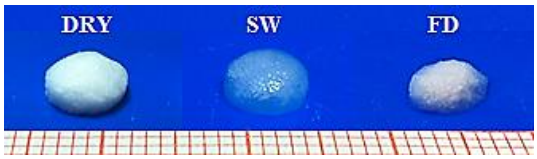

C80CSG

C80CS15HE

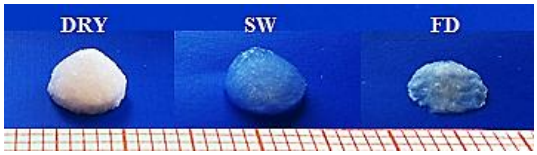

C80CS15HG

C60HE

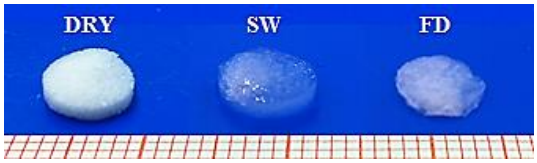

C60CSE

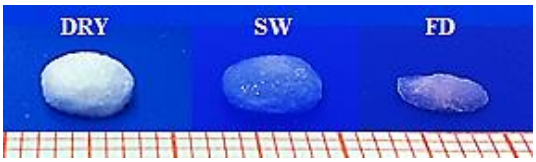

C60CS30HE

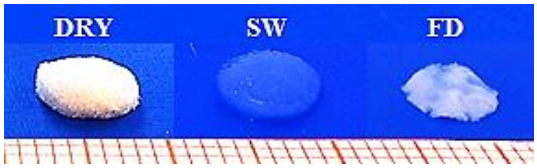

APPENDIX 3: COMPRESSIVE STRESS-STRAIN CURVES OF THE DRY SCAFFOLDS

Numbers appearing in each figure (from #01 to #06) stand for parallel scaffolds within each test group.

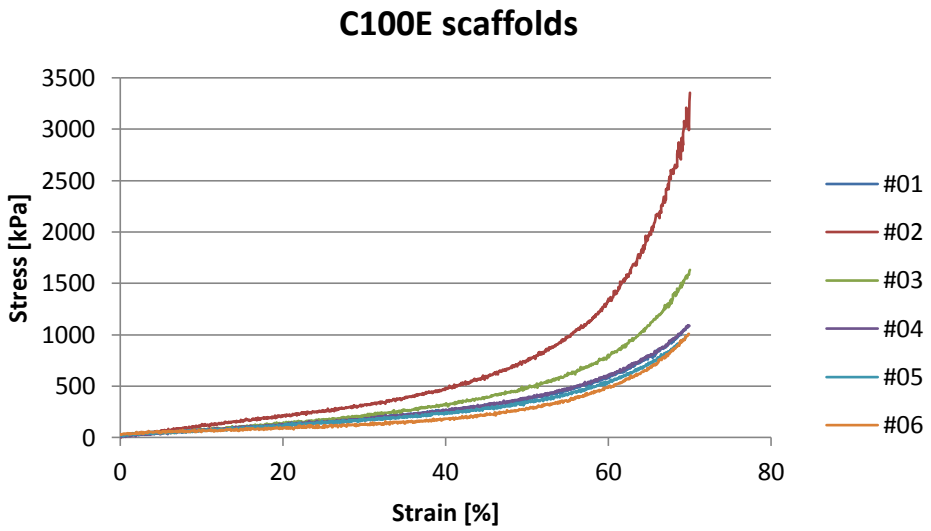

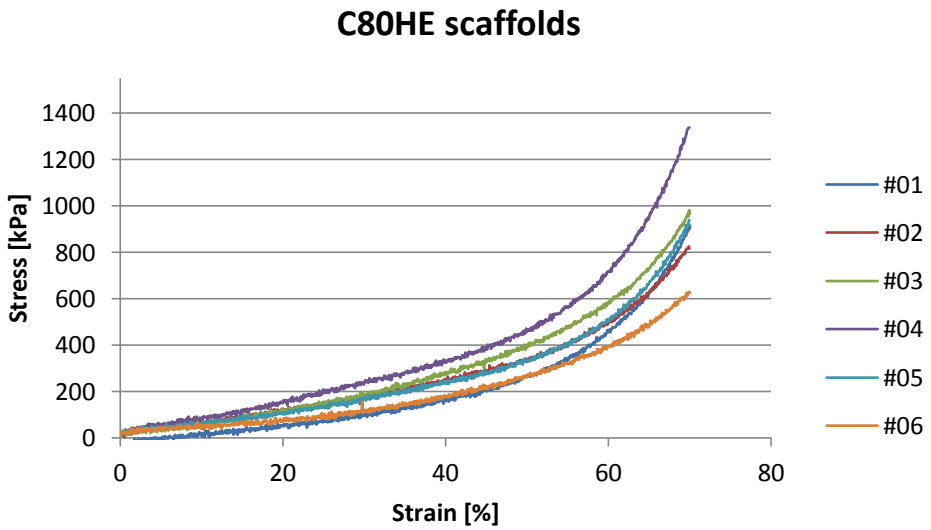

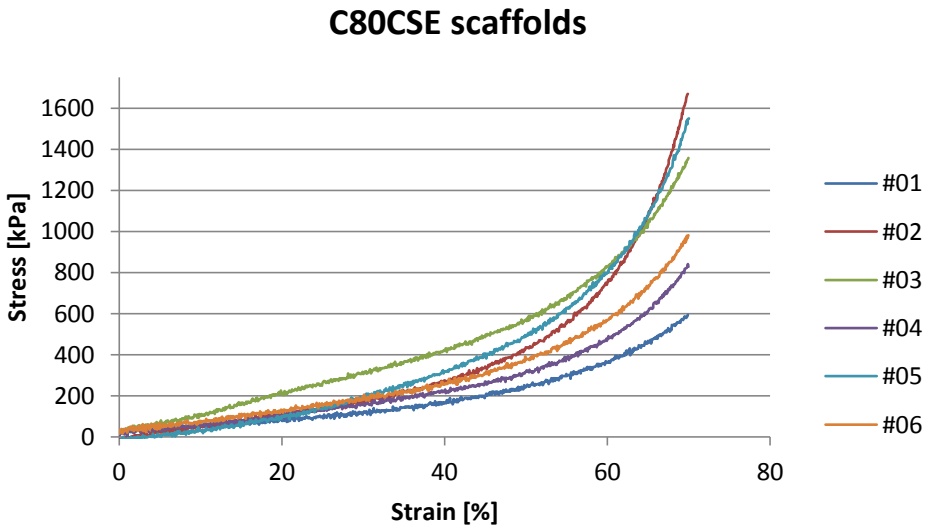
C80CSE scaffolds
Stress [kPa]
1600
1400
1200
1000
800
600
400
200
0
0
20
40
60
80
Strain [%]
#01
#02
#03
#04
#05
#06

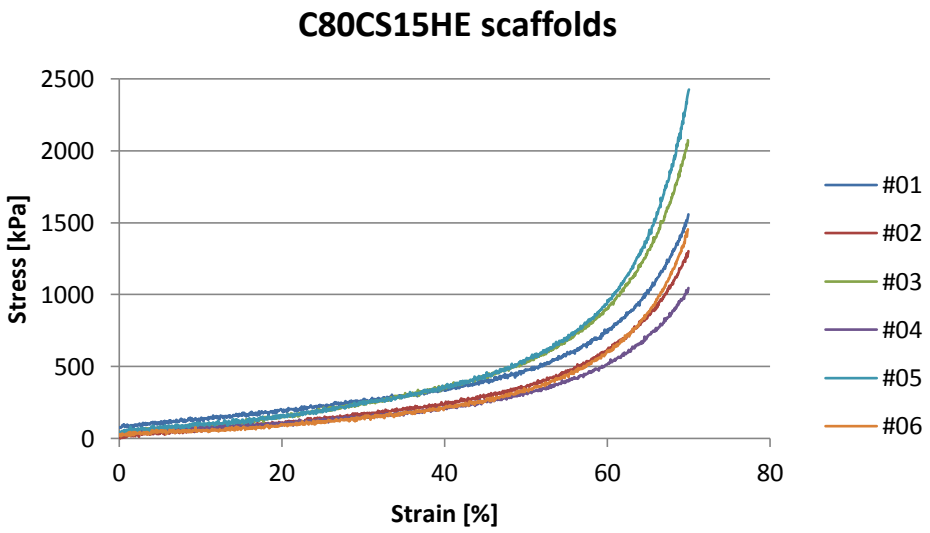
C80CS15HE scaffolds
Stress [kPa]
2500
2000
1500
1000
500
0
0
20
40
60
80
Strain [%]
#01
#02
#03
#04
#05
#06

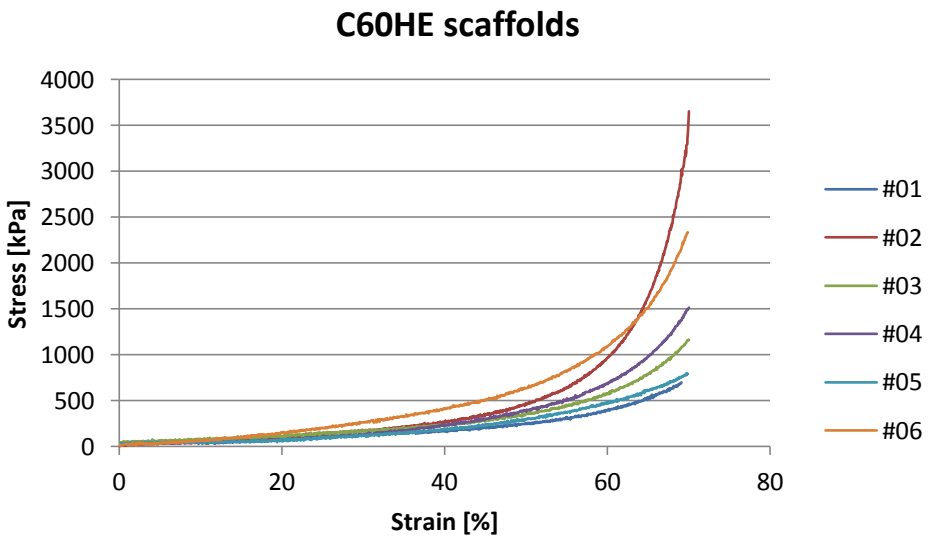
C60HE scaffolds
Stress [kPa]
4000
3500
3000
2500
2000
1500
1000
500
0
0
20
40
60
80
Strain [%]
#01
#02
#03
#04
#05
#06

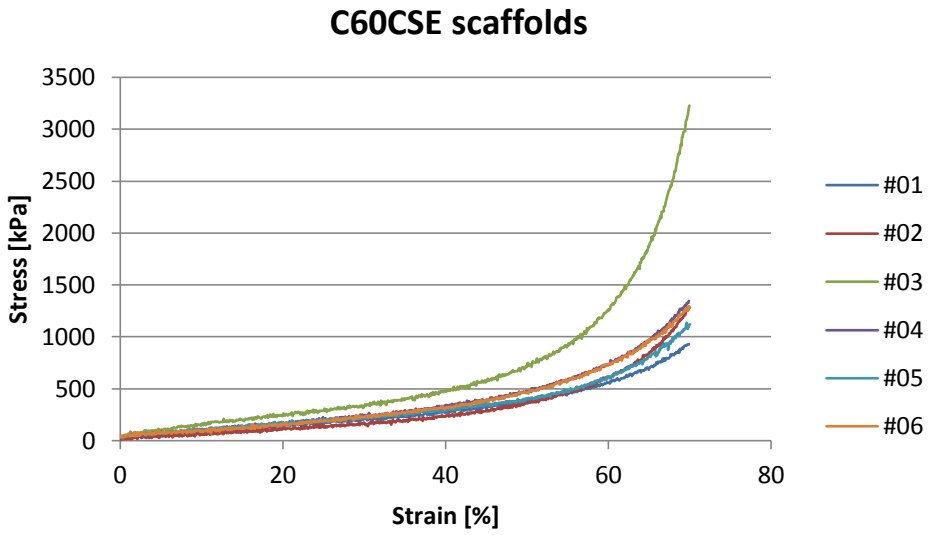
C60CSE scaffolds
Stress [kPa]
3500
3000
2500
2000
1500
1000
500
0
0
20
40
60
80
Strain [%]
#01
#02
#03
#04
#05
#06

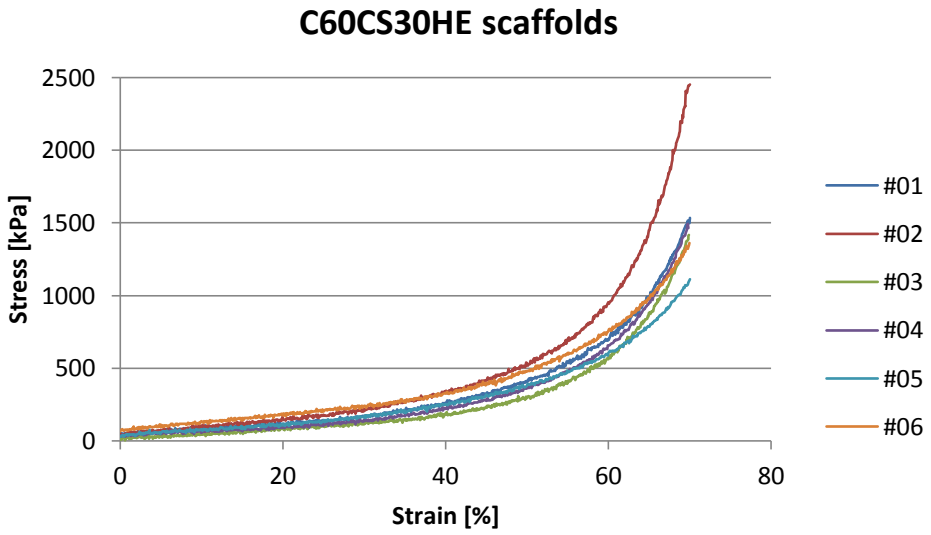
C60CS30HE scaffolds
Stress [kPa]
2500
2000
1500
1000
500
0
0
20
40
60
80
Strain [%]
#01
#02
#03
#04
#05
#06

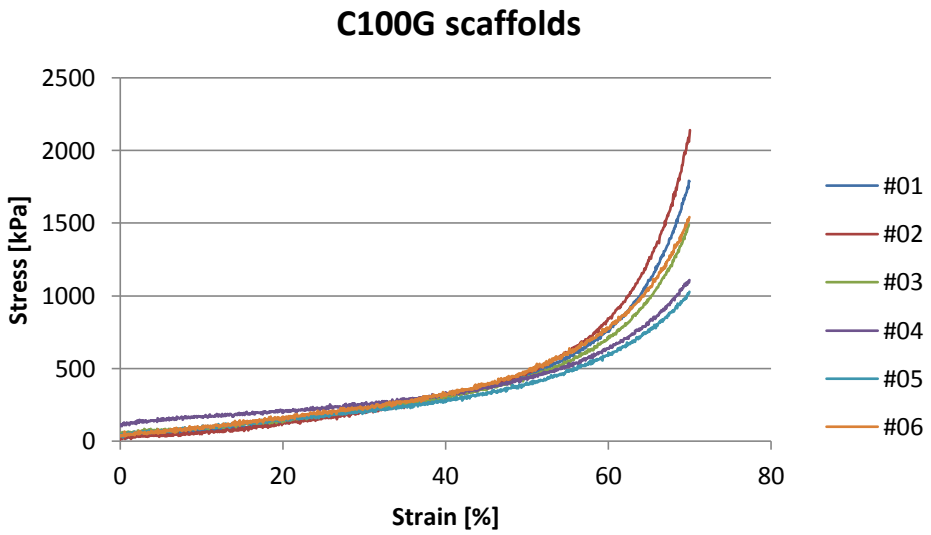
C100G scaffolds
Stress [kPa]
2500
2000
1500
1000
500
0
0
20
40
60
80
Strain [%]
#01
#02
#03
#04
#05
#06

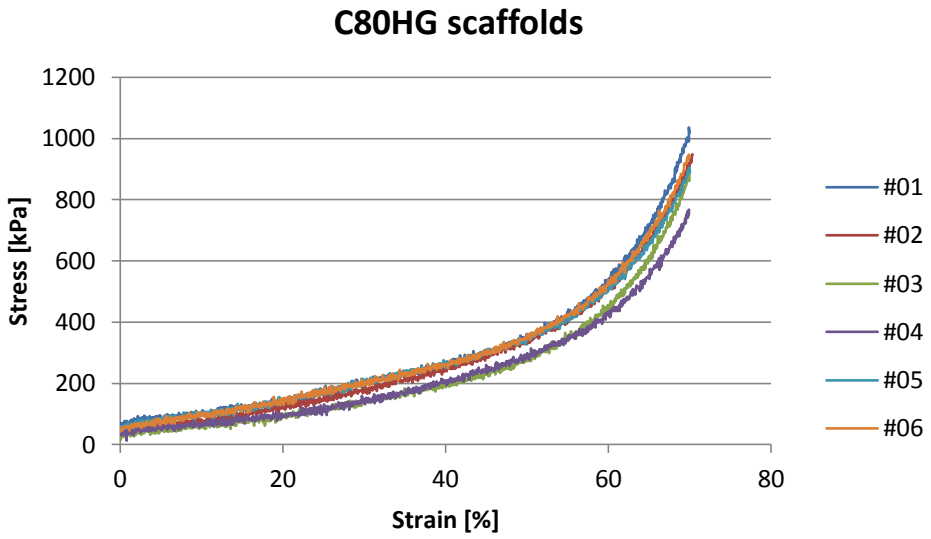
C80HG scaffolds
Stress [kPa]
1200
1000
800
600
400
200
0
0
20
40
60
80
Strain [%]
#01
#02
#03
#04
#05
#06

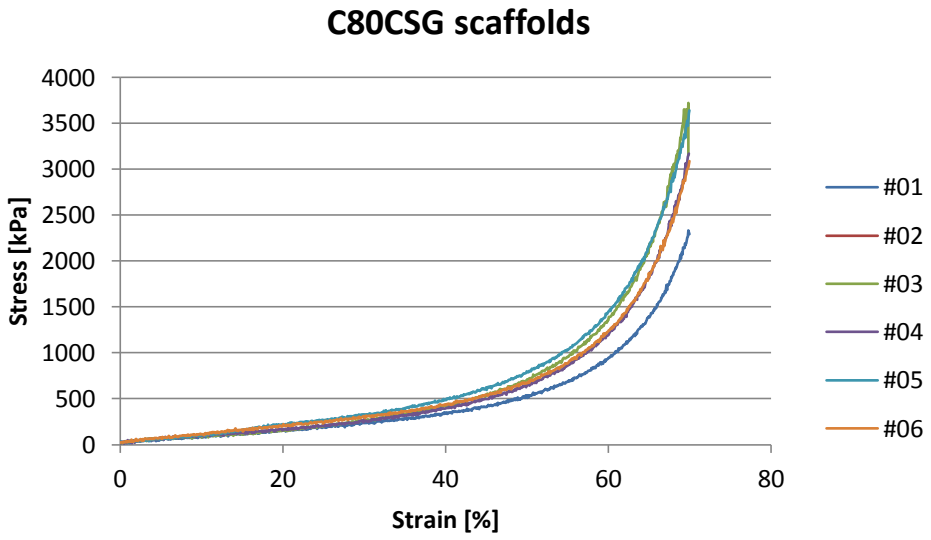
C80CSG scaffolds
Stress [kPa]
4000
3500
3000
2500
2000
1500
1000
500
0
0
20
40
60
80
Strain [%]
#01
#02
#03
#04
#05
#06

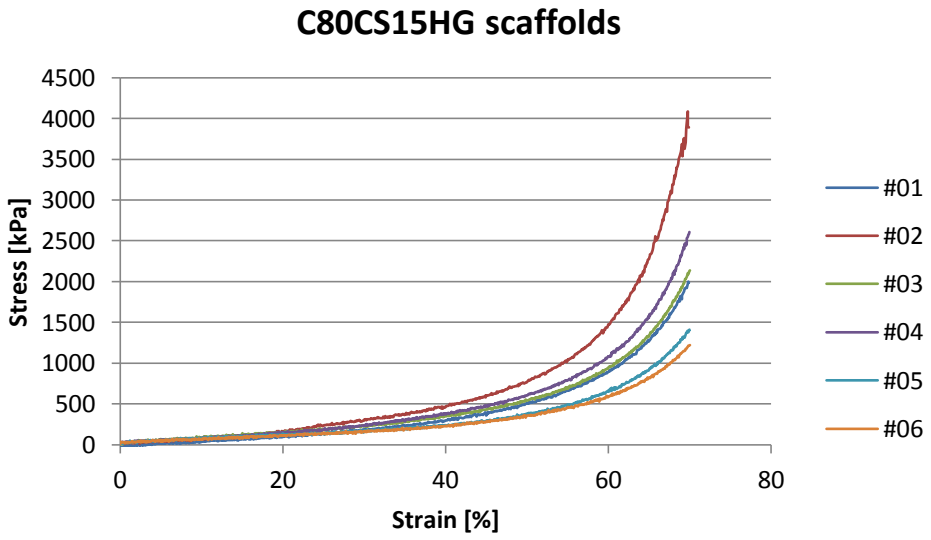
C80CS15HG scaffolds
Stress [kPa]
4500
4000
3500
3000
2500
2000
1500
1000
500
0
0
20
40
60
80
Strain [%]
#01
#02
#03
#04
#05
#06

APPENDIX 4: COMPRESSIVE STRESS-STRAIN CURVES OF THE WET SCAFFOLDS

Numbers appearing in each figure (from #01 to #06) stand for parallel scaffolds within each test group.

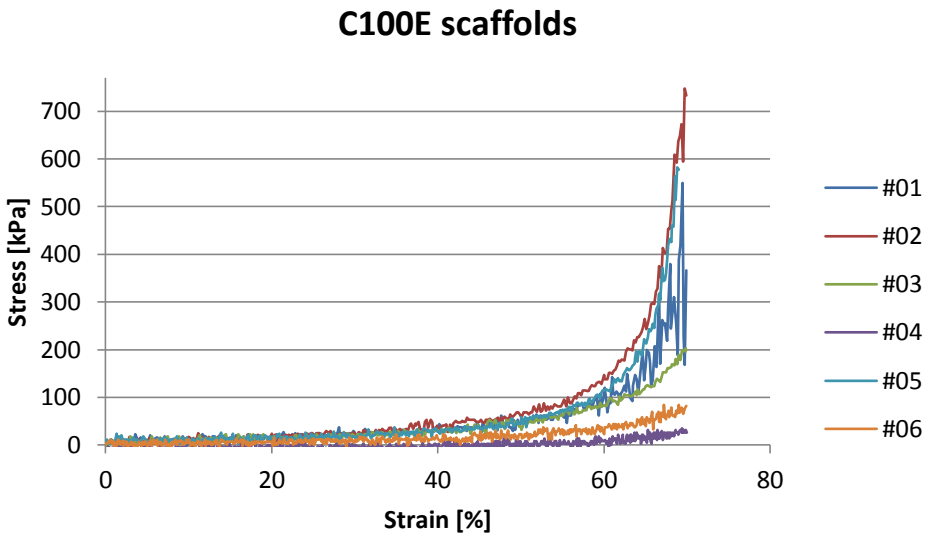

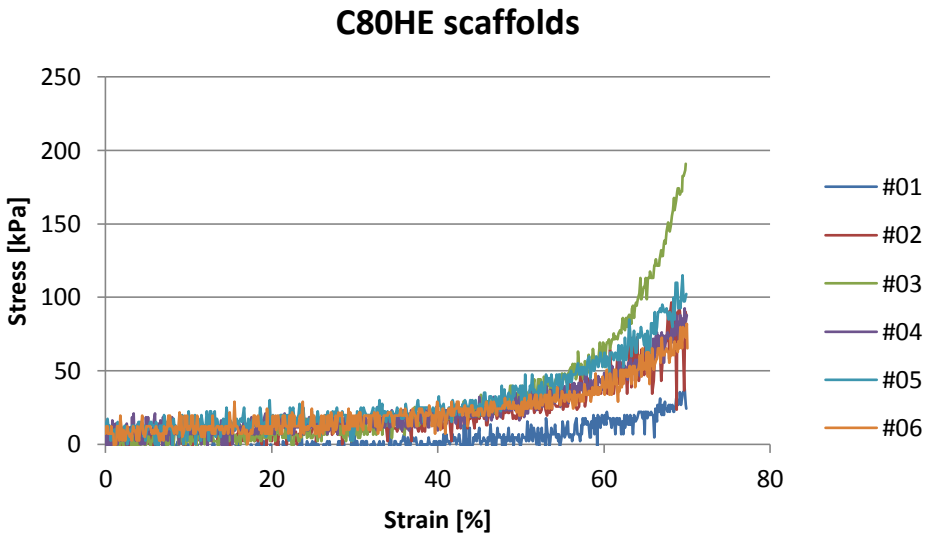

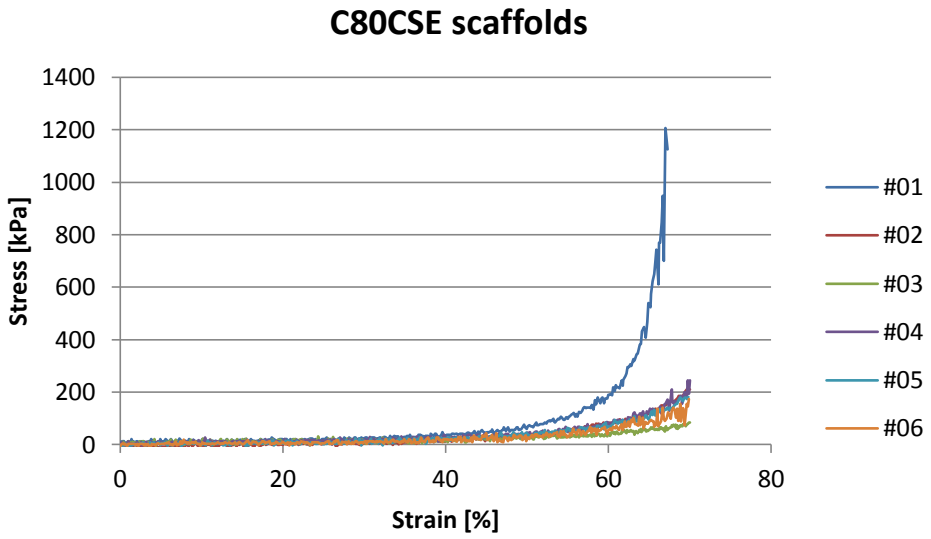
C80CSE scaffolds
1400
1200
1000
800
600
400
200
0
Stress [kPa]
0
20
40
60
80
Strain [%]
#01
#02
#03
#04
#05
#06

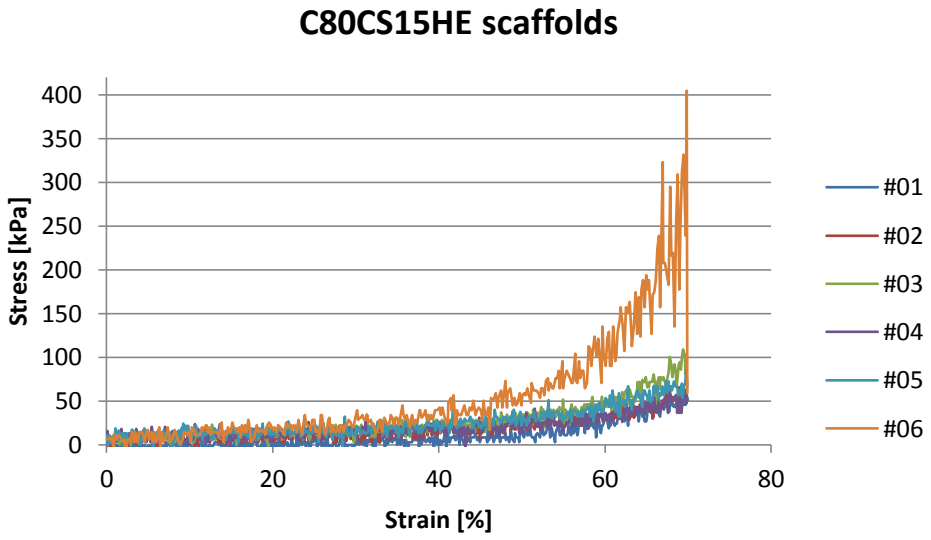
C80CS15HE scaffolds
400
350
300
250
200
150
100
50
0
Stress [kPa]
0
20
40
60
80
Strain [%]
#01
#02
#03
#04
#05
#06

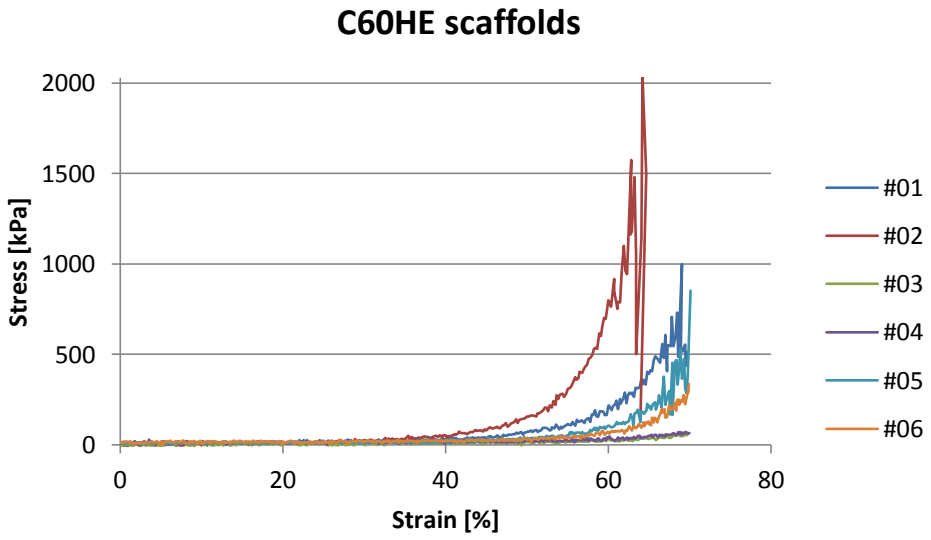
C60HE scaffolds
2000
1500
1000
500
0
Stress [kPa]
0
20
40
60
80
Strain [%]
#01
#02
#03
#04
#05
#06

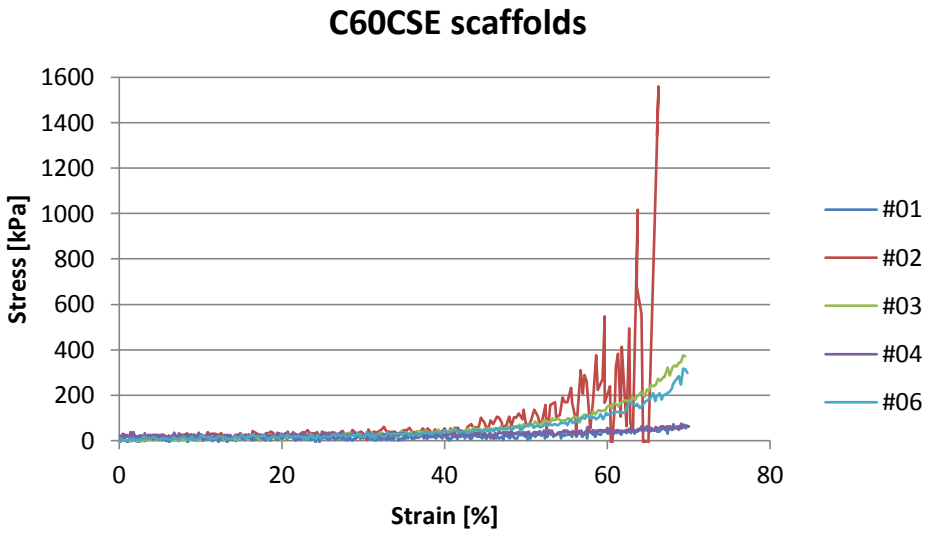
C60CSE scaffolds
Stress [kPa]
1600
1400
1200
1000
800
600
400
200
0
0
20
40
60
80
Strain [%]
#01
#02
#03
#04
#06

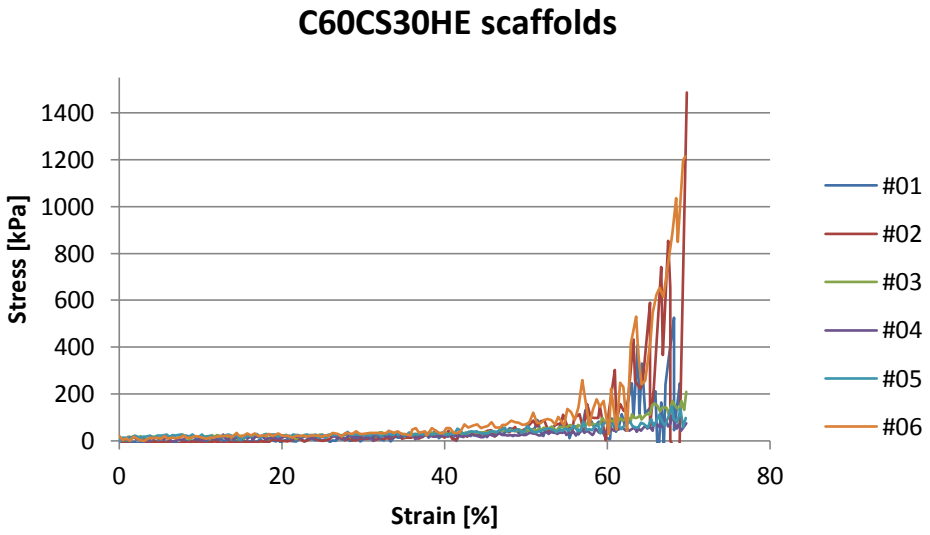
C60CS30HE scaffolds
Stress [kPa]
1400
1200
1000
800
600
400
200
0
0
20
40
60
80
Strain [%]
#01
#02
#03
#04
#05
#06

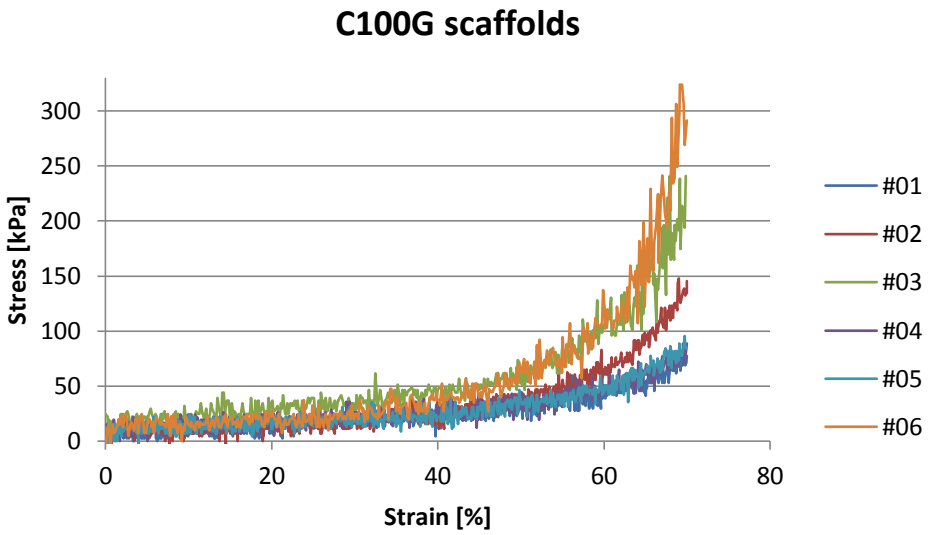
C100G scaffolds
Stress [kPa]
300
250
200
150
100
50
0
0
20
40
60
80
Strain [%]
#01
#02
#03
#04
#05
#06

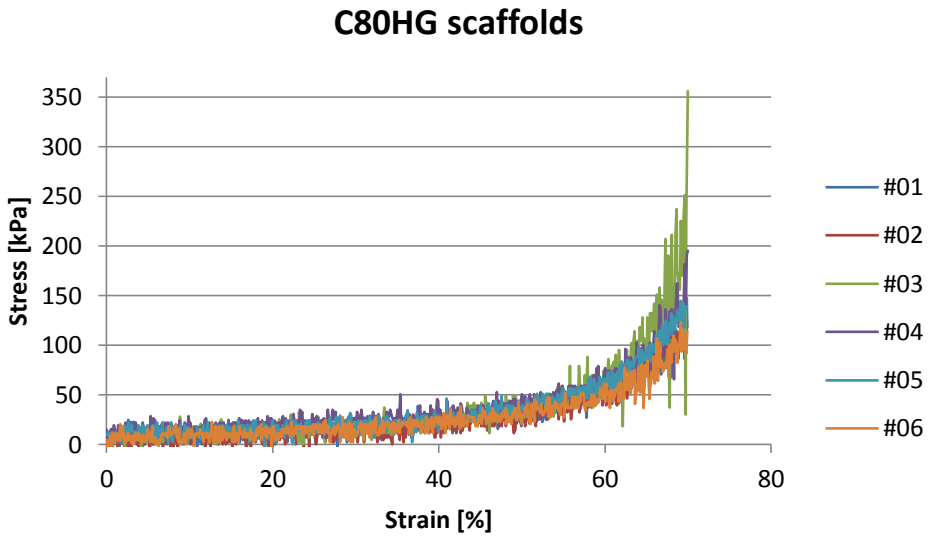
C80HG scaffolds
Stress [kPa]
350
300
250
200
150
100
50
0
0
20
40
60
80
Strain [%]
#01
#02
#03
#04
#05
#06

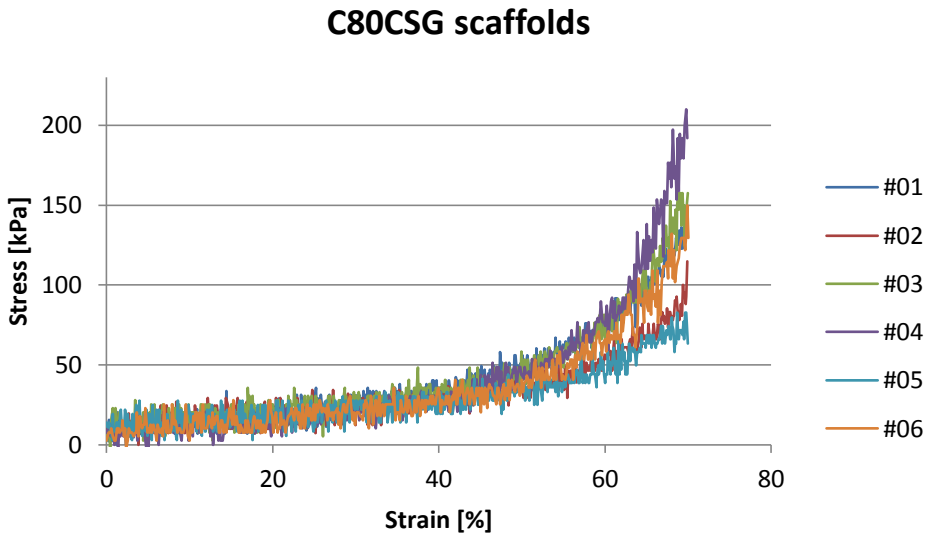
C80CSG scaffolds
Stress [kPa]
200
150
100
50
0
0
20
40
60
80
Strain [%]
#01
#02
#03
#04
#05
#06

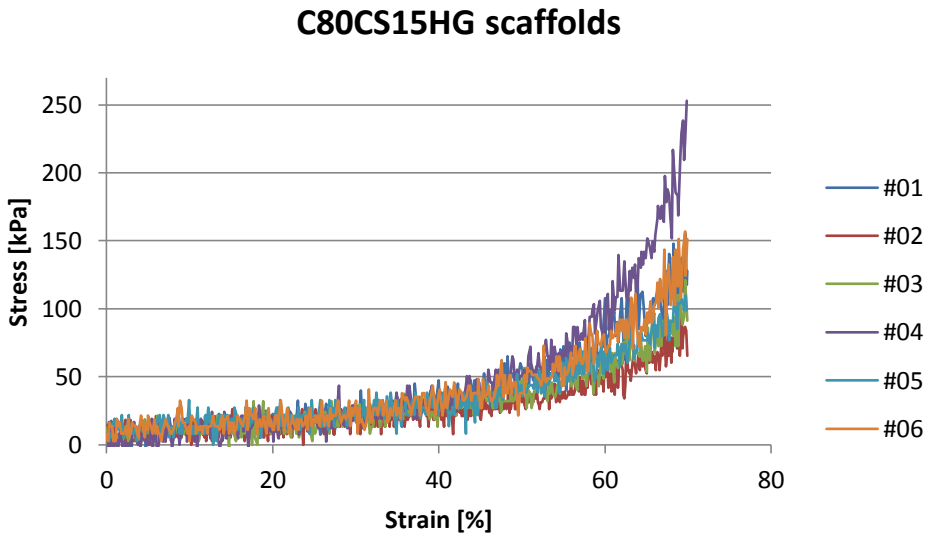
C80CS15HG scaffolds
Stress [kPa]
250
200
150
100
50
0
0
20
40
60
80
Strain [%]
#01
#02
#03
#04
#05
#06

APPENDIX 5: MICRO-COMPUTED TOMOGRAPHY IMAGES OF THE SCAFFOLDS

Image shown on top left represent a partial 3D reconstruction of the scaffold taken from 1 mm x 1 mm x 1 mm area of the scaffold (scale bar = 500 µm). The other three images are 2D photographs taken from different areas of the scaffold (scale bar = 300 µm).

C100E

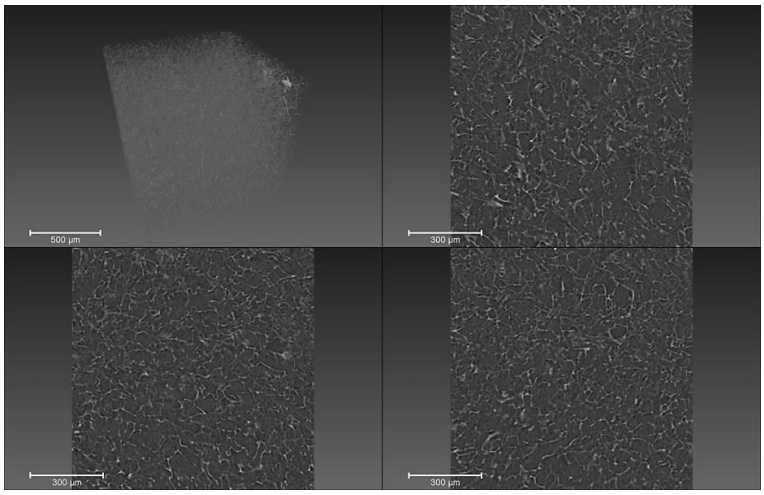

C100G

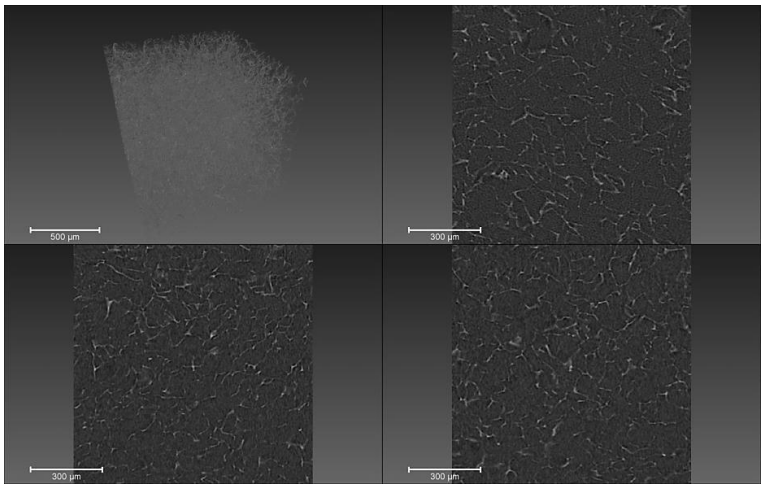

C80HE

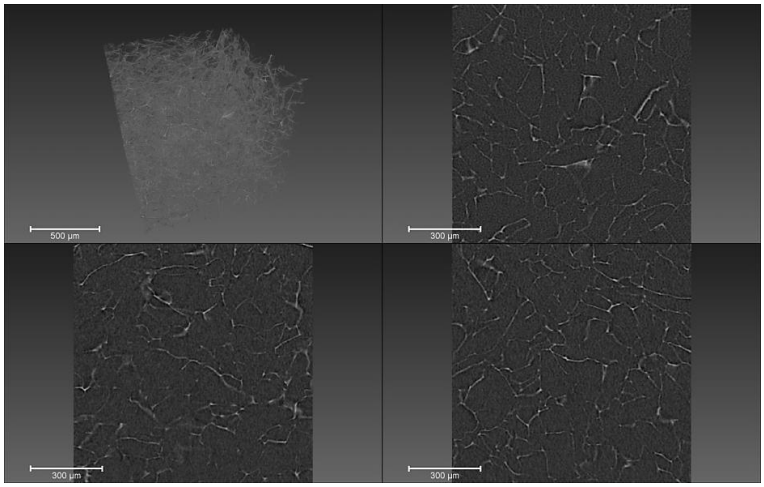

C80HG

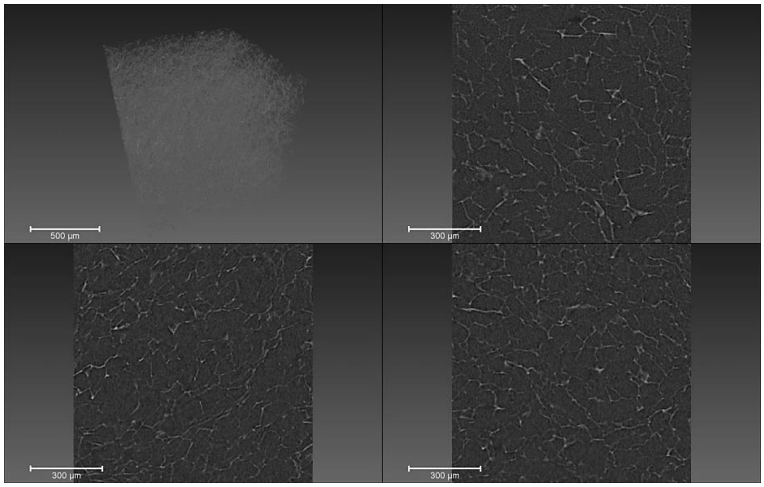

C60HE

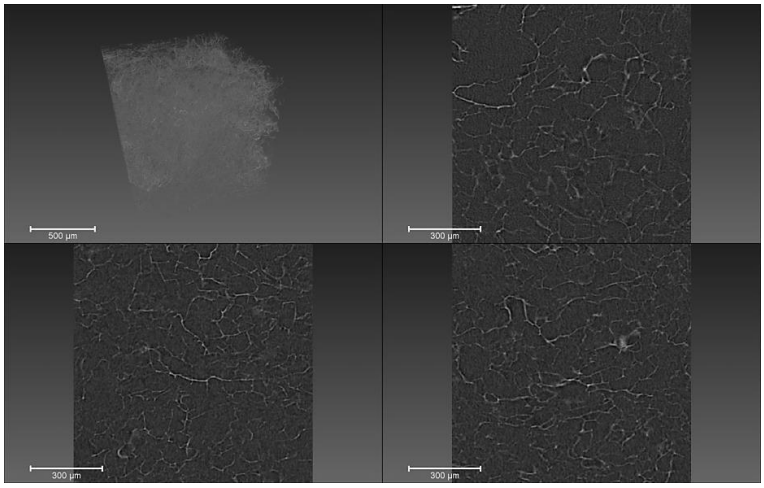

C80CSE

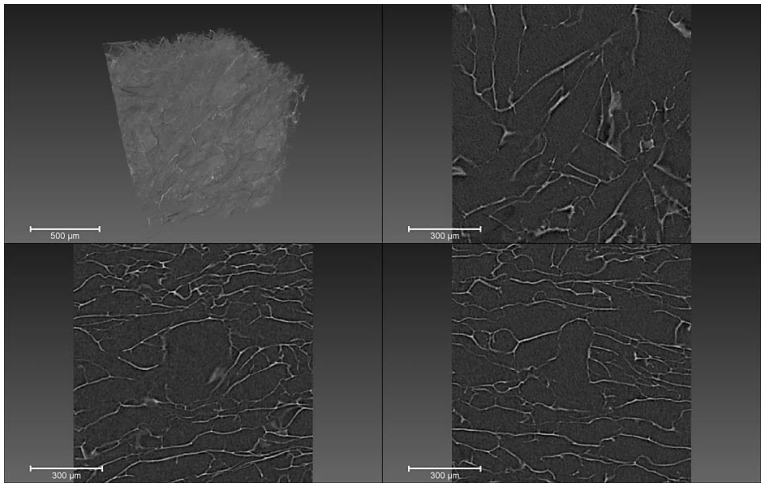

C80CSG

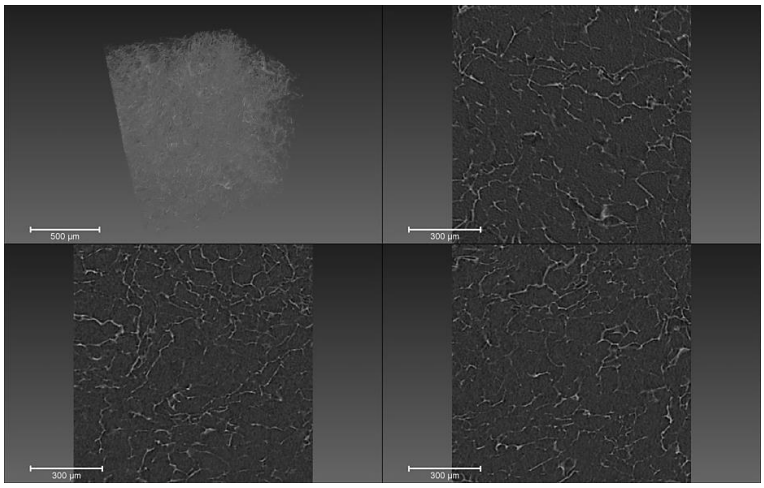

C60CSE

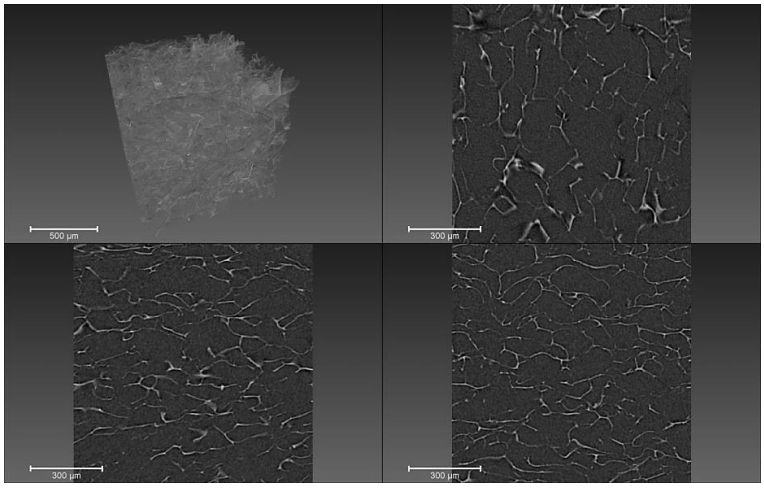

C80CS15HE

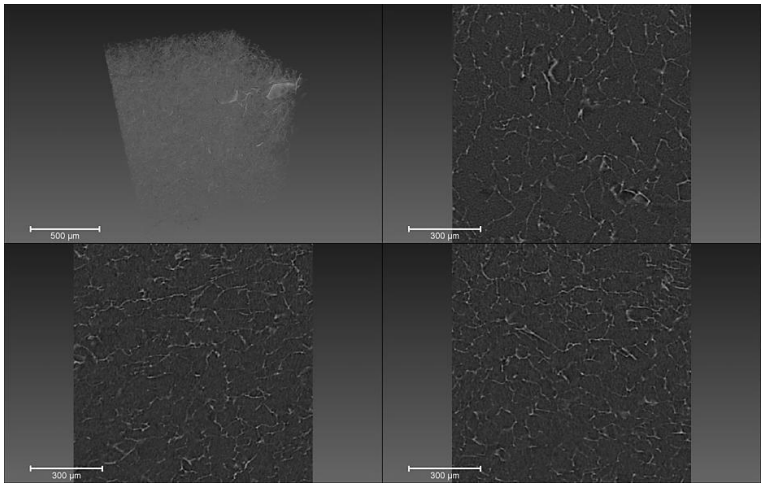

C80CS15HG

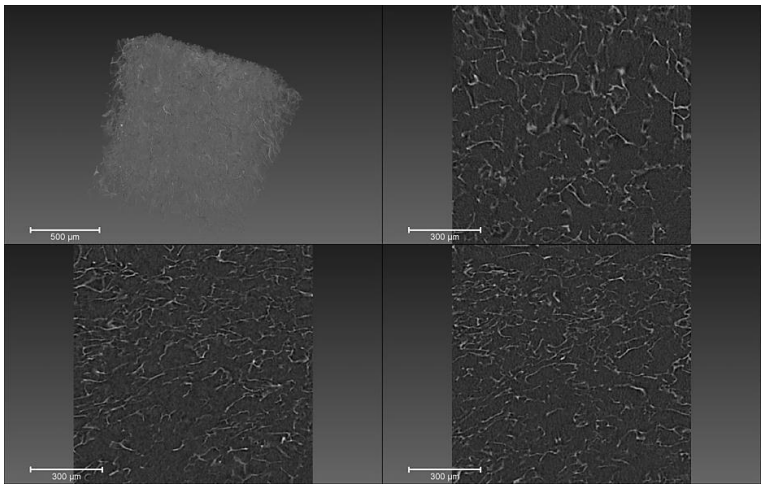

C60CS30HE

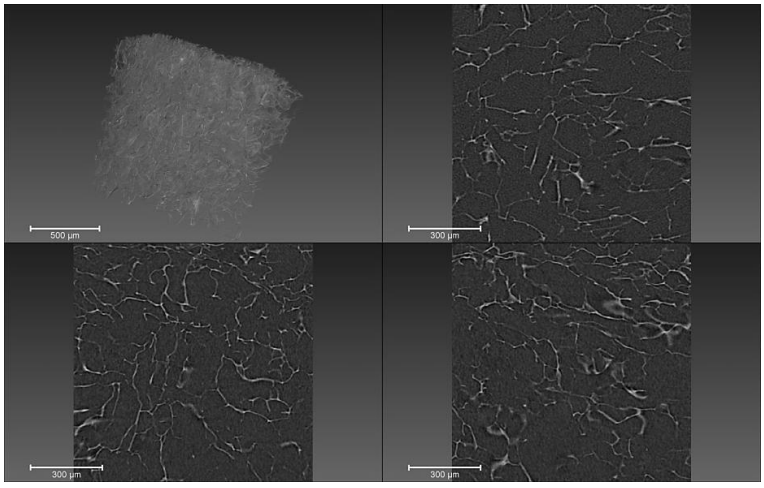

APPENDIX 6: FOURIER TRANSFORM INFRARED SPECTRA OF THE SCAFFOLDS

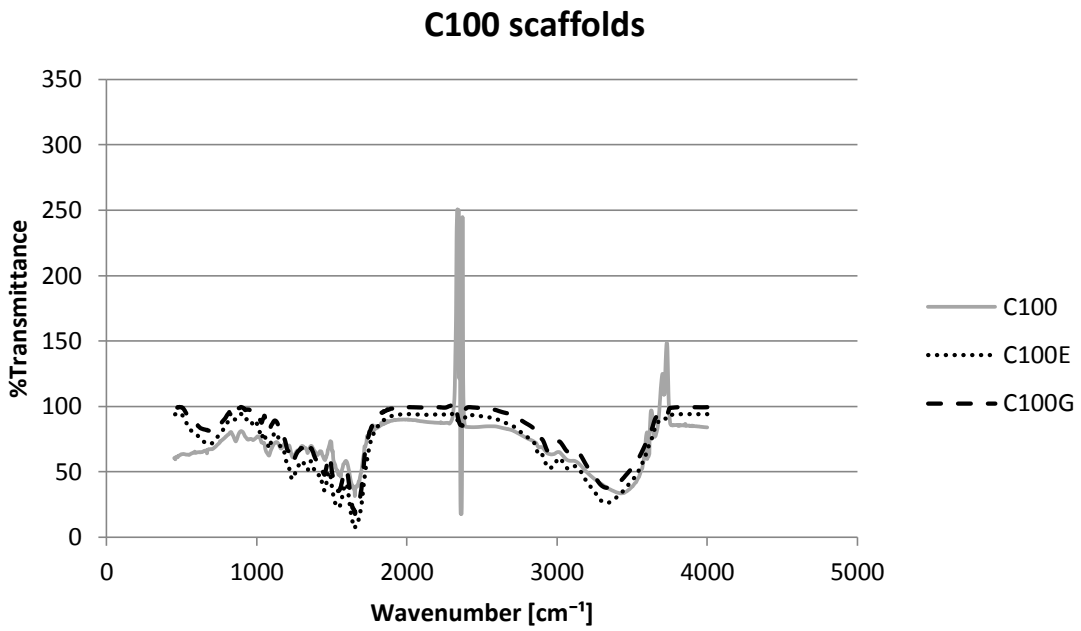

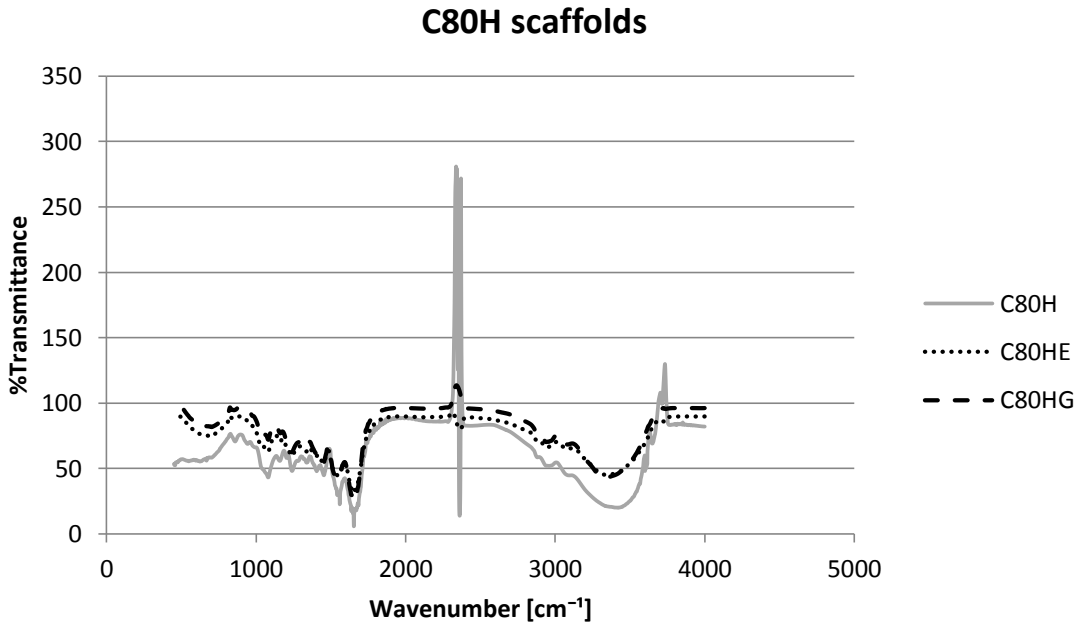

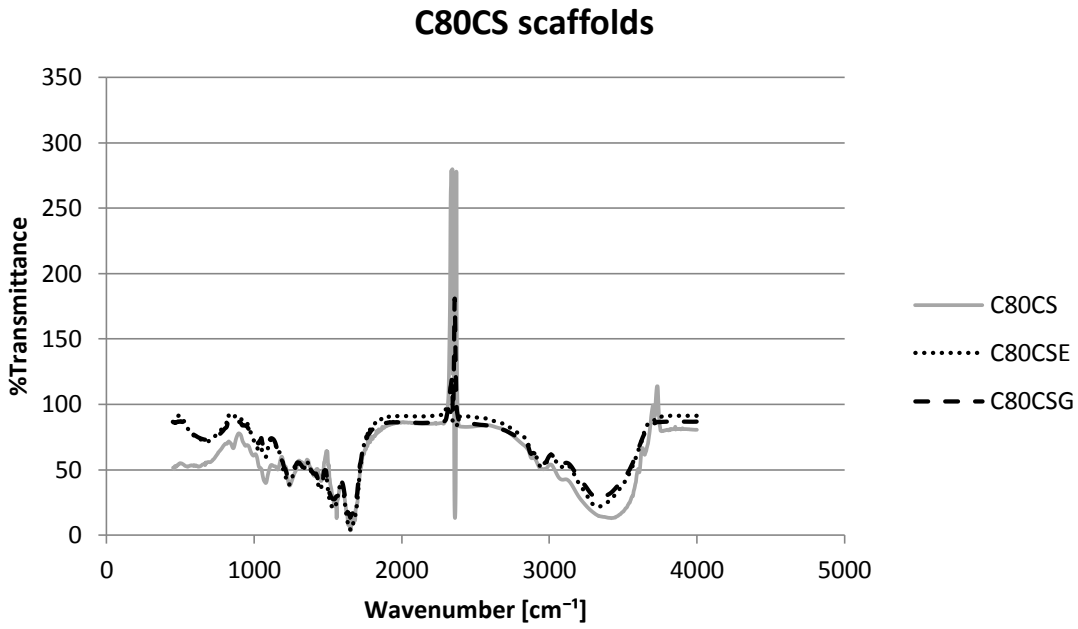
C80CS scaffolds
%Transmittance
350
300
250
200
150
100
50
0
0
1000
2000
3000
4000
5000
Wavenumber [cm⁻¹]
C80CS
C80CSE
C80CSG

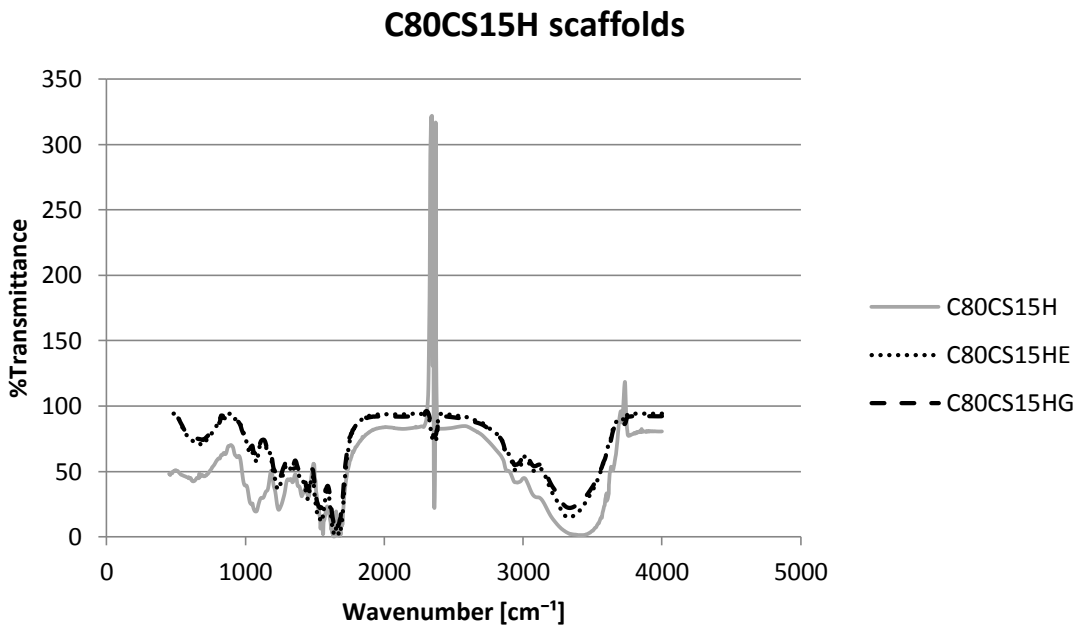
C80CS15H scaffolds
%Transmittance
350
300
250
200
150
100
50
0
0
1000
2000
3000
4000
5000
Wavenumber [cm⁻¹]
C80CS15H
C80CS15HE
C80CS15HG

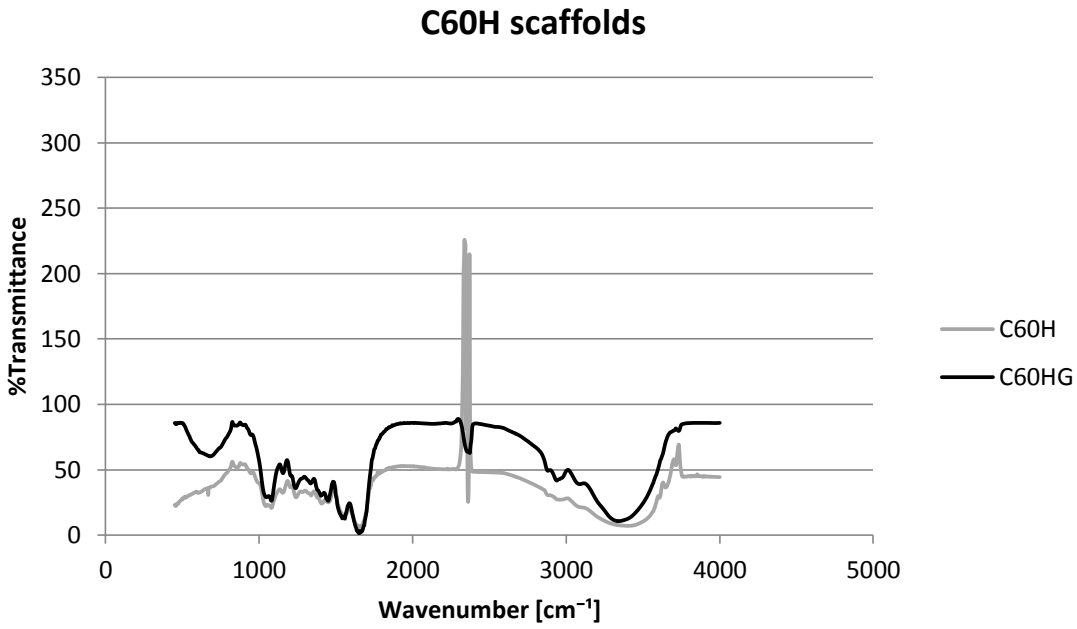
C60H scaffolds
%Transmittance
350
300
250
200
150
100
50
0
0
1000
2000
3000
4000
5000
Wavenumber [cm⁻¹]
C60H
C60HG

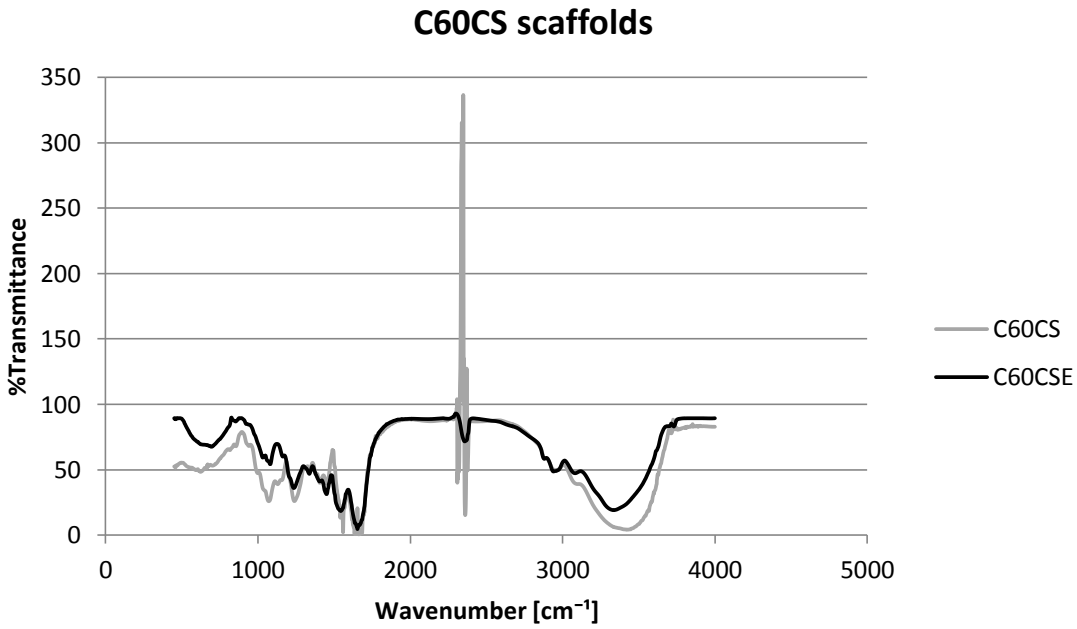
C60CS scaffolds
%Transmittance
350
300
250
200
150
100
50
0
0
1000
2000
3000
4000
5000
Wavenumber [cm⁻¹]
C60CS
C60CSE

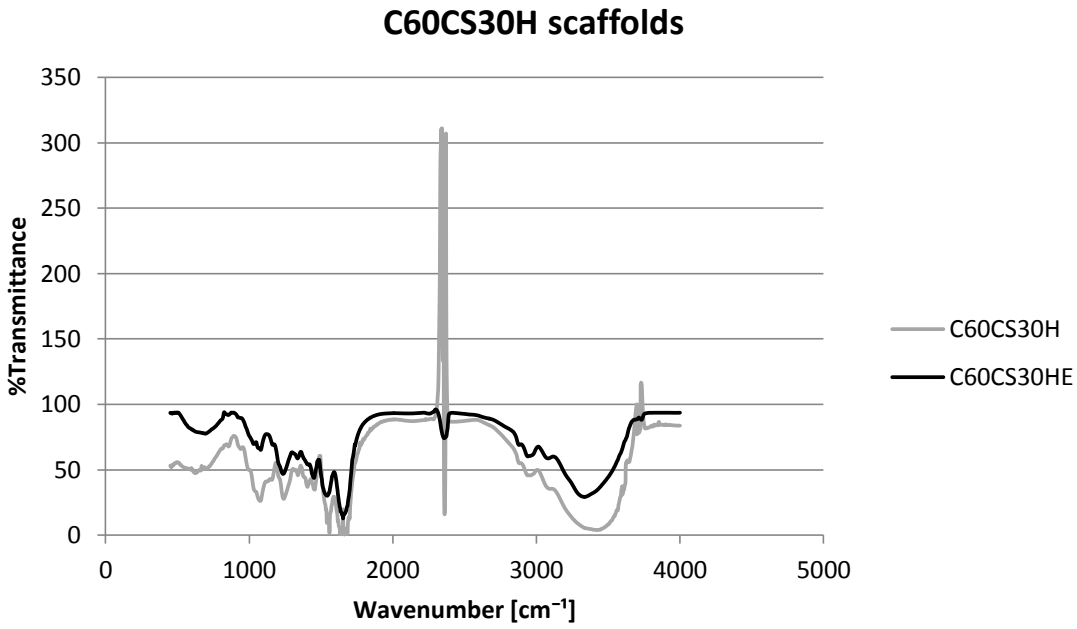
C60CS30H scaffolds
%Transmittance
350
300
250
200
150
100
50
0
0
1000
2000
3000
4000
5000
Wavenumber [cm⁻¹]
C60CS30H
C60CS30HE

APPENDIX 7: COMPARABLE COMPRESSIVE MODULUS RESULTS

All the scaffolds presented in the table below are cylindrical shaped. Abbreviations used in the table: d = diameter, h = height, ADH = adipic dihydrazide and DHT = dehydrothermal.

Reference	Composition	Form	Dimensions (d x h) [mm]	Freeze -dried	EDC/NHS cross-linked	GP cross-linked	Compression modulus [kPa]	Other modifications
DRY COLLAGEN scaffolds								
[95]	COL	Hydrogel	34,6 x 13,5	no	yes	yes	44,44 ± 0,13	ADH cross-linked
[137]	COL	Scaffold	8 x 2	yes	yes	no	115,1 ± 22,6	
Present study	COL	Scaffold	8 x 2	yes	yes	no	522 ± 52	
Present study	COL	Scaffold	8 x 2	yes	no	yes	437 ± 96	
WET COLLAGEN scaffolds								
[137]	COL	Scaffold	8 x 2	yes	yes	no	5,0 ± 0,5	
[81]	COL	Scaffold	8-9,5 x 4	yes	no	no	0,2 ± 0,08	Uncross-linked
[81]	COL	Scaffold	8-9,5 x 4	yes	no	no	0,43 ± 0,21	DHT cross-linked
Present study	COL	Scaffold	8 x 2	yes	yes	no	43 ± 13	
Present study	COL	Scaffold	8 x 2	yes	no	yes	44 ± 21	
DRY COLLAGEN + CHONDROITIN SULFATE + HYALURONIC ACID scaffolds								
[95]	COL+CS+HA	Hydrogel	34,6 x 13,5	no	yes	yes	44,93 ± 0,66	ADH cross-linked
[95]	COL+CS+HA-0,6	Hydrogel	34,6 x 13,5	no	yes	yes	48,09 ± 0,62	ADH cross-linked
[95]	COL+CS+HA-0,75	Hydrogel	34,6 x 13,5	no	yes	yes	51,53 ± 0,54	ADH cross-linked
[95]	COL+CS+HA-1	Hydrogel	34,6 x 13,5	no	yes	yes	53,67 ± 0,36	ADH cross-linked
Present study	COL+CS+HA 80:15:5	Scaffold	8 x 2	yes	yes	no	391 ± 142	
Present study	COL+CS+HA 80:15:5	Scaffold	8 x 2	yes	no	yes	559 ± 131	
Present study	COL+CS+HA 60:30:10	Scaffold	8 x 2	yes	yes	no	316 ± 110	
WET COLLAGEN + CHONDROTIN SULFATE scaffolds								
[136]	COL+CS	Scaffold	d = 8-20	no	yes	no	0,18-0,23 ± 0,05	Frozen by cooling rate technique, DHT cross-linked
[81]	COL+CS	Scaffold	8-9,5 x 4	yes	no	no	2,4 ± 0,08	Uncross-linked
[81]	COL+CS	Scaffold	8-9,5 x 4	yes	no	no	5,7 ± 0,07	DHT cross-linked
Present study	COL+CS 80:20	Scaffold	8 x 2	yes	yes	no	29 ± 13	
Present study	COL+CS 80:20	Scaffold	8 x 2	yes	no	yes	32 ± 16	
Present study	COL+CS 60:40	Scaffold	8 x 2	yes	yes	no	60 ± 9	

DRY COLLAGEN + CHONDROITIN SULFATE scaffolds								
[136]	COL+CS	Scaffold	d = 8-20	no	yes	no	28,5-39,4 ± 4,5	Frozen by cooling rate technique, DHT cross-linked
Present study	COL+CS 80:20	Scaffold	8 x 2	yes	yes	no	380 ± 181	
Present study	COL+CS 80:20	Scaffold	8 x 2	yes	no	yes	699 ± 114	
Present study	COL+CS 60:40	Scaffold	8 x 2	yes	yes	no	545 ± 97	
WET COLLAGEN + HYALURONIC ACID scaffolds								
[81]	COL+HA	Scaffold	8-9,5 x 4	yes	no	no	2,5 ± 0,06	Uncross-linked
[81]	COL+HA	Scaffold	8-9,5 x 4	yes	no	no	5,1 ± 0,23	DHT cross-linked
Present study	COL+HA 80:20	Scaffold	8 x 2	yes	yes	no	34 ± 7	
Present study	COL+HA 80:20	Scaffold	8 x 2	yes	no	yes	26 ± 5	
Present study	COL+HA 60:40	Scaffold	8 x 2	yes	yes	no	28 ± 13	

APPENDIX 8: REPORTED GENIPIN CROSS-LINKING PROCEDURES

Abbreviations used in the table: Chi = chitosan, CL = cross-linking, DMEM = Dulbecco’s modified Eagle's medium, DPBS = Dulbecco's PBS, ELN = elastin, Gel = gelatin, TE = tissue engineering and ELAC = electronically aligned collagen.

Samples	Application / Aim of study	GP concen-tration	Solvent	Amount of CL solution	CL time	CL tempera-ture	Washing procedures after CL	CL degree	Remarks	Reference
COL+Chi scaffolds	Fabricating scaffolds for articular cartilage TE.	(w/v) 0.3 % 0.1-0.5 %	PBS (pH 7.4)	4 ml /well*	24 h	RT	washed with deionized water	63.93 - 74.14 % 48.28 - 80.71 %	* Scaffolds placed in a 6-well cell culture plate; each scaffold occupying a single well.	[144]
COL gels	Characterizing the effects of GP CL in COL gels: correlation of mechanical properties to fluorescence.	1 mM 5 mM* 10 mM*	PBS	4.8 ml /petri dish**	2 h 4 h 6 h	37°C	rinsed generously with PBS		* GP has marked cytotoxic effects at concentrations of 5 mM and above. ** seemingly one sample/one petri dish	[122]
COL+Chi+ELN constructs	Vascular media regeneration.	1 mM 5 mM 10 mM 25 mM	PBS		5 h*	37°C	washed 6 times with 30 min each wash using sterile 1 x DPBS		* After 5 h, the GP solutions were removed and replaced with 1 mL of PBS per well. The culture plate was then maintained overnight at RT.	[85]
Gel films	Stabilization of gelatin films by CL with GP.	0.07-2 % (w/w)	PBS (pH 7.4)	10 ml /sample	24 h	RT	repeatedly washed with double distilled water and air dried at RT	85 %	The films treated with GP at concentrations higher than 0.67% were quite similar.	[5]
COL+HA+CS hydrogel scaffolds	Develop a biomimetic hydrogel scaffold with good operability and stability by COL self-assembly and reinforce mechanical properties with GP CL.	0.6 mM 0.75 mM 1 mM			5 h	37°C		20.14 % 33,32 % **	** No significant variations observed when GP concentration was greater than 0.75 mM.	[147]

Bovine pericardia	Study effects of CL degree of an acellular biological tissue on its tissue regeneration pattern.	0.00625 % 0.05 % 0.625 %	PBS (pH 7.4) 0.1 M		3 days	37°C		30 % 60 % 95 %		[78]
Porcine pericardia	See the difference in CL tissues treated with either GP or GA.	0.625 %	PBS (pH 7.4)		3 days	37°C	Tissues sterilized in a graded series of ethanol solutions with a gradual increase in concentration (20-75%) over a period of 4 h, and rinsed in sterilized PBS.			[125]
Gel scaffolds <-- gelatin stock solutions of 5 wt.%, 7.5 wt.%, and 10 wt.%	Fabricating scaffolds for articular cartilage TE.	0.5 wt%			48 h	RT	*	85 % with all stock solutions	* Freeze-drying procedure in all methods is to rinse the cross-linked scaffold with glycine first and then with deionized water 3 times to remove residual chemicals; these steps also contribute to the swelling of the scaffold.	[80]
COL+HA+CS	Fabricating scaffolds for cartilage TE.	0.1 % (w/v)	70 % ethanol (pH 7.4)		48 h	37°C	4 times with sterile PBS, once with 70% alcohol, and once with DMEM			[63]
Gel hydrogels	Investigation on CL structures.	4 mM	PBS (pH 7.4)		6 h	37°C		90 %		[77]

ELAC treads	Improve the mechanical strength of ELACs treads.	(w/v) 0.625 % 0.625 % 0.625 % 0.625 %	 70 % ehanol 80 % ethanol 90 % ethanol 100 % ethanol		 72 h				Increasing the GP concentration from 0.625 % to 2 % increased the CL degree. However the difference was only marginal (4%).	[136]
ELAC treads		0.1 % 2 % 6 %	80 % ethanol		72 h					
ELAC treads		0.625 % 0.625 % 0.625 %	80 % ethanol		6 h 12 h 24 h					
ELAC treads		**0.625 %** 0.625 % *2 %*	**1X PBS** 90 % ethanol *90 % ethanol*		**72 h** 72 h *72 h*			**25 %** 60 % *65 %*	**Least successful; e.g. higher swelling ratio (~ 300%)** 2nd best; superiority compared to 2 % GP was however only 4 % *Best; ultimate wet tensile stress*	
COL+Chi sheets constructs COL+ELN fibers constructs	Developing potential vascular graft materials.	10 mM			5 h		*		* After CL, all the constructs were retrieved and stored in 1 x DPBS.	[86]

COL+HA+CS	Fabricating scaffolds for articular cartilage therapy.	0.25 % (w/v)	70 % ethanol (pH 7.4)		48 h	37°C	matrices were immersed in 70% (v/v) ethanol (4 times × 30min), followed by washing with PBS (pH 7.4) (5 times × 20min)	56 %		[64]
COL	Control scaffolds.	0.25 % (w/v)	70 % ethanol (pH 7.4)		48 h	37°C		65 %		
Porcine pericardium	Study CL characteristics, mechanical properties, and resistance against enzymatic degradation of biological tissues after fixation with GP.	30 mM	PBS (pH 7.4)	~100ml GP-solution / 6 x 6 cm tissue	72 h	RT				[123]
Porcine cartilage	Cartilage-derived matrix for human adipose- derived stem cell chondrogenesis.	0.005 % 0.05 % 0.5 %			3 days	37°C	3 times with distilled water	3.5 % 50 % 89 %		[17]
COL+Chi+Gel scaffolds	Novel scaffold materials for biomedical applications.	(w/w) 0.5 %** 1 % 2 %	ethanol		3 h*	12°C		7.3 %** 13.3 % 27.64 %	* intensive stirring for 10 minutes ** exhibited a homogenous porous structure (33.1%)	[34]
Chi hydrogels	Hydrogels as biomedical and pharmaceutical aids.	0.01-0.1 %			24 h*	RT	washed with 1 N NaOH to remove residual acid, and finally rinsed with ultrapure water		* intensive stirring for 2 minutes	[95]

Chi scaffolds	Fabricating scaffolds for TE applications.	4 % (w/v)			2 h*	40°C-20°C*			* 200 bar pressure and a flow of CO_2 applied through the sample. Then the pressure was released slowly to the atmosphere and the temperature reduced to 20°C.	[67]
Gel microspheres	For cell delivery.	0.5 %	100 % ethanol 90 % ehanol* 80 % ehanol 50 % ehanol	5 ml / 1 g dried gelatin spheres	24 h 36 h* 24 h 24 h	37°C			* Best CL degree achieved in these conditions.	[69]

APPENDIX 9: STUDIES REPORTED ON COLLAGEN-HYALURONIC ACID SCAFFOLDS

ABBREVIATIONS

All the initial concentrations of blends as well as the final composition ratios of composite scaffolds are noted in the table according to original source. Abbreviations used in the table: AFM = atomic force microscopy, CL = cross-linking, COL1 = collagen type I, COL2 = collagen type II, dH_2O = distilled water, DIW = deionized water, Gel = gelatin, GMHA = glycidyl methacrylate-modifed hyaluronic acid, HCPDE = hollow-centered parallel disc electrode, IPN = interpenetrating polymeric network, PEM = polyelectrolyte multilayer, PIC = polyion complex, PU = polyurethane, (E)SEM = environmental scanning electron microscopy, TE = tissue engineering and UNS = unspecified.

Composite Material	Scaffold Stucture	Processing Method	Cross-linking	TE Application	Aims of Research	Research Results	Refe-rence
COL+HA	3D porous composite scaffolds, MSC-seeded, disk shaped 1 % (w/v) COL2 (in HCl) + UNS HA blend → COL:HA = UNS (phase I)	Freeze-drying (phase II) MSC-seeding (phase V)	DHT cross-linking (phase III) EDC/NHS cross-linking (phase IV)	Bone and cartilage TE	➢ Fabricate scaffolds that promote cellular attachment and bone regeneration. ➢ Different carbodiimide cross-linking protocols targeting to the scaffolds in order to control the compressive resistance and to see the effect on chondrogenesis. ➢ Investigate the association of aggregation of MSCs and chondrogenesis in vitro.	Histologic examination: scaffolds of highest cross-link density maintained an open, porous structure Swelling test: decrease in swelling ratio with increase of EDC cross-linking treatment Cross-linking and scaffold contraction analysis: low cross-link densities resulted in cell-mediated contraction, increased cell number densities, and a greater degree of chondrogenesis compared to more highly cross-linked scaffolds resisting cellular contraction In vitro cell culture test with MSCs: COL+HA scaffolds promoted cellular attachment, uniform cell distribution after 24 h	[140]
COL+HA	3D porous composite scaffolds 1 % COL1 + 1 % HA blend (wt.%) → COL:HA = 92.5:7.5 and 75:15 (wt.%) (phase I)	Freeze-drying (phase II, IV)	EDC/NHS cross-linking (phase III)	Adipose TE	➢ Fabricate a robust freely permeable, porous, 3D COL+HA matrix applicable to mammary stromal tissue development in vitro.	X-ray micro tomography, FTIR, SEM and pore size analysis: interconnected pore structure with total porosity of ~85% in all scaffolds, no signs of COL denaturation during successful cross-linking treatment DSC and TG analysis: presence of HA enhanced the cross-linking efficiency Water uptake and dissolution tests: cross-linking reduced the swelling, COL+HA scaffolds swelled more and had higher dissolution resistance than plain COL matrix Mechanical tests: compressive modulus and elastic collapse stress higher in COL+HA scaffolds, compared to plain COL	[22]

						In vitro cell culture test with 3T3-L1 preadipocytes: all scaffolds supported cell proliferation and differentiation	
COL+HA	3D porous composite scaffolds, disk shaped 1 % COL1 (aqueous solution) + UNS HA blend → COL:HA = 100:0 95:5,90:10 and 80:20 (%, w/w) (phase I) *Porous PU matrix as control*	Freeze-drying (phase II, IV)	EDC cross-linking (phase III)	Dermal tissue restoration	➢ Prepare COL+HA composite matrix applicable for wound dressing and skin substitute.	SEM and pore size analysis: interconnected pores in all of the COL+HA matrices, more irregular and fibrous pore structure with increasing HA content Retention and water uptake test: HA content decreased slowly after rapid decrease over 24 h, HA had no significant effect on water uptake In vitro cell culture test with fetal human dermal fibroblasts: good cell adhesion, *compared to PU matrix*, and 9.6 % increase in cell proliferation after 2 weeks In vivo animal test with guinea pigs: thicker dermis after COL+HA treatment, *compared to PU treated dermis*, also accelerated epithelial regeneration and COL synthesis, however HA had no significant effect on wound size reduction	[106]
COL+HA	3D porous composite scaffolds, sponge-like 1 % COL1/2 (in HCl) + 1 % HA (in dH_2O) blend (wt.%) → COL:HA = 2:1, 1:1 and 1:2 (phase I)	Freeze-drying (phase II, IV)	EDC/NHS cross-linking (phase III)	Brain TE	➢ Produce 3D sponge-like COL+HA scaffolds with open porous structure applicable for brain TE. ➢ Provide mechanical stability by EDC cross-linking.	Optical microscopy, SEM and pore size analysis: successful COL+HA scaffolds with interconnecting pore structure and homogenous pore size distribution, COL2 scaffolds had slightly larger (10 %) pore diameter than COL1; in both pore Ø increased with increasing HA content Water absorption test: addition of HA increased water uptake capacity of COL+HA scaffolds, in contrast more extensive cross-linking decreased water uptake HA release degradation test: higher COL, resulted in slower HA degradation rate,	[142]

						pure cross-linked HA scaffolds were not totally degraded after 28 days, pure non-cross-linked HA was degraded immediately Tensile testing: adding HA reduced significantly compressive strength and modulus, COL1 had lower (15 %) strength and modulus than COL2; both had similar compressive behavior, mechanical properties of COL:HA 1:2 and pure HA sponges most comparable with brain tissue In vitro cell culture test with neural stem cells: suitable for NSC growth and differentiation, neurite extensions with neuronal and glial phenotypes observed	
COL+HA	Porous composite scaffolds, membrane shaped UNS COL1 dispersion (in dH_2O) + 3 % HA (wt.%, aqueous solution) blend → COL:HA = 8:2 (weight ratio) (phase I)	Freeze-drying (phase II, IV)	EDC cross-linking (phase III) *GA cross-linked membranes as comparison*	Tissue regeneration	➢ Fabricate porous scaffold material applicable for tissue regeneration. ➢ Achieve better mechanical stability with cross-linking.	SEM and pore size analysis: porosity of 58-66 % depended on freezing temperature, all scaffolds had porous and interconnected structure before and after cross-linking Swelling test: no significant differences in the swelling behavior of EDC treated membranes with increasing cross-linking degree Enzymatic degradation test: *compared to GA treated membranes*, EDC cross-linked membranes showed significant enhancement of resistance to collagenase activity In vitro cell culture test with L929 fibroblast cells: no significant cytotoxity observed	[107]

COL+HA	3D macroporous, nanofibrous hybrid scaffolds 0 %, 5 % and 20 % COL1 + 10 % HA blend (wt.%) →COL:HA = 5:95 20:80 (weight ratio) (phase I)	Electro-spinning combined with salt leaching technique (phase II) Freeze-drying (phase IV)	EDC cross-linking (phase III)	Cartilage TE	➢ Fabrication of HA-based scaffolds (able to swell in water) retaining macroporous and nanofibrous geometry. ➢ Achieve fluffy nanofiber web structure in the matrix.	SEM analysis: soft, fluffy appearance, most of the nanofibers extensively interconnected Tensile test: tensile strength increased with greater COL content, also the HA nanofibrous structure was thought to contribute to the enhanced mechanical strength Degradation test: slower degradation rate with greater COL content, also nanofibrous structure, blending COL+HA and EDC treatment were thought to enhance the structural integrity and produce less water-absorbing scaffolds In vitro cell culture test with bovine chondrocytes: enhanced cell adhesion and proliferation with increasing COL content, cells maintained round characteristics of chondroplastic morphology	[61]
COL+HA	Porous composite scaffold matrices, antibiotic-loaded, bi-layered 1% COL1 dispersion + 1% HA (aqueous solution) blend (phase I) → COL :HA = 80:20 (%, w/w)	Freeze-drying (phase II, IV, VI) Antibiotic loading (phase V)	EDC cross-linking (phase III)	Skin substitutes	➢ Antibiotic releasing scaffolds for the control of wound contamination and to promote wound healing. ➢ Investigate the effects of two antibiotics (tobramycin and ciprofloxacin) incorporated in COL+HA matrix.	SEM and pore size analysis: end result was dense membrane and porous COL+HA matrix, loaded drug nor cross-linking did not alter the 3D interconnected porous structure Tensile test: higher tensile stress with drug loaded COL+HA matrices In vitro cell culture test with fetal human dermal fibroblasts: 0.4 mg/ml concentration of ciprofloxacin had cytotoxic effect In vivo wound size reduction analysis with full thickness dermal defect model: tobramycin had no significant effect on wound healing	[105]

COL+HA	3D porous hybrid scaffolds, disk shaped 0.1 %, 0.3 % or 0.5 % COL + 1 % HA (in dH_2O) blend → COL:HA = UNS (phase I)	Freeze-drying (phase III)	EDGE cross-linking (phase II)	Cartilage TE	➢ Easily prepared and processed scaffolds applicable to cartilage regeneration.	SEM and pore size analysis: COL+HA scaffolds had structure within chondrocytes and tissue could grow well Tensile and degradation tests: increased tensile strength and degradation period with greater COL concentration In vitro cell culture test with human chondrocytes: increased cell proliferation with greater COL concentration, even cell distribution and good adhesion In vivo cell culture test with rabbits: increase in GAG concentration in COL+HA scaffolds (compared to plain HA scaffold) indicating cartilage formation	[59]
COL+HA	3D composite microspheres 0.35, 0.5 and 0.7 % COL + 0.7 % HA blend (wt.%) → COL:HA = 1:1 (volume ratio) (phase II)	Freeze-drying (for COL only) (phase I) HCPDE system (phase III) Thermal reconstitution (phase V)	Two-step cross-linking treatment: gelation by $FeCl_3$ + cross-linking by EDC (phase IV)	Drug delivery encapsulating materials for cell/tissue carriers and bone grafting	➢ To create 3D microspheres that could provide a larger surface area for cell adhesion and possess easy estimation of diffusion and mass-transfer behavior. ➢ To create 3D microspheres that can be delivered to the targeted and hard-to-reach areas easily. ➢ To offer an effective alternative method for microsphere preparation, as compared to emulsion processes.	Two-step cross-linking: $FeCl_3$ gelation treatment caused the microspheres to decrease in size Optical microscopy and SEM analysis: microspheres exhibited good spherical structure shape, the higher COL content the greater morphological heterogeneity Mechanical durability test: EDC cross-linking increased significantly mechanical durability of COL+HA microspheres Water content and swelling test: higher water content after $FeCl_3$ gelation, which decreased after EDC treatment; produced firmer structure and limited swelling Thermal analysis: increase in water holding capacity with greater COL concentration Fluorescence analysis: COL and HA can be well mixed with the method introduced in present study	[13]

COL+HA	3D composite scaffolds, nanofiber mesh, disk shaped 7.5 % COL1 + 7.5 % HA (wt/vol) blend → COL:HA = 5:95 (wt ratio) (phase I)	Electro-spinning (phase II) Addition of gold particles (additional conjugation step, phase IV)	EDC cross-linking (phase III)	Bone TE	➢ Fabricate scaffolds that promote cell proliferation and bone regeneration. ➢ Produce nanofiber scaffold matrix with electro-spinning. ➢ Achieve insolubility with EDC cross-linking. ➢ Enhance biocompatibility and cellular attachment by adding gold particles.	SEM and FTIR analysis: meshes with uniformed nanostructure and successful gold particle attachment EDC cross-linking: scaffolds insoluble in aqueous solutions In vitro WST cell culture test with L929 fibroblast cells: meshes promoted cellular attachment	[31]
COL +GMHA	3D composite hydrogels, IPN, disc shaped 1% (w/v) HA + 50:50 water:acetone blend → GMHA (phase I) UNS COL1 (in acetic acid) + 12.5, 25, 50 and 75 mg/ml GMHA blend → COL:GMHA:DMEM &HEPES = 8:1:1 (phase III)	Freeze-drying (phase II)	Photo cross-linking (phase IV)	TE	➢ Prepare a biohybrid and biomimetic scaffold composed of natural ECM components. ➢ Introduce a novel photo cross-linkable IPNs of COL+HA with precisely controlled structural and biomechanical properties. ➢ Offer possibility to fine-tune scaffold properties by performing structural modifications and patterned scaffolds with the hydrogels prepared in present study.	SEM and rheological analysis: COL+HA IPNs denser than semi-IPNs (where COL is in network form) resulting in molecular reinforcement Swelling test: decrease in swelling ratio of COL+HA IPNs with increasing GMHA concentration, no significant difference with semi-IPNs Degradation test: slower degradation with COL+HA IPNs compared to semi-IPNs In vitro cell culture test with human dermal fibroblasts and Schwann cells: no cytotoxity observed with COL+HA IPNs nor semi-IPNs Patterned cross-linking analysis (phase V): successful creation of heterogeneous hydrogels (IPN + semi-IPN regions in one)	[126]
COL+HA	Porous composite matrices 1.25 % (w/v) COL2 + UNS HA blend (in dH_2O)	PIC formation in aqueous solution (phase I)	EDC cross-linking (phase II)	Cartilage TE	➢ Introduce an improved method to prepare COL+HA composite scaffolds applicable to cartilage regeneration.	FTIR analysis: successful cross-linking between COL ja HA molecules SEM and pore size analysis: matrices had multi pore structures Swelling test: swelling ratio decreased with increasing EDC concentration and with 0-20% HA content, and again increased from >40% HA content	[127]

	→ COL:HA = 1:1, 2:1, 4:1, 8:1 (weight ratios) (phase I)						
COL+HA	Composite scaffolds, nanofibrous, membrane shaped 0.5 % COL1 + 0.75 % HA (wt.%, in water) blend → COL:HA = UNS (phase I)	Self-assembling strategy and coating technique: overlaying COL solution on top of the HA solution (phase II)	None	Targeted tissue regeneration	➢ Introduce a novel self-assembling and coating technique to create COL+HA membranes and encapsulating structures.	SEM analysis: COL and HA had dense membrane structure, HA had more beaded architecture, cross-section images revealed multilayered nanofibrous structure In vitro cell culture test with hMSCs: membranes supported cell proliferation and viability Protein delivery test: slow and steady protein release profile	[18]
Additional component on COL+HA scaffolds							
COL+HA +Gel	Composite films 0.6 % COL1 (in HCl) + UNS Gel (in HCl) + UNS HA (in DIW) blend → COL:Gel:HA = 6:3:1, 6:3:0.5, 6:3:0 (w/w) (phase I)	Air drying (phase III)	EDC/NHS cross-linking (phase II)	Cornea TE	➢ Fabricate biomimetic films applicable to cornea TE applications. ➢ Achieve composite films that have similar hydrophilic, tensile enduring and optical performance than human cornea.	Tensile test: tensile strength increased with higher HA content, no significant differences between the scaffolds concerning elongation at break, all in all 6:3:1 composite film had the best mechanical properties Swelling and water absorption test: water absorption and hydrophilicity improved with HA content, 6:3:1 composite film had best hydrophilicity properties Diffusion coefficient analysis: 6:3:1 composite film had diffusion property similar to human cornea In vitro cell culture test with human corneal epithelial cells: good cell adhesion and proliferation	[83]
COL+HA +PEM-coating + fluorescent probes	Composite films, multilayered 0.46 mg/mL COL1 film (in acetic acid) +	PEM layer-by-layer deposition technique (phase II)	EDC/NHS cross-linking (phase III)	Tailored cell and tissue interactions, design of	➢ Introduce a novel polyelectrolyte multilayer coating technique to create COL+HA films applicable to tailored TE and ECM	AFM and ESEM analysis: increase in PEM thickness and refractive index with increasing collagen concentration; corresponding but opposite effects with increasing HA concentration	[55]

fluorescent probes	0.46 mg/mL COL1 film (in acetic acid) + 0.46 mg/mL HA solution (in acetic acid) → COL and HA = 0.46 mg/mL (phase I)	technique (phase II) Fluorescence labeling (phase IV)		artificial ECM	to tailored TE and ECM designing with tailored cell/tissue interactions.	corresponding but opposite effects with increasing HA concentration EDC/NHS cross-linking: PEM layers stable at physiological pH, no dissolution of the coating Fluorescence analysis: successful insertion of covalently linked fluorescence labels showed the potential of incorporating also other functionalities	

APPENDIX 10: STUDIES REPORTED ON COLLAGEN-CHONDROITIN SULFATE SCAFFOLDS

All the initial concentrations of blends as well as the final composition ratios of composite scaffolds are noted in the table according to original source. Abbreviations used in the table: BP = benzophenone, CDI = 1,1-carbonyldiimidazole, Chi = chitosan, CL = cross-linking, COL1 = collagen type I, COL2 = collagen type II, ELN = elastin, (E)SEM = (environmental) scanning electron microscopy, TE = tissue engineering and UNS = unspecified.

Composite Material	Scaffold Stucture	Processing Method	Cross-linking	TE Application	Aims of Research	Research Results	Refe-rence
COL+CS	Porous composite scaffolds UNS COL1 matrix (phase I) + UNS CS (covalently attached, phase III) → COL:CS = 97.25:2.75 (%, w/v)	Freeze-drying (phase II, IV)	EDC/NHS cross-linking (phase III)	Cartilage TE	➢ Investigate the effect of the presence of CS in COL+CS scaffolds on metabolic activity of seeded chondrocytes.	SEM and optical microscopy analysis: equally distributed chondrocytes throughout the porous scaffold structure, increase in the amount of cells with COL+CS scaffolds compared to plain COL scaffolds, however no penetration of cells into the deeper layers, chondrocytes maintained round morphology throughout the experiment; only sparse elongated cells with fibroblastic appearance found In vitro cell culture test with bovine chondrocytes: CS influenced positively on bioactivity of chondrocytes; proliferation and total amount of proteoglycans were significantly higher in COL matrix with CS present	[138]
COL+CS	Composite scaffolds UNS COL1 + UNS C6S blend (in acetic acid) → COL:CS = 92:8 (wt.%) (phase I)	Freeze-drying (phase II)	DHT cross-linked (phase III) AND/OR EDC/NHS cross-linking (phase III/IV)	TE	➢ Demonstrate COL+CS scaffolds degradation by collagenase and chondroitinase. ➢ Provide information for the COL+CS scaffold production with desired compressive strength.	Compression test: EDC cross-linked scaffolds had higher compressive stiffness compared to non-cross-linked or DHT cross-linked scaffolds Degradation test, ESEM and video imaging analysis: EDC cross-linked scaffolds had greater resistance against degradation compared to non-cross-linked or DHT cross-linked scaffolds, collagenase degradation resulted in loss of microstructural topography, chondroitinase degradation of scaffolds resulted in swelling as well as smaller, rounder pores	[108]

COL+CS	3D porous composite scaffolds 0.5 % COL1 + 0.05 % C6S blend (wt.%, in acetic acid) → COL:CS = UNS (phase I)	Freeze-drying (phase II)	DHT cross-linking (phase III) EDC/NHS cross-linking (phase IV)	Skin TE	➢ Mechanical characterization of porous, 3D COL+CS scaffolds.	Tensile and compression tests, and AFM analysis: scaffolds showed characteristic of low-density, open-cell foams with distinct linear elastic, collapse plateau and densification regimes, scaffolds with equiaxed pore were characterized as mechanically isotropic	[42]
COL+CS	3D porous composite scaffolds, anisotropic, cylindrical shaped UNS COL1 + UNS C6S blend (in acetic acid) → COL:CS = UNS (phase I) *Isotropic COL+CS scaffolds as control.*	Freeze-drying (phase II)	DHT cross-linking (phase III) EDC/NHS cross-linking (phase IV)	Tendon TE	➢ Fabricate 3D scaffolds with aligned tracks of ellipsoidal pores that mimic native tendon physiology.	SEM and optical microscopy analysis: anisotropic scaffolds had aligned, ellipsoidal pores regardless of different freezing temperatures, and significantly elongated pores in longitudinal vs. transverse planes In vitro cell culture test with horse tendon cells: compared to isotropic scaffolds, anisotropic scaffolds showed better cell attachment, metabolic activity, cell-mediated contraction and alignment, pore size influenced significantly cell viability, proliferation, penetration and metabolic activity	[10]
COL+CS	3D porous composite scaffolds, scaffold + membrane structured, cylindrical shaped 0.5 % COL1 + 0.05 % C6S blend (w/v, in acetic acid) → COL:CS = UNS (phase I); multiple variations with membrane thickness - *see the source for more details*	Evaporation (phase II) Freeze-drying (phase III)	DHT cross-linking (phase IV) EDC/NHS cross-linking (phase V)	Tendon TE	➢ Fabricate porous, biomimetic core-shell composites with high bioactivity and improved mechanical properties.	SEM and pore size analysis: all variants had consistent relative density (0.6 %) Tensile test: increasing thickness of the membrane shell increased composite tensile elastic modulus, also cross-linking was found to increase tensile strength In vitro cell culture test with horse tendon cells: composites supported cell viability, proliferation and metabolic activity	[11]

COL+CS	Porous composite scaffolds, fiber reinforced 0.92 % COL1 + 0.08 % C6S blend (wt.%, in HCl) → COL:CS = UNS (phase III) *6 % fiber volume after initial freeze-drying, and 75 % of the dried mass of the final samples.*	COL fiber bundle fabrication by extrusion (phase I) Freeze-drying (phase II, IV, VI)	EDC/NHS cross-linking (phase V)	Soft tissue and cartilage TE	➢ Fabricate scaffolds for repair and regeneration of tissues like tendon, ligaments and cartilage. ➢ Show that integrating fibers into the scaffold matrix result in scaffolds with higher mechanical properties.	SEM and optical microscopy analysis: cross-linked scaffolds had open interconnected pore structure, dense fibers had little internal porosity or cracking (i.e. freeze-drying result in minimal damage to fibers), non-cross-linked scaffolds showed larger channels and pores inside the structure, and also lower interaction between fibers Swelling test: non-cross-linked has higher swelling than cross-linked (~20-50 % higher) Tensile test: non-cross-linked scaffolds had significantly reduced mechanical properties (6-fold lower tensile strength), cross-linked fiber scaffolds increased tensile strength over 100 times, all in all the presence of fibers together with cross-linking increased tensile strength and strain to failure significantly	[117]
COL+CS	Porous composite scaffolds 0.019 % COL1 + 0.002 % C6S blend (wt.%, in acetic acid) → COL:CS = UNS (phase I)	Freeze-drying (phase II)	DHT cross-linking (phase III)	Soft TE	➢ Fabricate composite scaffolds applicable to tendon and ligament regeneration, i.e. soft TE applications.	SEM and optical microscopy analysis: all samples had low-density open-cell structure, pore diameter decreased but wall thickness remained roughly constant with larger material densities Compression and tensile tests: increasing density of the scaffolds resulted in higher compressive and tensile strength; in both dry and hydrated states In vitro cell attachment test with MC3T3-E1 mouse osteogenic cells: attachment of cells was directly proportional to specific surface area of the scaffold	[57]

COL+CS	Composite scaffolds, disk shaped 0.5 (%, w/v) COL2 (in dilute ethanoic acid) + 0.5 g C4S (in ethanoic acid) blend → COL:CS = 1:1 (wt) (phase I)	Freeze-drying (phase II)	None	Cartilage TE	➢ Scaffold characterization to highlight the effects of fibrillogenesis, CS addition on viscosity, pore structure, porosity and mechanical properties.	SEM and optical analysis: fibrillogenesis increased the circularity of pores significantly in plain COL scaffolds, no significant change observed in CS-containing scaffolds, adding CS to COL-scaffolds increased the circularity of the pores and the proportion of pores between 50 and 300 µm suitable for chondrocytes growth FTIR analysis: bonding between COL and CS was observed Compression test: CS increased the compressive modulus 10-fold to 0.28 kPa in COL-scaffolds Rheological test: bonding of COL and CS was confirmed	[128]
COL+CS	3D composite scaffolds 0.5 % COL1 + 0.044 % C6S blend (w/v, in glacial acetic acid) → COL:CS = UNS (phase I)	Freeze-drying (phase II)	DHT cross-linking (phase III)	Skin TE	➢ Investigate the effects of DHT treatment on COL+CS scaffolds; on their mechanical properties, cross-linking density and denaturation.	Compression and tensile tests: cross-linking at 180°C (vs. 105°C) increased compressive modulus up to 2-fold, increasing exposure duration increased tensile modulus at 120 and 150°C but not in 105°C, increasing temperature from 105 to 150°C increased tensile properties up to 3.8-fold FTIR analysis: increasing exposure period at 120 and 150°C increased denaturation of collagen in the composite scaffolds Altogether: increase in temperature and duration of DHT treatment increased mechanical properties of COL+CS scaffolds	[43]

COL+CS	3D porous composite scaffolds 0.5 % COL1 + 0.05 % C6S blend (wt.%, in acetic acid) → COL:CS = UNS (phase I)	Freeze-drying (phase II)	DHT cross-linking (phase III)	Skin TE	➢ Study the effect of pore size on cell adhesion in porous scaffolds. ➢ Study relationship between cell viability and cell attachment in COL+CS scaffolds and their structure.	Pore size analysis: all COL+CS scaffolds had consistent, homogenous pore structure with no obvious non-uniformity, largest mean pore size achieved with -10°C freezing temperature In vitro cell culture test with MC3T3-E1 mouse clonal osteogenic cells: no significant difference in cell attachment with different mean pore sizes, but increase in mean pore size resulted in lower amount of viable cells	[100]
COL+CS	3D porous composite scaffolds 0.5 % COL1 + 0.05 % C6S blend (wt.%, in acetic acid) → COL:CS = UNS (phase I)	Modified conventional freeze-drying method (phase II)	DHT-cross-linking (phase III)	TE	➢ Produce more homogenous COL+CS scaffold structures by varying the cooling rates freeze-drying method. ➢ Achieve more uniform contact between the pan containing COL+CS suspension and the freezing shelf with use of smaller, less warped pans.	Optical microscopy analysis: smaller and stiffer stainless steel pans resulted in more homogenous and smaller mean pore sized scaffolds ESEM and micro-CT analysis: constant cooling rate technique produced more randomly oriented and more homogenous solid scaffolds, and showed no significant spatial variation in pore size as well as equiaxed pores compared to scaffolds produced with quenching technique	[99]
COL+CS	Composite gels 0.3 % COL1 + 3 mg/ml C6S blend (w/v) → COL:CS = 80:20 (%) (phase I)	None	EDAC and CDI cross-linking (phase II)	Skin TE	➢ Investigate biological stability of COL+CS gels and their contraction seeded with fibroblasts and keratinocytes.	Gel contraction test: fibroblasts caused more contraction to the gel variants than keratinocytes, adding CS did not influence significantly to the contraction in presence of either cell type Biological stability test: most stable gels were non-cross-linked COL+CS, EDAC nor CDI agents had no additive effect on stability	[102]

Additional component on COL+CS scaffolds							
COL+CS + ELN	Porous composite scaffolds (COL fibrils + elastin fibers + CS) 1 % COL + UNS ELN blend (in acetic acid) → COL:ELN = 9:1, 1:1, 1:9 (phase I) + 2.75 % CS (w/v, covalent attachment, in EDC cross-linking solution) → COL:ELN:CS = UNS (phase III)	Freeze-drying (phase II)	EDC/NHS cross-linking (phase III)	TE	➢ Provide useful information for the design and application of tailor-made biomaterials applicable for TE in general.	SEM, TEM and optical microscopy analysis: COL and ELN interacted with each other physically, and ELN fibers were enveloped by COL, more CS bound to COL scaffolds (10 %) than to COL+ELN (2.4-8.5 %) scaffolds Water-binding test: attachment of CS increased water-binding abilities (up to 65 %) Tensile test: higher COL content resulted in higher tensile strength, increase of ELN content increased elasticity In vitro cell culture test with human myoblasts and fibroblasts: cytocompatible	[21]
COL+CS + Chi	3D composite scaffolds, membrane shaped UNS COL + UNS Chi → COL:Chi = 1:1 (phase I) + 1 % CS blend COL:Chi:CS = UNS (phase III)	Freeze-drying (phase II and IV)	DHT cross-linking (phase III) EDC/NHS cross-linking (phase III)	Skin TE	➢ Preparation and characterization of collagen-chitosan-chondroitin sulfate membranes applicable for wound dressing or skin scaffold.	XPS analysis: COL+Chi+CS scaffolds had higher hydrophilic and lower hydrophobic properties compared to COL+Chi scaffolds FTIR analysis: COL+Chi+CS had lower content of primary amine (i.e. degree of cross-linking was much higher) compared to COL+Chi scaffolds Tensile test: COL+Chi+CS scaffolds had higher mechanical strength compared to COL+Chi scaffolds Degradation test: with addition of CS to the scaffold structure, antizymohydrolysis ability was improved, also it was evident that cross-linked scaffolds endured degradation better than unmodified scaffolds	[56]

COL+CS + titanium disks	Composite scaffolds or coatings Preparation of COL fibrils (phase I) 0.1 % COL1/2 + UNS C4S/C6S blend (wt.%) → COL:CS = 1.5:1 – 6:1 (w/w) (phase II)	Fibrillogenesis (phase III) Surface coatings onto titanium disks (phase IV)	EDC/NHS cross-linking (phase V)	Bone TE	➢ Fabricate implant coatings or TE scaffolds suitable for osteoblast adhesion. ➢ Compare the ability of the collagen types I and II to bind preparations of different chondroitin sulfate types. ➢ Provide results that could help selecting COL or CS type as materials for implant coatings or TE scaffolds.	Binding of CS to COL 1 or 2: COL2 bound more CS than COL1; more precisely C6S, CS caused COL fibrils to become thinner In vitro cell attachment test with rat calvarial osteoblasts: cells cultured on COL1 and 2 had more flattened appearance compared to those cultured on plain titanium disks, variations on cell spreading and rounded form of cells attached to the scaffold surface; *see the source for more details*	[23]
COL+CS + BP + covalently photo-immolized biomolecules	3D porous composite scaffolds UNS COL1 + UNS C6S blend (in acetic acid) → COL:CS = UNS (phase I)	Freeze-drying (phase II) BP photolitho-graphy (phase IV) Photoattachment of biomolecules (phase V)	DHT cross-linking (phase III) *BP photolithography further cross-links the scaffold structure*	TE	➢ Fabricate highly porous scaffolds with improved bioactivity by using direct photolithography.	Tensile test and XRD analysis: increase in mechanical properties and COL crystallinity, no significant difference in mean pore size with COL+CS+BP scaffolds compared to COL+CS scaffolds Optical microscopy analysis: BP photolithography does not affect scaffold microstructural or compositional properties In vitro cell culture test with MC3T3-E1 mouse: BP photolithography does not influence negatively cell adhesion, viability or proliferation	[88]

APPENDIX 11: STUDIES REPORTED ON COLLAGEN-HYALURONIC ACID/CHONDROITIN SULFATE SCAFFOLDS

All the initial concentrations of blends as well as the final composition ratios of composite scaffolds are noted in the table according to original source. Abbreviations used in the table: CL = cross-linking, COL1 = collagen type I, COL2 = collagen type II, TE = tissue engineering and UNS = unspecified.

Composite Material	Scaffold Stucture	Processing Method	Cross-linking	TE Application	Aims of Research	Research Results	Refe-rence
COL+HA/ CS	3D porous composite scaffolds, cylindrical shaped 1.5 % COL1 + UNS HA/C6S blend (w/v) → COL:HA/CS = 11.28:1 (w/v) (phase I)	Freeze-drying (phase II)	DHT cross-linking (phase III) EDC/NHS cross-linking (phase IV)	Tendon TE	➢ Produce bioinspired alteration in GAG content of COL+GAG scaffolds in order to regulate cell activity.	SEM and pore size analysis: all scaffolds had highly porous, sponge-like features with only minimal microstructural differences In vitro cell culture tests with horse tendon cells and hMSCs: GAG sulfation improved tenocyte metabolic activity; *see the source for more details*	[47]
COL+HA/ CS	Porous composite scaffolds, membrane shaped 0.5 % COL + 0.05 % HA/CS blend (wt.%) → COL:HA/CS = UNS (phase I)	Freeze-drying (phase I)	DHT cross-linking (phase II) EDC/NHS cross-linking (phase III)	Cartilage and bone TE	➢ Study changes in stiffness and composition of the scaffolds, and how they effect on MSC cell differentiation. ➢ Fabricate composite materials that differ from their stiffness values, by using two cross-linking treatments.	Compression test: scaffolds with the lowest stiffness (0.5 kPa) got MSCs directed towards a chondrogenic lineage, in contrast, in the stiffest scaffolds (1.5 kPa), MSCs are directed towards an osteogenic lineage In vitro cell differentiation test with MSCs: within the COL+HA scaffolds compared to COL+CS scaffolds, HA further influences chondrogenic differentiation, in contrast, in the COL+CS scaffolds compared to COL+HA scaffolds, CS on MSC differentiation suggests an osteogenic influence	[94]
COL+HA/ CS	Porous composite scaffolds 0.5 % COL1 + 0.05 % UNS HA/C6S (w/v, in glacial acetic acid) blends → COL:HA/CS = UNS (phase I)	Freeze-drying (phase II)	DHT cross-linking (phase III)	Cartilage TE	➢ Study effect of HA vs. CS to compressive modulus and morphological mean pore size of COL-based scaffolds, as well as their effect on MSC cell differentiation.	SEM and pore size analysis: adding HA resulted in a significant reduction in scaffold mean pore size compared to COL+CS and GAG-free scaffolds, addition of CS resulted in largest mean pore size, all scaffolds were highly porous (98 %) with or without GAGs FTIR analysis: presence of GAGs did not affect DHT cross-linking mechanism, evidence of COL intermolecular cross-links as well as between COL and GAGs	[89]

						Compression test: after DHT treatment all three scaffolds had increased compressive strength, however there was no significant difference between COL+GAG and GAG-free scaffolds In vitro cell culture, gene expression etc. tests: COL+HA scaffolds showed greater levels of MSC infiltration compared to COL+CS scaffolds, COL+HA scaffolds showed significant acceleration of early stage gene expression of COL2 and cartilage matrix production compared to COL+CS scaffolds Altogether: combining their ability to stimulate MSC migration and chondrogenesis in vitro, COL+HA scaffolds show great potential for promoting cartilage tissue repair	

APPENDIX 12: STUDIES REPORTED ON COLLAGEN-CHONDROITIN SULFATE-HYALURONIC ACID SCAFFOLDS

All the initial concentrations of blends as well as the final composition ratios of composite scaffolds are noted in the table according to original source. Abbreviations used in the table: ADH = adipic dihydrazide, CL = cross-linking, COL1 = collagen type I, COL2 = collagen type II, CSMA = chondroitin sulfate methacrylic anhydride, dH_2O = distilled water, HAMA = hyaluronic acid methacrylic anhydride, IPN = interpenetrating polymeric network, TE = tissue engineering and UNS = unspecified.

Composite Material	Scaffold Stucture	Processing Method	Cross-linking	TE Application	Aims of Research	Research Results	Refe-rence
COL+HA +CS	3D hybrid hydrogel scaffolds, cylindrical 80 mg/ml HA+CS (in dH_2O) blend → CS:HA = 15:1 (phase I) 7 mg/ml COL1 (in acetic acid) + CS+HA blend → COL:HA:CS = 4:1 (phase IV)	Freeze-drying (phase VI)	ADH cross-linking (phase II) EDC cross-linking (phase II) GP cross-linking: 0.5, 0.75, 1 mM (phase V)	Cartilage TE	➢ Fabricate biomimetic hydrogel scaffold with good operability and stability by means of COL self-assembly. ➢ Improve physical and chemical performance with GP cross-linking.	SEM and pore size analysis: composite hydrogels had interconnected and homogenously distributed porous structure, no significant phase separation observed, increase in GP concentration (from 0 to 0.75 mM) decreased pore size significantly; no such effect when GP concentration exceeded 0.75 mM Compression test: non-cross-linked COL+HA+CS hydrogels had slightly greater compressive strength than plain COL hydrogels, compressive strength increased slightly with increase of GP concentration Swelling test: higher cross-linking degree resulted in lower water uptake, however in 1 mM GP concentration the swelling tendency increased significantly Degradation test: COL+ HA+CS hydrogels degraded slower than plain COL hydrogels, higher amount of GP decreased degradation rate In vitro cell culture test with rabbit chondrocytes: COL+HA+CS hydrogels showed excellent cytocompatibility and evidence of possible promotion of cell proliferation	[147]

COL+HA +CS	3D porous composite scaffolds, sponge-like 1 % COL2 (wt/vol, in acetic acid) (phase I) + 2 % HA + 1 % C6S blend (wt/vol, in GP solution) → COL:HA:CS = UNS (phase III)	Freeze-drying (phase II)	GP cross-linking: 0.1 % (wt/vol) (phase III)	Cartilage TE	➢ Fabricate porous 3D scaffolds that mimic the natural ECM of articular cartilage.	SEM and pore size analysis: after GP cross-linking COL+HA+CS scaffolds had interconnected pores with porosities of 92-95 % Degradation test: cross-linked scaffolds became significantly more resistant to degradation compared to non-cross-linked, after 14 days COL+HA+CS composites were the least degraded In vitro cell culture, gene expression test with human articular chondrocytes: after 14-day culture, morphologically round chondrocytes uniformly distributed throughout the scaffolds, expression of aggrecan genes etc. was increased with CS and HA present compared to scaffolds without them	[63]
COL+HA +CS	Porous composite scaffolds 0.5 % COL2 (w/v, in acetic acid) (phase I) + 2 % HA + 1 % C6S blend (w/v, in GP solution) → COL:HA:CS = UNS (phase III)	Freeze-drying (phase II)	GP cross-linking, 0.25 % (w/v) (phase III)	Articular cartilage therapy	➢ Fabricate porous 3D scaffolds that mimic the natural ECM of articular cartilage.	SEM and pore size analysis: after GP cross-linking pore structure stained mostly intact, except that surface pores collapsed to some extent, porosity was less in cross-linked COL+HA+CS scaffolds (90 %) compared to cross-linked plain COL scaffolds (95 %), and to non-cross-linked COL scaffolds (96 %) Swelling test: water absorption was greatest in GP cross-linked COL scaffolds, cross-linked COL+HA+CS scaffolds second and non-cross-linked COL scaffolds swelling the least In vitro cell culture, gene expression test with human articular primary cells: GP cross-linked scaffolds showed no significant cytotoxity	[64]

COL +HAMA +CSMA	3D composite hydrogel scaffolds, IPN, cylindrical shaped 5 mg/ml COL1 + 0.3 mg/ml HAMA + 2.2 mg/ml CSMA → COL:HAMA:CSMA = UNS (with varying methacrylation and IPN degrees) (phase III)	HA and CS dissolved separately into dH_2O and MA (phase I) Freeze-drying (phase II, IV) COL self-assembly (phase III)	Cross-linking polymerization of MA groups (phase III)	Cartilage TE	➢ Fabricate and characterize 3D COL+HA+CS composite hydrogel scaffolds with IPN structure applicable for cartilage regeneration.	SEM and pore size analysis: all hydrogels had interconnected fibrillar porous structure, increase of methacrylation degree resulted in more sheet-like structure and decrease in the amount of fibers Swelling test: presence of IPNs, higher methacrylation and cross-linking degree resulted in decrease of swelling Degradation test: presence of IPNs extended degradation time Compression test: presence of IPNs enhanced compressive modulus (see source for more information) In vitro cell culture test with rabbit chondrocytes: no significant difference about cell viability; all samples showed good cytocompatibility and helped maintain chondrocytic phenotype	[36]